Singularities and Resonances in Complex Adaptive Systems

Diploma Thesis in Physics

John-Oliver Engler

1st Referee: PD Dr. R. Haussmann, Fachbereich Physik, Universität Konstanz

2nd Referee: Prof. Dr. G. Burkard, Fachbereich Physik, Universität Konstanz

Supervisors: Dr. S. Reimann, Prof. Dr. D. Sornette

Department of Management, Technology and Economics, ETH Zürich

March 27, 2010

Contents

List of Abbreviations

CIR-CEV	Cox-Ingersoll-Ross - constant elasticity of variance
CIR-VR	Cox-Ingersoll-Ross with variable rate
CPF	cumulative probability function
FPE	Fokker-Planck equation
FTS	finite-time singularity
ODE	ordinary differential equation
OU	Ornstein-Uhlenbeck
PDF	probability density function
SDE	stochastic differential equation

11:15, restate my assumptions:
1. Mathematics is the language of nature. 2. Everything around us can be represented and understood through numbers. 3. If you graph these numbers, patterns emerge. Therefore: There are patterns everywhere in nature.

Darren Arronofsky, π

Acknowledgements

Numerous people have contributed a great deal to the completion of this thesis: First and foremost, I am equally indebted to the following four persons: To Prof. Didier Sornette for giving me the opportunity to work at his chair and for giving me an idea of what it means to 'live science'. To Dr. Stefan Reimann for his supervision. I especially acknowledge his cooperation and help during a severe family emergency. To PD Dr. Rudolf Haussmann and Prof. Guido Burkard for their kind acceptance of refereeing my work.
Especially, I would like to thank Dr. Ryan Woodard for his kind help with whatever Python problem and way beyond.

Meinen Eltern gilt an dieser Stelle ein besonderes Dankeschön. Ihr habt mich nach Kräften moralisch und finanziell unterstützt und mir so dieses Studium möglich gemacht. Meiner Großmutter danke ich besonders für ihre finanzielle Unterstützung, die mir ein geldsorgenfreies Studium ermöglicht hat.

Und ganz besonders möchte ich mich bei Judith bedanken, die mit mir gemeinsam durch alle Höhen und Tiefen des Studiums gegangen ist und hoffentlich noch viele weitere Jahre Teil meines Lebens sein wird.

Konstanz, 15.03.2010
John-Oliver Engler

Deutsche Zusammenfassung

Die vorliegende Arbeit dokumentiert die Bemühungen und Resultate meines einjährigen Forschungsprojekts am Lehrstuhl für Unternehmensrisiken der Eidgenössischen Technischen Hochschule (ETH) Zürich. Es wurde versucht, ein möglichst eigenständiges und klares Dokument zu schreiben, dass ohne Zuhilfenahme von Sekundärliteratur verstanden werden kann. Andererseits hat eine wissenschaftliche Arbeit (in der Regel) kein vorab klares Resultat (wenn dem so wäre, warum sollte man sie dann tun?). Deshalb habe ich diese Arbeit in zwei Hauptteile unterteilt, die die beiden Hauptprojekte wiederspiegeln, mit denen ich während meines einjährigen Aufenthalts befasst war: Der erste Teil bietet eine allgemeine Einführung in das Forschungsfeld der Theorie komplexer Systeme und eine vollständige Darstellung des Ide-Sornette Modells für Finanzmärkte, sowie neue Erkenntnisse. Das Modell beschreibt einen Markt mit nur zwei Typen von Händlern: 'Mitläufer' (trend followers) und 'Fundamentalwertinvestoren' (fundamental value investors). Trotz dieser restriktiven und eher einfachen Annahmen zeigt das Modell singuläres Verhalten in endlicher Zeit. Das Hauptziel des ersten Teils der Arbeit ist die Erweiterung des Modells auf parametrisches (d.h. multiplikatives) Weißes Rauschen sowie die Detektion und Quantifizierung von Ähnlichkeiten und Unterschieden zur deterministischen Version des Modells. Die meisten heutigen Finanzmarktmodelle sind von erster Ordnung in der Zeit sowie linear oder - zum Zwecke der numerisch-analytischen Untersuchung - linearisiert. Das Ide-Sornette-Modell hingegen vereint in sich zwei Merkmale, die es zu einem besonders interessanten Forschungsobjekt im Kontext der mathematischen Finanzwissenschaften machen: (1) Die Gegenwart von Trägheit (d.h. einer zweiten Zeitableitung) im Markt, was von der Mehrheit der Ökonomen abgelehnt wird und (2) es ist nichtlinear.

Der zweite Teil stellt die Frage nach der Möglichkeit des Auftretens einer Singularität in endlicher Zeit in einer bekannten und etablierten Modellklasse zur Beschreibung von Finanzmärkten und Zinsraten, der CIR-CEV[1]-Klasse von Modellen. Das Auftreten solcher

[1] Cox-Ingersoll-Ross - constant elasticity of variance

Singularitäten wäre zum Beispiel relevant für bestimmte ökonometrische Tests, die eine unendliche Lebenszeit des Prozesses voraussetzen.

Diese zwei Teile sind wie folgt organisiert: In Kapitel 1 wird versucht, eine kurze allgemeine Einführung in das relativ neue Forschungsfeld der Theorie komplexer Systeme zu geben. Das Kapitel gibt keine erschöpfende Definition des Feldes (was auch nicht notwendigerweise möglich ist), sondern ist gemeint als Klärung und Trennung der beiden Begriffe *komplex* und *kompliziert*. Im zweiten Kapitel wird das Ide-Sornette-Modell motiviert und eingeführt und sein dynamisches Gesamtverhalten sowie dessen Komponenten werden analysiert. Die Originalarbeit von Ide und Sornette [6] wird dabei als Leitfaden verwendet, wobei wir auch einige Details liefern werden, denen vorher so noch nicht auf den Grund gegangen worden war. Kapitel 3 stellt den benötigten theoretischen Hintegrund für die analytische Behandlung von Zufallsprozessen sowie die für den Rest der Arbeit notwendigen Werkzeuge und Definitionen bereit. Kapitel 4 dokumentiert die Hauptergebnisse der Erweiterung des Ide-Sornette-Modells um Weißes Rauschen und stellt die für die Arbeit relevanten numerischen Aspekte zusammen. Die Ergebnisse werden zusammengefasst und ein Ausblick auf mögliche zukünftige Forschungsfragen wird auch gegeben.
Das fünfte Kapitel bildet den zweiten Teil der Arbeit in einer jedoch nicht völlig unabhängigen Form, da viele Aspekte des ersten Teils relevant bleiben. Nach einer Einführung in die CIR-CEV-Modellklasse wird von vier verschiedenen Blickwinkeln die Frage beleuchtet, ob es in diesem Modell in endlicher Zeit eine Singularität geben kann. Diese vier Blickwinkel umfassen: Stochastische Differentialgleichung, Fokker-Planck-Gleichung, Schrödinger-Formalismus und exakte Lösung der Gleichungen. Eine kompakte Zusammenfassung sowie ein kurzer Ausblick beschließen diesen Teil.
Zusätzlich findet der geneigte Leser einige theoretische Ausführungen in Anhang A, die detaillierte numerischen Konzepte und Programmiercodes in den Anhängen B und C, sowie einige Zusatzinformationen im Hinblick auf zukünftige Forschungsfragen das Ide-Sornette-Modell betreffend in Anhang D.

The Structure of This Thesis

The present work documents the efforts and results of my one-year long research project at the Chair of Entrepreneurial Risks at the Swiss Federal Institute of Technology (ETH) Zurich. It has been attempted to write this thesis as self-contained and clear as possible so that it can be understood without having to consult secondary literature. On the other hand, scientific work has (mostly) no pre-defined outcome (if it did, then why would one want to do it?). This is why I chose to split the thesis into two main parts that reflect the two main projects that I have been working on during this one-year project:

The first part provides a general introduction into the field of complex system theory and an exhaustive description of the Ide-Sornette model for financial markets as well as some new findings. This model describes a market with only two types of traders: Trend followers and fundamental value investors. In spite of these restrictive and rather simple assumptions, it features a singularity in finite time. The general objective of this thesis' first part is to extend the model towards parametric (i.e. multiplicative) white noise and to detect and quantify similarities and differences to the deterministic version of the model. To date, most of the models for financial markets are of first order in time and linear - or linearized - for a more convenient numerical and analytical investigation. The Ide-Sornette model however unites two rare features which make it a particularly interesting object of study in the context of mathematical finance: (1) the presence of an inertia (i.e. the presence of a second derivative with respect to time) in the market which is rejected by the majority of economists and (2) it features nonlinearity.

The second part probes the question of the possibility of occurrence of a finite-time singularity in a well-known and established model for financial markets and return rates, the CIR-CEV[2] class of models. The occurrence of a finite-time singularity in this class of models would be relevant for example in certain econometric tests that rely on an infinite lifetime of the process.

[2] Cox-Ingersoll-Ross - constant elasticity of velocity

These two parts are organized into five chapters as follows: In Chapter 1, we attempt to provide a brief general introduction to the relatively recent field of science called complex system theory or complexity theory. While the intention of this chapter is not to provide an exhaustive definition of the field (which is not necessarily possible), it is meant as a clarification of the two wordings *complex* and *complicated*. In Chapter 2, the Ide-Sornette model is introduced and motivated and its components as well as its overall dynamical behavior is analyzed. The original work by Ide and Sornette [6] is taken as a guideline while we also provide some details that have not been penetrated before. Chapter 3 compiles the required theoretical background for the analytical discussion of random processes as well as all necessary tools and definitions needed in the rest of this thesis. Chapter 4 documents the main results concerning the extension of the Ide-Sornette model towards multiplicative Gaussian white noise and a compilation about the numerical aspects that are relevant for this work. Findings are summarized and an outlook on possible future research questions concerning the model is also given. Chapter 5 constitutes Part II of this thesis in a non-self-contained manner as many of the aspects from the first part remain relevant. After introducing the CIR-CEV class of models, it sheds light on the question of the possibility of a singularity occurring in finite time in these models from four different perspectives: Stochastic differential equation, Fokker-Planck equation, Schrödinger formalism and closed-form solution of the processes. A compact summary and a brief outlook concludes this part. In addition, the interested reader can find some theoretical explanations in Appendix A, the detailed numerical concepts and codes in Appendixes B and C as well as some additional information related to future research questions related to the Ide-Sornette model in Appendix D.

Part I.

Singularities, Inertia and White Noise in A Nonlinear Twodimensional Model for Financial Markets

1. A Brief Introduction To Complex System Theory

> And so from that, I've always been fascinated with the idea that complexity can come out of such simplicity.
>
> Will Wright

This work will be concerned with a subfield of complex system theory, in particular two models for financial markets. In this first chapter, we will elaborate on the meaning of the wording *complex* system and relate it to the word *complicated* which is also frequently used when dealing with multilayer situations or systems in order to prevent complex system theory from being thought of as chameleon expression.

In everyday life, the wording *complex* might seem as just another hip substitute for anything that we really find *complicated*. Is complex system theory thus in the end just the gateway to the legendary 'theory for everything' that everyone has been looking for as long as science exists? Of course, the answer is 'No!'. In fact, as it turns out, there is no slip-proof definition of complex system theory. Richter and Rost [2] have pointed out that a *complicated* system is 'hard to overview but possible to break-down into sub-units' that can be analyzed separately *without loosing information about the behavior of the whole system*. In their view, a *complex* system cannot be analyzed in this fashion at all or it may be broken-down into sub-parts which however does not yield any further insight because it misses what qualifies the system as *complex*: emergencent behavior, i.e. the interplay and connection of individual parts of the system that lead to new features and characteristics. Examples for complex systems in this sense include swarms of birds and fish, sandpiles (the dunes of Barhan, Marocco) and avalanches, earthquakes, phase transitions (water $\leftrightarrow$ ice, ferro- $\leftrightarrow$ paramagnetism), societies (social unrest and civil wars) and the stock market (herding). On the other hand, an example

given by [2] for a system that is 'only' *complicated* would be the streets and alleyways in any Southern European historic city center. Another example would be the architectural sophistication of certain airports: It takes some time to get used to the arrangement of one-way streets or hallways and gates but once penetrated, orientation is no longer a problem. If we however implement some feedback mechanism, the system will be no longer just *complicated*, it will turn into a *complex* system. In the above two examples, such a feedback mechanism would be to couple the assignment of one-way streets or hallways and gates to the behavior of cars, pedestriants and passengers themselves so that analyzing parts of the system is still possible but does not lead to new insights. Complex system theory is thus about any system that consists of mutually interacting parts (often referred to as 'agents') that constitute the system and - at the same time - react to it. The following table lists a few agents and their corresponding sciences. The wording *complex adaptive system* (CAS) has been introduced by

Agent	**Science**
society	sociology
individual	psychology
organ	physiology
cell	cytology
biomolecule	biochemistry
atom	atomic physics
elementary particle	elementary particle physics

Table 1.1.: Agents and corresponding sciences according to [2]. Note the hierarchical structure of the scheme.

two scientists of the Santa Fe Institute (New Mexico, USA), namely John H. Holland[1] and Murray Gell-Mann[2]. There are several definitions of what a complex adaptive system actually is (there is again no textbook definition) and sometimes, CAS is simply used as a synonym for the science of complexity. According to [1], John H. Holland has coined the following definition:

> A Complex Adaptive System (CAS) is a dynamic network of many agents (which may represent cells, species, individuals, firms, nations) acting in parallel, con-

[1] John H. Holland, born 1929, American computer scientist most renowned for his work on genetic algorithms
[2] Murray Gell-Mann, born 1929, American physicist, Nobel prize in physics 1969

> stantly acting and reacting to what the other agents are doing. The control of a CAS tends to be highly dispersed and decentralized. If there is to be any coherent behavior in the system, it has to arise from competition and cooperation among the agents themselves. The overall behavior of the system is the result of a huge number of decisions made every moment by many individual agents.

We conclude this short introduction by naming a few examples that are often referred to as CAS: the cell, the developing embryo, political parties, ant colonies and the stock market. A model of the latter will be subject of the first part of this thesis.

2. The Ide-Sornette Model for Financial Markets

> All models are wrong, but some are useful.
>
> George Box

In this chapter, the nonstochastic Ide-Sornette model for financial markets is introduced and its features are developed and explained. The usual notation in finance, $x(t) = \ln \frac{p(t)}{p_f}$, will be used throughout the thesis, i.e. that prices are treated as logarithms to some fundamental price p_f. In what follows, the original publication by Ide and Sornette [6] serves as a guideline while we focus on understanding the dynamical properties of the model that are relevant for this work as the main results of [6] are reproduced and explained.

2.1. Motivation

In this section, the Ide-Sornette model for financial markets is derived and our motivation to study this particular model in the present work is pointed out.
As Lux and Marchesi [3] as well as Farmer [4] have shown, the presence of two classes of investors is essential for the generation of stock market price dynamics: technical analysts which are also often referred to as 'trend followers' and fundamental value investors often nicknamed 'fundamentalists' for the sake of simplicity. Farmer [4] also introduced the idea that the market return, i.e. the logarithm of the price relative $\ln \frac{p(t+1)}{p(t)}$, is a function of order size $\Omega(t)$:

$$r(t) = \frac{\Omega(t)}{L} \tag{2.1}$$

with L being the market's liquidity which is usually defined by

$$\frac{\mathrm{d}x}{\mathrm{d}t} = \frac{D(x) - S(x)}{L}$$

where D and S are the demand and supply functions of buyers and sellers at a certain price level, respectively. The order size is thought to consist of two components, the mean reverting component

$$\Omega_f(t) = -c \cdot x(t) \cdot |x(t)|^{n-1}, \quad n > 0 \tag{2.2}$$

and the trend following component

$$\begin{aligned} \Omega_t(t) &= a_1 r(t) + a_2 \cdot r(t) \cdot |r(t)|^{m-1} \\ &= a_1 \ln \frac{p(t)}{p(t-1)} + a_2 \ln \frac{p(t)}{p(t-1)} \cdot \left| \ln \frac{p(t)}{p(t-1)} \right|^{m-1} \qquad m > 1 \end{aligned} \tag{2.3}$$

so that the choice $a_1, a_2 > 0$ reflects the increase of the price if the preceding move was up. According to Ide and Sornette [6], financial models to date are mostly restricted to the case $a_2 = 0$, a fact that points out that these models tend to dismiss the most prominent features of trend following strategies in general, namely underreaction for small price movements and overreaction for large ones. Note also that, altogether, $\Omega(t) = \Omega_f(t) + \Omega_t(t)$. The exponents n and m are important measures for the nonlinearity of the mean reversal and the eagerness of traders to follow the trend, respectively. If we rewrite eqs. (2.1), (2.2) and (2.3) using the log-price notation and the time scale δt (instead of putting $\delta t = 1$) corresponding to one arbitrarily small time step, we may write

$$\begin{aligned} x(t+\delta t) - x(t) = \frac{1}{L}(a_1[x(t) - x(t-\delta t)] + a_2[x(t) - x(t-\delta t)] \\ \cdot |x(t) - x(t-\delta t)|^{m-1} - cx(t)\,|x(t)|^{n-1}) \end{aligned} \tag{2.4}$$

Since one will want to consider small time steps δt rather than large ones, it is sensible to expand eq. (2.4) as Taylor series in powers of δt [6]:

$$\begin{aligned} (\delta t)^2 \frac{\mathrm{d}^2 t}{\mathrm{d}t^2} = -\left(1 - \frac{a_1}{L}\right) \delta t \frac{\mathrm{d}x}{\mathrm{d}t} + \frac{(\delta t)^m a_2}{L} \frac{\mathrm{d}x}{\mathrm{d}t} \left| \frac{\mathrm{d}x}{\mathrm{d}t} \right|^{m-1} \\ -\frac{c}{L} x(t) \cdot |x(t)|^{n-1} + \mathcal{O}[(\delta t)^3] \end{aligned} \tag{2.5}$$

As argued in [6], choosing $a_1 = L$ simplifies the situation without destroying significant features of the model. For $m > 1$, the effects of this damping term are dominated by the second term

on the right-hand side. Thus, introducing the shortcuts

$$\alpha = a_2(\delta t)^{m-2}/L \tag{2.6}$$

$$\gamma = c/L(\delta t)^2 \tag{2.7}$$

yields

$$\frac{\mathrm{d}^2x}{\mathrm{d}t^2} = \alpha \left| \frac{\mathrm{d}x(t)}{\mathrm{d}t} \right|^m - \gamma \left| x(t) \right|^n, \quad n, m > 1. \tag{2.8}$$

which is known throughout the literature as Ide-Sornette model. It is worth noting that this model features two properties entirely new to the models of quantitative finance that have been introduced so far: First and foremost, it is *nonlinear*. Nonlinearity however can capture quite well the behaviour of the price movements of stocks or whole markets in that it accounts for the salient overreaction of traders to price changes that are significantly larger than average or the relative nonchalance to small price movements on the other hand [6]. When wanting to investigate the formation and dynamics of extreme events such as stock market crashes in complex systems, it is therefore desirable to have nonlinearity inherent in the model. Other models are to the author's knowledge not all a priori nonlinear but they are linearized for more convenient treatment. The second speciality of this model is the appearance of a second derivative with respect to t. Physically speaking, this is an *inertia* (of the unit mass M). This is noteworthy because the presence of inertia in a market has been either rejected or ignored among economists which is surprising since trend following strategies are based on the assumption of an inertia in price trajectories ('the price variation from present to tomorrow is based on analysis of price change between yesterday and present' [6]). There is thus no *a priori* reason to reject models with inertia. We will recapitulate the most important dynamical properties of the Ide-Sornette model in the rest of this chapter.

2.2. Investigation of the Model

In the following paragraph, an extensive review of the properties of the model (2.8) will be given. This includes investigation of the cases $\gamma = 0$, $\alpha = 0$ (nonlinear oscillator) and $\alpha \neq 0, \gamma \neq 0$ (Ide-Sornette model).

2.2.1. Case $\gamma = 0$

Working with $B = \frac{\mathrm{d}x}{\mathrm{d}t}$ and adding stochasticity to the model, this case is known as the Sornette-Andersen model for financial bubbles and has been introduced by Sornette and Andersen in 2002 [5]. While the exact scientific textbook definition of what a 'bubble' exactly is, is still subject to a lively and changeful debate and thus is still absent, this model was shown to capture the price dynamics of two recent crashes: the crash of Nasdaq in April 2000 and (one of) the Hongkong market crash(es) in 1994. In [13], the model was enhanced by the possibility to qualify time series - commonly accepted as bubbles - as 'fearful' or 'fearless' depending on the behaviour of the volatility prior to the crash with the characteristic 'super-exponential' price growth occuring in any case and thus being the hallmark of any bubble. By 'super-exponential', it is meant that the growth rate is growing itself with time, a fact which is explained below (see eq. (2.9) and explanations thereafter). It is worth noting that crashes and therefore bubbles that have been investigated with this rather simple approach include the Dow Jones Industrial Average (DJIA) from 1927 to 1929, the Nasdaq Future 100 Index from June 1999 to March 2000, the S&P500 from mid-1985 to mid-1987, the aforementioned Hang Seng Index for the same period and for 1995 till 1997 but also currency crashes like the USD/CHF crash of 1985. One of the most important results of these investigations is that markets do not always anticipate crashes or severe corrections in that the volatility level remains comparably low prior to the crash. As long as 'worry' or 'fear' is measured by the volatility, these 'fearless' financial bubbles are not at all in agreement with the theory of rational expectations from macroeconomics which states that "the agents' expectations are correct on average" [14]. After these introductory remarks, let us now turn to the model:

Putting $r(t) = \dot{x}(t)$, one obtains

$$\frac{\mathrm{d}r(t)}{\mathrm{d}t} = \alpha r(t)^m, \quad m > 1 \tag{2.9}$$

Equations of this type are the simplest type of equations that exhibit so-called finite time singularities. By this term, it is meant that a critical time t_C exists where $r(t)$ grows over all boundaries. This can be understood by just looking at the plain equation (2.9): Since the growth rate $\dot{r}(t)$ grows with r^m, the time needed to double r decreases so fast that it converges to zero sufficiently fast to give rise to a singularity in finite time. Hence,

$$\lim_{t \to t_C} r(t) \longrightarrow \infty$$

Eq. (2.9) can be solved easily by separation of variables by demanding without loss of gener-

ality that $r(t) \geq 0 \; \forall t \in \mathbb{R}^+$. Integration then yields

$$\begin{aligned} r(t) &= r_0 \left[\frac{\alpha(1-m)(t-t_0)}{r_0^{1-m}} + 1 \right]^{\frac{1}{1-m}} \\ &= r_0 \left[\frac{\alpha(m-1)t_0}{r_0^{1-m}} - \frac{\alpha(m-1)t}{r_0^{1-m}} + 1 \right]^{\frac{1}{1-m}} \\ &= \frac{r_0}{t_C^{\frac{1}{1-m}}} (t_0 - t + t_C)^{\frac{1}{1-m}} \\ &= (\alpha(m-1)(t_0 - t + t_C))^{\frac{1}{1-m}} \end{aligned} \tag{2.10}$$

where we introduced the critical time t_C by putting

$$t_C = \frac{r_0^{1-m}}{\alpha(m-1)} \tag{2.11}$$

and where we can always set $t_0 = 0$ since eq. (2.9) is an autonomous ordinary differential equation. This means that the critical time depends on the initial growth rate $r_0 = r(t=0)$ and on the strength of the positive feedback measured by the parameter m. In a stock market model, m can be interpreted as cooperation parameter since a stronger cooperation means a stronger tendency to follow the trend collectively, i.e. imitation effects play a stronger role. In a more physical language, the greater m, the greater also the *correlation length* of traders participating in the market.
Notice also that

$$r(t) \propto (t_C - t)^{1/(1-m)}$$

which diverges at the approach of t_C since $m > 1$ just as we expected.
The logarithmic price $x(t)$ can be derived equivalently by remembering the original ansatz $\dot{x}(t) = r(t)$:

$$\begin{aligned} x - x_0 &= r_0 \int_{t_0}^{t} \left(\frac{t_C - t'}{t_C} \right)^{-\frac{1}{m-1}} \mathrm{d}t' \\ &= -r_0 t_C \left[\frac{m-1}{m-2} \left(\frac{t_C - t'}{t_C} \right)^{\frac{m-2}{m-1}} \right]_{t'=t_0}^{t'=t} \\ &= \frac{r_0^{2-m}}{\alpha(2-m)} \cdot \left((1 - \frac{t}{t_C})^{\frac{m-2}{m-1}} - (1 - \frac{t_0}{t_C})^{\frac{m-2}{m-1}} \right) \cdot \\ &\overset{t_0=0}{=} \frac{r_0^{2-m}}{\alpha(2-m)} \left[(1 - \frac{t}{t_C})^{\frac{m-2}{m-1}} - 1 \right]; \quad m \neq 2 \end{aligned} \tag{2.12}$$

From eq. (2.12), we see that the finite-time singularity at t_C where the growth rate r explodes

beyond every limit has in fact a finite price $x(t_C)$:

$$x(t) = x_0 + C\left((1 - \frac{t}{t_C})^{\frac{m-2}{m-1}} - 1\right) \tag{2.13}$$

where we have defined

$$C = \frac{r_0^{2-m}}{\alpha(2-m)}$$

Thus, we can write

$$\lim_{t \to t_C} x(t) = x_0 - C \tag{2.14}$$

and assert that, for $r_0 > 0$, it holds that $C < 0$ for $m > 2$ and $C > 0$ for $1 < m < 2$. Figure 2.1 illustrates the behaviour exemplarily for the case $m = 2.1$, $r_0 = 0.6 > 0$ and $x_0 = 0$.

This result can be generalized by also accounting for the case $m = 2$ which can be accomplished using l'Hôpital's rule, i.e.

$$\lim_{x \to 0} \frac{f(x)}{g(x)} = \lim_{x \to 0} \frac{f'(x)}{g'(x)}.$$

Thus, substituting $m = 2 + \varepsilon$, we can write

$$\begin{aligned} x(t) - x_0 &= \frac{1}{\alpha} \lim_{\varepsilon \to 0} \left\{ (1+\varepsilon)^{\frac{\varepsilon}{1+\varepsilon}} \cdot \frac{1}{\varepsilon} \left[(t_C - t)^{\frac{\varepsilon}{1+\varepsilon}} - (t_C - t_0)^{\frac{\varepsilon}{1+\varepsilon}} \right] \right\} \\ &= \frac{1}{\alpha}(\ln(t_C - t) - \ln(t_C - t_0)); \quad m = 2 \end{aligned} \tag{2.15}$$

in agreement with [6]. Choosing again $t_0 = 0$ and taking the limit $t \to t_C$, one obtains that $x(t \to t_C) \to -\infty$ which means for the price that $p(t \to t_C) \to 0$.

2.2.2. Case $\alpha = 0$

This case is known as nonlinear oscillator which has been extensively studied because of the general relevance of oscillatory processes in physics and science (see [7], [6], [9], [10], [11] and references therein). The special feature of nonlinear oscillations is that they exhibit a frequency-amplitude relationship in contrast to the linear case where the period T of oscillations is independent of the amplitude A. The study of approximatory methods to find the frequency-amplitude relationship of nonlinear oscillators is a very rich and challenging subject of applied mathematics which easily covers several hundred pages. For an extensive review of these methods, the reader is referred to the book of Nayfeh and Mook [7]. For our purposes however, we will in the following outline the very simple but effective way of tackling

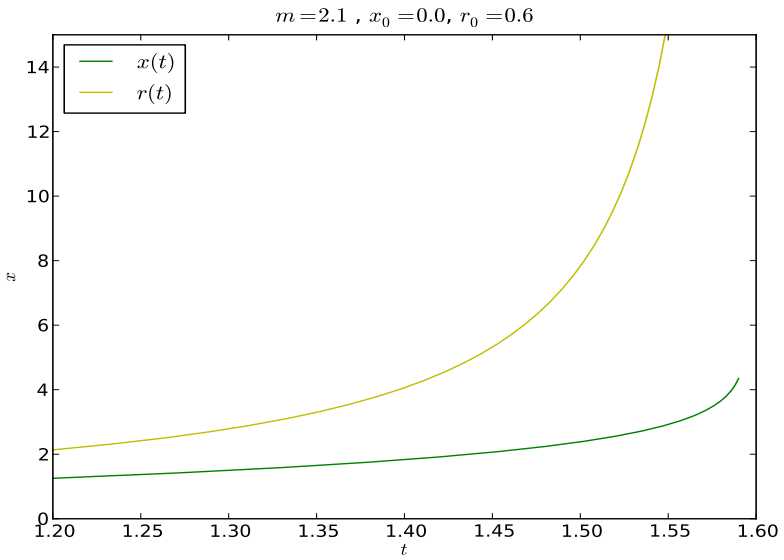

Figure 2.1.: Behaviour of log-return r and log-price x as function of time t: From eq. (2.11), we obtain $t_C \approx 1.594$. It is clearly visible that the price remains finite but $> x_0$, as expected for $m > 2$, while $r \to \infty$

this problem introduced by Mohazzabi [12] which makes use of the energy function of the oscillator: The equation of interest reads

$$\frac{\mathrm{d}^2 x}{\mathrm{d}t^2} = -\gamma x(t)^n, \quad n > 1, x(t) > 0. \tag{2.16}$$

where the mass M has been chosen to be equal to one to keep the notation as simple as possible. The corresponding total energy function of this oscillator can be written as

$$\frac{\dot{x}^2}{2} + V(x) = E \tag{2.17}$$

where the identity $E = V(A) = \frac{\gamma}{n+1} A^{n+1}$ with A being the amplitude holds. Eq. (2.17) can be rewritten as

$$\mathrm{d}t = \pm \left(\frac{1}{2E}\right)^{1/2} \frac{\mathrm{d}x}{\sqrt{1 - \frac{V(x)}{E}}} \tag{2.18}$$

so that the period of oscillations can be found by integration

$$\frac{T}{4} = \left(\frac{1}{2E}\right)^{1/2} \int_0^A \frac{\mathrm{d}x}{\sqrt{1 - \frac{V(x)}{E}}} \tag{2.19}$$

In our case, $V(x) = \frac{\gamma}{n+1}x^{n+1}$, so that we are looking for a solution of the equation

$$\frac{T}{4} = \left(\frac{1}{2E}\right)^{1/2} \int_0^A \frac{\mathrm{d}x}{\sqrt{1 - \frac{\gamma x^{n+1}}{(n+1)E}}} \tag{2.20}$$

which we do by considering the substitution

$$x = \left(\frac{E(n+1)}{\gamma}\right)^{\frac{1}{n+1}} \cdot (\sin(\Theta))^{\frac{2}{n+1}} \tag{2.21}$$

$$\Rightarrow \frac{\mathrm{d}x}{\mathrm{d}\Theta} = \left(\frac{E(n+1)}{\gamma}\right)^{\frac{1}{n+1}} \frac{2}{n+1} \cos(\Theta)(\sin(\Theta))^{\frac{2}{n+1}-1} \tag{2.22}$$

This can be simplified[1] to finally obtain[2]

$$\omega = \sqrt{\frac{\gamma\pi}{2(n+1)}} \cdot \frac{\Gamma(\frac{n+3}{2(n+1)})}{\Gamma(\frac{n+2}{n+1})} A^{\frac{1}{2}(n-1)} \tag{2.23}$$

Note that the identity $z\Gamma(z) = \Gamma(z+1)$ has been utilized in the last step. Figure 2.2 illustrates the dynamic behavior of this nonlinear frictionless oscillator.

There is a very nice oscillator picture that comes to mind related to the current financial crisis: Let us imagine a rod that is mounted on a slide that can move along a rail. The task is now to stabilize the system in the labile rest position which is a very prominent task in graduate engineering courses known as the inverse pendulum. Of course, the most efficient way to keep the pendulum in the desired position is to make only very little but frequent 'white noise'-like moves as too large movements will ultimately perturbate the pendulum from remaining at the labile rest position very much like a wire dancer trying to prevent himself from falling down. What has happened in the first few months following the outbreak of the financial crisis however is exactly the opposite: Almost any central reserve bank in the world has lowered the prime rate to a de facto 0% level and huge financial support packages and cash injections have been adopted by the major goverments in the world with the intention to provide extra liquidity in an otherwise sold out market with no market participator willing to lend money anymore to anybody. Although these steps are understandable and logic on first sight and have been 'hoorayed' by the overwhelming majority of economists, the analogy to the inverse pendulum should teach us some awareness for the possible dangers of such huge external stimuli since too large movements might as well destabilize the system as a whole[3].

[1] using $\int_0^{\pi/2}(\sin(\Theta)^{\frac{2}{n+1}-1}) = \sqrt{\pi}\frac{\Gamma(\frac{1}{n+1})}{2\Gamma(\frac{n+3}{2(n+1)})}$

[2] since $T = 2\pi/\omega$

[3] let alone that the monetary policy of almost every national bank in the western world and also the abolishment of the gold standard (Bretton Woods System) in 1973 have led to a more than remarkable increase

In blatantly simple words, the problem that the system itself is deficient will not be cured by interventions from the outside and moreover severe corrections and system inherent crashes will only be postponed.

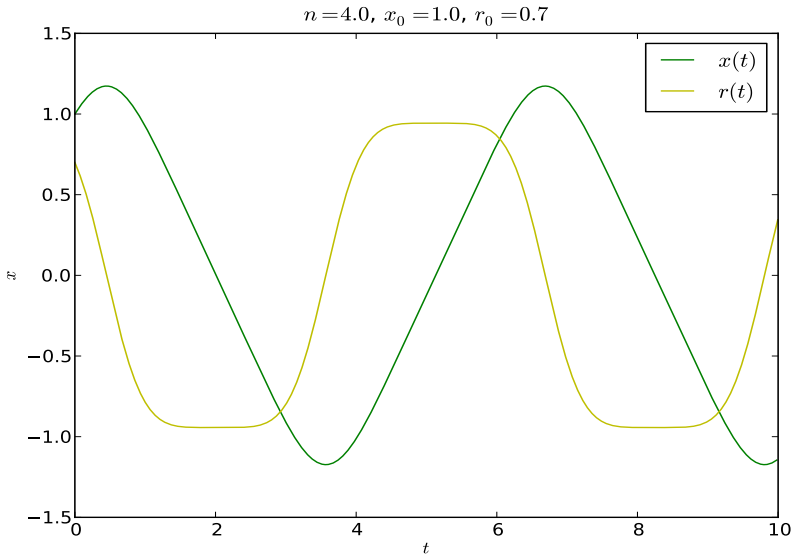

Figure 2.2.: Behaviour of log-price $x(t)$ and log-return $r(t)$ in the case $\alpha = 0$.

2.2.3. Case $\alpha \neq 0$, $\gamma \neq 0$

This case introduced in 2002 by Ide and Sornette [6] now unites the features we have unraveled so far which means that one will observe an interplay between singular and oscillatory behaviour. Moreover, it is clear that the oscillations will have their frequency increased with time since the amplitude, i.e. the price increases with time. In the following, we will outline the general features of the model in dependence of the cooperation parameter m and the coefficient α of the 'bubble term'.
For a general hint about how this model will behave as t_C is approached, we modify Mohazzabi's exact solution (2.23) for the frequency amplitude relation of the nonlinear oscillator by substituting $A = x(t)$ to obtain (with $x(t)$ taken from eq. (2.13))

$$\omega(t) = \sqrt{\frac{\gamma\pi}{2(n+1)}} \cdot \frac{\Gamma(\frac{n+3}{2(n+1)})}{\Gamma(\frac{n+2}{n+1})} \cdot \left[x_0 + C \left((1 - \frac{t}{t_C})^{\frac{m-2}{m-1}} - 1 \right) \right]^{\frac{n-1}{2}} \tag{2.24}$$

One thus finds two different behaviors of the frequency as the critical time t_C is approached:

of the amount of money in circulation and thus a looming inflation making the value of the money we own and spend a rather fragile quantity [15]

- $1 < m < 2$: $\omega \to \infty$
- $m > 2$: $\omega \to 0$

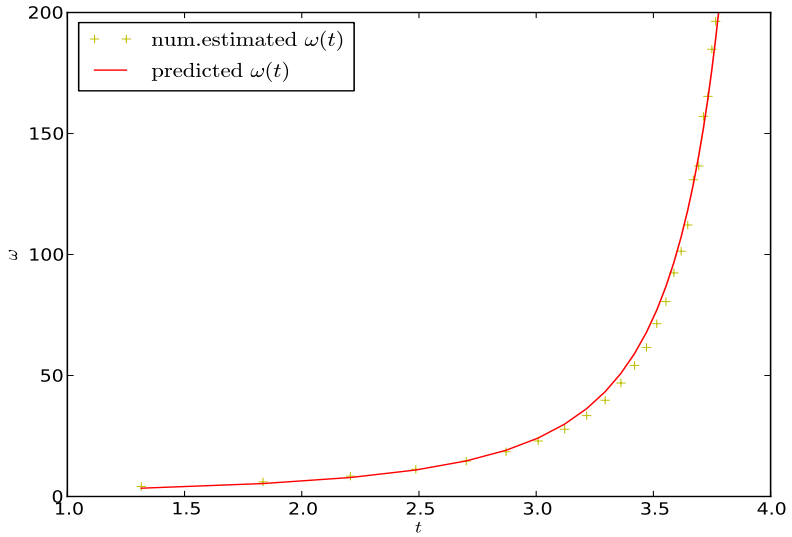

Figure 2.3.: Comparison of theoretical prediction according to eq. (2.24) (solid red line) and a comparably rough numerical estimate of the local frequency $\omega(t)$ (yellow crosses). Estimation of $\omega(t)$ is done by considering the difference of two consecutive zeros (z_{i+1}, z_i) of the log-price trajectory $x(t)$. The resulting time interval is then regarded as an estimated value of $T/2$ at $t = \frac{z_{i+1}-z_i}{2}$, so that $\omega = \frac{2\pi}{T}$ can be calculated as an approximation for $\omega(t)$.

$1 < m < 2$, $\alpha > 0$: Looking back at eqs. (2.10) and (2.12), it is clear that both expressions diverge if $t \to t_C$ since $r(t)$ diverges for any $m > 1$ and for $1 < m < 2$, $x(t) \propto (t_C - t)^{-z}, \quad z > 0$. As one can see in figure (2.4), the log-price remains relatively stable around its initial value for a comparatively long time, before the oscillations become more and more frequent as t progresses, as expected because of eq. (2.23). Also, the expected power law behaviour of the envelop of $x(t)$ can be observed. However, one has to keep in mind that the actual values of z and t_C might have been altered in comparison to section 2.2.1 since we are not neglecting the oscillatory component anymore. In [6], it is reported that the inclusion of the oscillatory term is correcting z downwards, namely the expected value of $(m-2)/(m-1) \approx -2.33$ for the choice $m = 1.3$ is countered by a numerically estimated exponent of -1.5.

$1 < m < 2$, $\alpha < 0$: When looking at the equation of the Sornette-Andersen model, it is clear that (the sign of) α models the nature of the feedback of the log-return on itself. If $\alpha > 0$, then there is a self-reinforcement meaning that higher returns in the past automatically lead to a higher growth rate of the return and thus to higher prices in the futute. From that, it is obvious that exactly the converse holds if $\alpha < 0$. The effect is illustrated in figure (2.5).

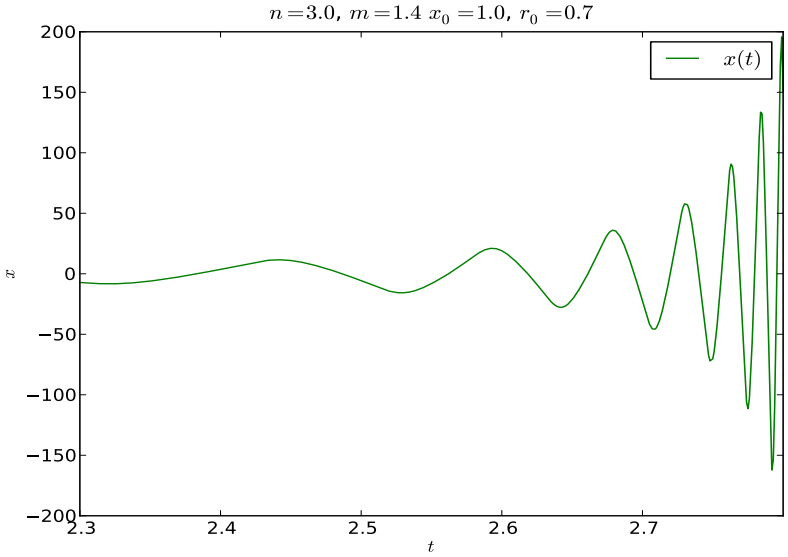

Figure 2.4.: Numerical solution of eq. (2.8) for the indicated parameters with $t_C \approx 2.8$, $\alpha = 1$, $\gamma = 10$. Note that $\omega \to \infty$ as t_C is approached in agreement with equation (2.24).

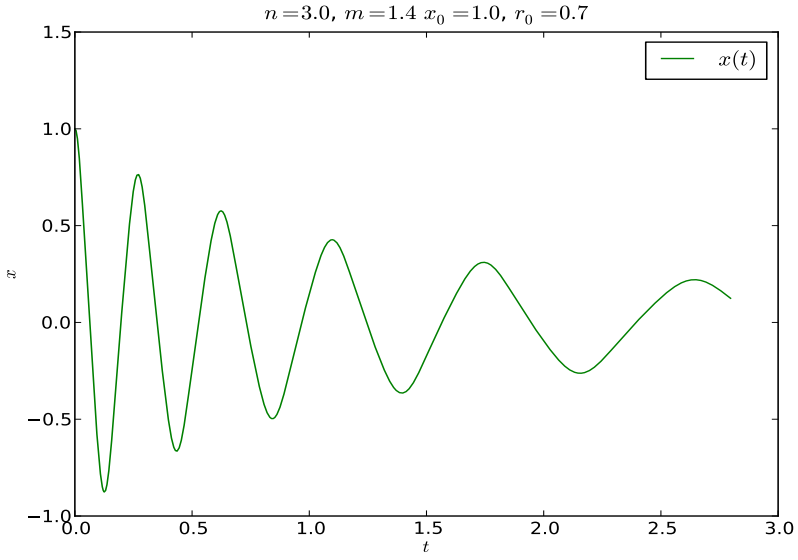

Figure 2.5.: The Ide-Sornette model for negative α: The feedback is now negative and thus self-downsizing. Note also that $\gamma = 1000$ in this picture while in fig. 2.4 $\gamma = 10$.

$m > 2$, $\alpha > 0$: Since we are interested in stock market *crashes* and *bubbles*, we will in this work not focus on the decaying regime ($\alpha < 0$) introduced in the preceding paragraph for this regime corresponds to *anti-bubbles*, a term coined in various different articles ([17], [16]). What can be learnt from numerical simulations of the case $m > 2$, $\alpha > 0$ is that the system qualitatively exhibits the same features as the Sornette-Andersen model ($\gamma = 0$) which is quite clear since the singular term dominates the oscillatory term at least in the vicinity of t_C. That

means that we expect the log-price $x(t)$ to remain finite while the growth rate of x, i.e. the return r explodes over all limits, so that we expect

$$x(t) \propto x_C - A(t_C - t)^{\frac{m-2}{m-1}}$$

with A being a constant factor. Also a striking feature of the system is the influence of γ: The larger its absolute value is, the more oscillations can be observed prior to t_C and the closer $r_0 = r(t = 0)$ to the unstable fixed point (0,0) of the dynamical sytem

$$\begin{aligned} \dot{x} &= r \\ \dot{r} &= \alpha r|r|^{m-1} - \gamma x|x|^{n-1} \end{aligned} \tag{2.25}$$

the more oscillations occur before the system is finally driven to the critical point [6]. This is illustrated by the following figures:

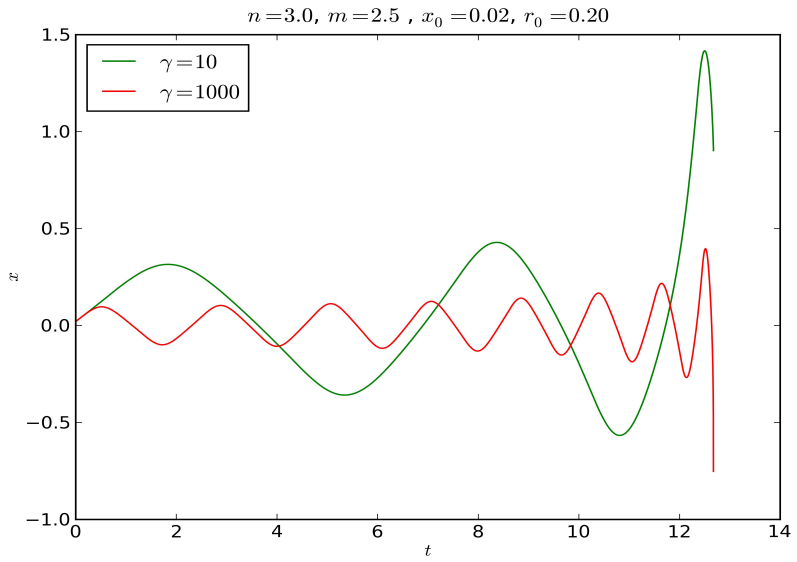

Figure 2.6.: The Ide-Sornette model for two mutually different values of γ and equal choice of $r_0 = 0.2$, as indicated in the graph ($\alpha = 1$, $t_C \approx 12.7$). It is also noteworthy that the oscillation simply stops as t_C is reached reflecting our prediction that $\omega \to 0$ since $m > 2$.

2.3. Summary

To conclude this chapter, a short recapitulation of the most important features of the Ide-Sornette model shall be given.

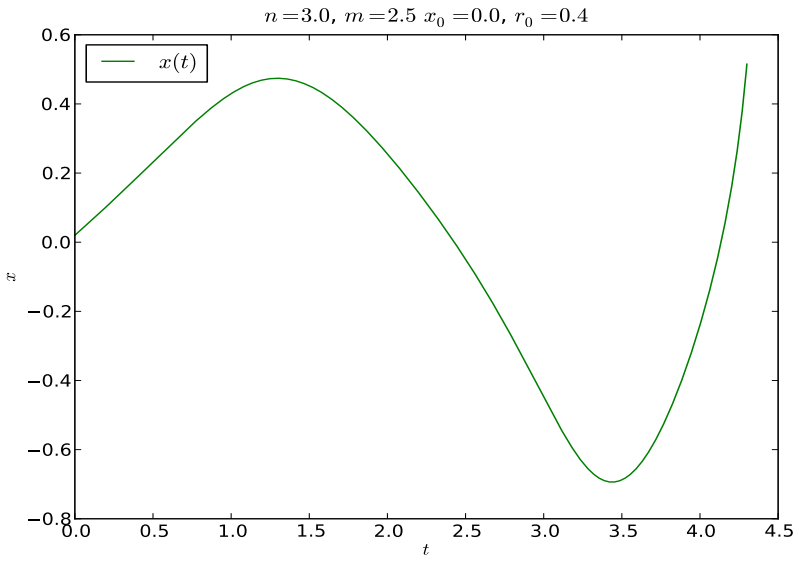

Figure 2.7.: The effect of a choice of $r_0 = 0.4$ which is farther away from (0,0): As expected, we observe less oscillations before reaching $t_C \approx 4.4$.

- The Ide-Sornette model was introduced in 2002 as a model exhibiting prominent features of empirical time series such as the formation of bubbles, crashes and the leverage effect although only assuming the existence of two classes of investors: 'trend followers' and 'fundamental value investors'.

- The model is an autonomous differential equation of second order in time which reads $\ddot{x} = \alpha \left|\dot{x}\right|^m - \gamma \left|x(t)\right|^n$ where $x = \ln p$. The four parameters α, γ, n and m are real numbers, two of which are inversely proportional to the market liquidity L. n measures the degree of nonlinearity of the oscillatory part of the equation, m quantifies the willingness of the market participants to cooperate.

- The fundamental new feature of this equation besides its nonlinearity is the presence of a second derivative of the log-price with respect to time, i.e. the presence of inertia which ultimately generates oscillations.

- The key to the understanding of the influence of the oscillatory part of the equation to the overall dynamics is the frequency-amplitude relation of nonlinear oscillators which is known to behave according to $\omega \propto A^{\frac{1}{2}(n-1)}$. This is the case if $\alpha = 0$.

- The case $\gamma = 0$ (with $B = \frac{\mathrm{d}x}{\mathrm{d}t}$ and stochasticity, see Chapter 3) is known as Sornette-Andersen model of financial bubbles, an example of a very simple equation that can feature a finite-time singularity.

- The parameter m determines the nature of the price dynamics as the critical time t_C is approached where two different regimes exist: For $1 < m < 2$, the frequency of oscillations grows to infinity as $t \to t_C$ whereas for $m > 2$, ω tends to zero.

- The origin of the phase space acts as unstable fixed point and the initial position of the system in the phase space considerably influences the dynamics: The closer the system initially is to (0,0), the more oscillations can be observed prior to crash.

- The sign of α determines the general regime, i.e. bubble or anti-bubble, the absolute value of γ influences the number of oscillations before crash, the greater γ the more oscillations occur.

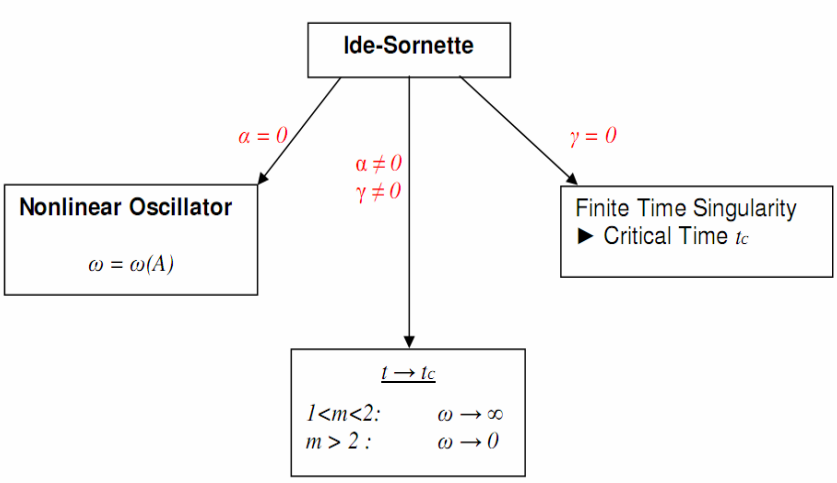

Figure 2.8.: Schematic illustration of the Ide-Sornette model and its dynamic components

3. Mathematical Treatment of Random Fluctuations

> So much of life, it seems to me, is determined by pure randomness.
>
> Sydney Poitier

In this chapter, we will introduce the necessary basics of stochastic calculus that are required for this work. The most important stochastic processes, Brownian motion (the Wiener process) and the Brownian motion with mean-reversion (Ornstein-Uhlenbeck process) will be introduced and we will discuss the difference between additive and multiplicative noise which is fundamental for later research questions concerning the stochastic Ide-Sornette model. The important Lamperti transform, which will be used in the second part of this thesis, is introduced along the way as a consequence of the lemma of Itô. The discussion in this chapter mainly follows the presenations by Horsthemke and Lefever [20] and van Kampen [21].

3.1. Fundamentals of Stochasticity and Stochastic Calculus

Stochastic calculus has evolved from man's desire to describe nature, i.e. from physics. The most prominent example for a natural phenomenon giving rise to a stochastic differential equation (SDE) is the thermal motion of a particle (Brownian[1] motion). The theoretical description followed by Einstein, Smoluchovski and Langevin (see [19] and references therein) in early 20th century. Langevin considered an equation of motion for the position $x(t)$ of the

[1] after Scottish botanist Robert Brown's (1773 - 1858) discovery in 1827

Brownian particle while Smoluchovski and Einstein investigated

$$m\frac{\mathrm{d}v}{\mathrm{d}t} = \gamma v + \xi(t) \tag{3.1}$$

with a systematic viscous friction force $-\gamma v$ and a randomly fluctuating force $\xi(t)$. Nonetheless, eq. (3.1) is referred to as 'Langevin equation' in standard literature. Looking at this equation, one can note several things: Firstly, the randomly fluctuating $\xi(t)$ which is called 'noise' to appreciate its randomness is *added* on the right-hand side of eq. (3.1) and thus, we call it *additive noise*. As we will point out later in this chapter, this has important consequences for the whole system. Secondly, it is not yet clear what noise exactly is supposed to mean. We will consequently define some fundamental variables to describe and characterize noise in the following while, for our purposes, it always holds that $\langle \xi(t) \rangle = 0$: Let us define the *correlator* as

$$\langle \xi(t)\xi(t') \rangle = f(t'-t) \tag{3.2}$$

To characterize noise, one typically uses the two integrals of (3.2):

$$D = \frac{1}{2}\int_0^\infty \langle \xi(t)\xi(t+z) \rangle \, \mathrm{d}z, \tag{3.3}$$

and

$$\tau = \frac{1}{D}\int_0^\infty z \, \langle \xi(t)\xi(t+z) \rangle \, \mathrm{d}z \tag{3.4}$$

with D being called the 'noise strength' and τ named 'correlation time'. For computer-based simulations in complex system theory, finance and economics, *white noise* is usually employed (for reasons of computability) for which the correlator reads

$$\langle \xi(t)\xi(t') \rangle = 2D\delta(t'-t) \tag{3.5}$$

so that, no matter how close t and t' may be, they are always statistically independent. Any other type of noise is called *coloured noise* which shall not be further investigated in this thesis. In quantitative finance, the white noise assumption for market fluctuations can be justified from both, the theoretical and the empirical point of view: Any market consists of mutually independent traders and investors that follow their own strategies (however, mostly driven by greed and fear which makes great sense from an evolutionary point of view: Greed boosting motivation and fear providing the sensitivity for potentially dangerous situations). That means that, in a normal regime, the superposition of the trading decisions of the market participants forms some background noise that ornaments the overall market behavior. Looking at the price data of a stock of one's choice of any trading day, one will find that the white noise

assumption is in very good agreement with the actual behavior of prices and indexes (as weighted averages of prices) since thousands or millions of independent trading orders - which can be placed within seconds due to computer trading - make the price fluctuate sufficiently fast. An important feature of SDEs such as equation (3.1) is that sample solutions are shaped

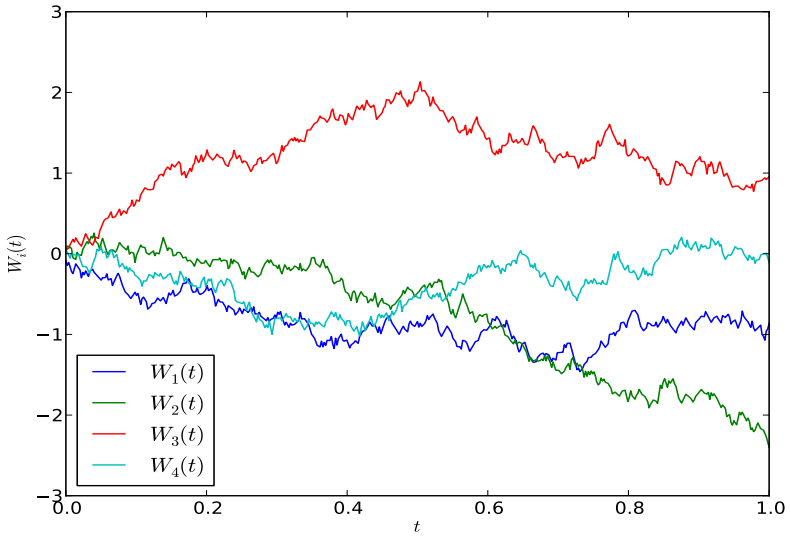

Figure 3.1.: Four sample Wiener paths

by the realization of the white noise $\xi(t)$. This implies that, unlike the in the ODE[2] case, one has to look at ensembles of solution paths rather than single sample paths. This is a crucial difference compared to the deterministic case since, after all, knowing the solution of an ODE tells you all about the system's behavior if the initial conditions are specified. Moreover, it turns out that solving SDEs requires a concept of integration of stochastic processes just like solving ordinary differential equations requires a concept of 'normal integration'. That is, one needs some standard about integrating processes that are nowhere differentiable but continuous everywhere. Hence, let us consider the equation

$$\mathrm{d}X_t = f(t, X_t)\mathrm{d}t + g(t, X_t)\mathrm{d}W_t \tag{3.6}$$

in which $f(t, X_t)$ is called *drift term* while $g(t, X_t)$ is called *diffusion term*. Equivalently, we can write (3.6) as

$$X_t = X_0 + \int_0^t f(s,X_s)\mathrm{d}s + \int_0^t g(s, X_s)\mathrm{d}W_s. \tag{3.7}$$

W_t denotes a standard Wiener process which is characterized by $\langle \mathrm{d}W_t \rangle = 0$ and $\mathrm{d}W_t = \xi(t)\mathrm{d}t$ with $\xi(t)$ being delta-correlated Gaussian white noise. Note that eq. (3.7) requires two

[2]ordinary differential equation

mutually different integrations: The first integral on the right-hand side involves a standard Lebesgue integration (which is a generalization of the Riemann integral) whereas the second one apparently calls for a definition of stochastic integration which we will promptly deliver in the graphic spirit of [19]: The white noise $\xi(t)$ causes the process X_t to jump. It is therefore debatable at which point of this jump process $g(t, X_t)$ has to be evaluated. If $g(t, X_t)$ is evaluated at the beginning of the jump, then the second integral in eq. (3.7) is called *Itô integration* and the process X_t, $t \geq 0$ is consequently called Itô[3] process, if $g(t, X_t)$ is evaluated in the middle of the jump, the above integral is called *Stratonovich integral*[4] thus giving rise to the corresponding Stratonovich process. As a natural consequence, the integrations yield different results according to the choice one has taken and, to use the words of van Kampen, eqs. (3.6) and (3.7) are only 'pre-equations' [21] since their full message is only delivered once we have specified which type of integration to use. It should also be kept in mind that, once specified whether Itô or Stratonovich interpretation applies to the SDE, two mutually different Fokker[5]-Planck[6] equations[7] (FPEs) arise that can be transformed into one another and thus, the same conclusions about the whole stochastic system X_t can be drawn [21]! Hence, we give, for the sake of completeness, the FPE corresponding to (3.6) in the Itô sense of stochastic integration and will stick to Itô's definition of stochastic integration from this point on to avoid any possible confusion:

$$\frac{\partial}{\partial t}p(x,t) = -\frac{\partial}{\partial x}(f(x,t) \cdot p(x,t)) + \frac{1}{2}\frac{\partial^2}{\partial x^2}(g(x,t) \cdot p(x,t)) \tag{3.8}$$

where x denotes the actual value of the random process X_t. The SDE of a process describes single paths of this process (which may be undestood as paths of single particles) whereas the corresponding FPE describes the behavior of an *ensemble* of particles that undergo the stochastic process (3.6). One is therefore free to analyze either SDE or FPE (or both). In the second part of this work, we will demonstrate this equivalence for an example from finance. Note that the FPE as it stands is a deterministic equation that does not contain any random expressions. The impact of the stochasticity is fully reflected by the purely probabilistic statement of the solution of the FPE since $p(x,t)$ is a probability density, a concept familiar to physicists from quantum mechanics ($|\psi|^2$). Also worth noting is the fact that the FPE (3.8) turns into the familiar heat equation for a vanishing drift term, hence its alias 'diffusion equation':

$$\partial_t u(x,t) = a\partial_{xx} u(x,t) \tag{3.9}$$

[3] Kyoshi Itô, Japanese mathematician, 1915-2008
[4] after Ruslan Leont'evich Stratonovich (1930-1997), Russian physicist and engineer
[5] Adriaan Daniel Fokker (1887-1972), Dutch physicist and musician
[6] Max Karl Ernst Ludwig Planck (1858-1947), German physicist, Nobel price 1918
[7] mathematicians rather prefer the term Kolmogorov equation

The real constant a is the heat conductivity. The solution of eq. (3.9) is also referred to as heat kernel. For the sake of completeness, we give the transformation formula from Itô to Stratonovich for the diffusion process (3.6) understood as Itô SDE [20]:

$$\mathrm{d}X_t = \left[f(t, X_t) - \frac{\sigma^2}{2} g'(X_t) g(X_t)) \right] \mathrm{d}t + g(t, X_t) \mathrm{d}W_t \tag{3.10}$$

Note that the drift term changes while the diffusion term is unaffected and that both interpretations coincide if we deal with additive noise. As we have seen so far, stochastic calculus has some peculiarities. The lemma of Itô is one of the most prominent results of research conducted in this field. It is often referred to as *stochastic chain rule* and consequently, it answers the question of what happens when wanting to change variables in a SDE.

Lemma 1. *Be $Y_t = h(t,X_t)$ some relation to change variables in the Itô process (3.6). Then,*

$$\mathrm{d}Y_t = \left(\frac{\partial h(t,X_t)}{\partial X} f(t,X_t) + \frac{\partial h(t,X_t)}{\partial t} + \frac{1}{2} \frac{\partial^2 h(t,X_t)}{\partial X^2} g^2(t,X_t) \right) \mathrm{d}t + \frac{\partial h(t,X_t)}{\partial X} g(t,X_t) \mathrm{d}W_t \tag{3.11}$$

is also an Itô process given that $h(t,X_t)$ exists and is twice continuously differentiable.

A very important example of application is the *Lamperti transform* which transforms multiplicative noise into additive noise. If the diffusion coefficient, i.e. the prefactor $g(t,X_t)$ in the process (3.6) is of the general form σX_t^β where $\beta > 1$, then the corresponding Lamperti transformation reads

$$Y_t = \frac{1}{\sigma(1-\beta)} X_t^{1-\beta} \tag{3.12}$$

Transforming multiplicative noise into additive noise can be advantageous for numerical simulations as well as for the analytics as it may be possible to find an explicit analytical solution of the SDE for Y_t which then provides the solution in terms of X_t.

3.2. Ornstein-Uhlenbeck process

Besides the standard Wiener process introduced in the previous section, the Ornstein-Uhlenbeck process is one of the most important processes in mathematical finance. It is often referred to as OU process or mean-reverting Brownian motion. This process will be used in Part II of this thesis where it will be part of the analytical solution of a special SDE. The OU process is

defined over the stochastic initial value problem

$$\mathrm{d}X_t = \Theta(\mu - X_t)\mathrm{d}t + \sigma \mathrm{d}W_t, \quad X(0) = a. \tag{3.13}$$

The real parameters μ, Θ and σ have the following meaning [35]:

- μ is the mean-reversion level. Thus, if $X_t > \mu$, the drift term of the OU process is negative (given $\Theta > 0$) which will draw the process down (towards μ) and vice versa.
- Θ is the mean-reversion rate which affects the level of 'gravity' of the mean value μ. If Θ is large, then the process will fluctuate in only a very tight corridor around μ.
- The parameter σ affects the level of influence of the random Brownian increment $\mathrm{d}W_t$

There is also an explicit solution of the process (3.13) which reads

$$X_t = ae^{-\Theta t} + \mu(1 - e^{-\Theta t}) + \int_0^t \sigma e^{\Theta(s-t)} \mathrm{d}W_s. \tag{3.14}$$

We will need this process in the second part of this thesis to prove the explicit closed form solution of the CIR-CEV model. An illustration of the process is provided in figure 3.2.

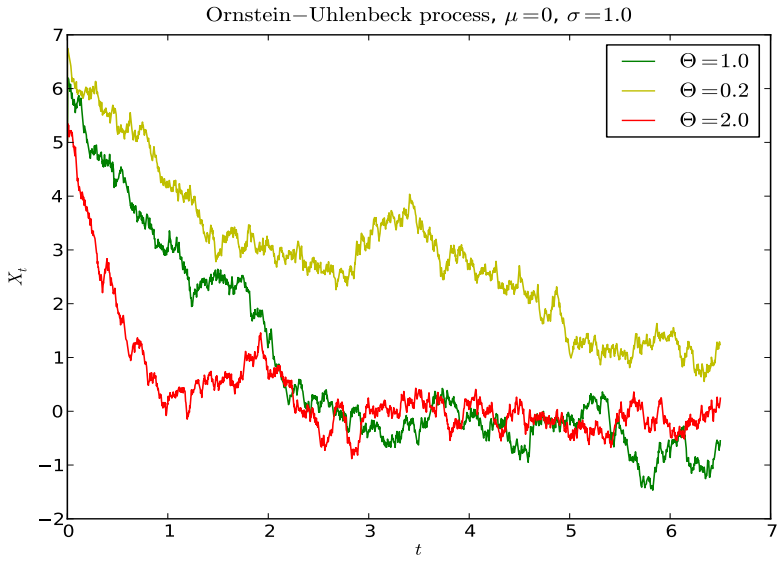

Figure 3.2.: Three OU processes with different mean-reversion rates (to $\mu = 0$) each

3.3. Stationary Solution of the FPE

In this paragraph, the reader is given an overview on how a stationary solution of a FPE can be derived and how it is defined. This concept will be needed to point out the difference between additive and multiplicative noise.

Remembering quantum mechanics, one could ask the question whether the solution of the FPE of a system described by

$$\mathrm{d}X_t = f(X_t)\mathrm{d}t + \sigma g(X_t)\mathrm{d}W_t \tag{3.15}$$

that means its probability density $p(x,t)$, can be stationary, i.e. invariant under elapsing time ($\partial_t p(x,t) = 0$). As is shown in great detail in [20], this question can be adressed by writing the FPE as continuity equation, so that

$$\partial_t p(x,t|x_0,0) + \partial_x J(x,t|x_0,0) = 0 \tag{3.16}$$

where we have defined the probability current density

$$J(x,t|x_0,0) = f(x)p(x,t|x_0,0) - \frac{\sigma^2}{2}\partial_x g^2(x)p(x,t|x_0,0) \tag{3.17}$$

$p(x,t|x_0,0)$ denotes the probability density at position x at time t given the initial conditions x_0 and $t_0 = 0$. The condition for $p(x,t)$ to be stationary, that is, explicitly time-independent, reads $\partial_t p(x,t) = 0$ and thus, $\partial_x J(x,t) = 0$. The stationary probability density $p_s(x)$ is then given by (refer to [20] for a detailed calculation)

$$p_s(x) = N g^{-2}(x) \cdot \exp\left(\frac{2}{\sigma^2}\int \frac{f(x)}{g^2(x)}\right)\mathrm{d}x \tag{3.18}$$

N is a normalization factor since $\int p_s(x)\mathrm{d}x \stackrel{!}{=} 1$. Furthermore, employing statistical physics, we have the following theorem: Be $g(x) > 0$ for any x arbitrarily drawn from the state space Ω. Then, a solution $p(x,t)$ of the FPE with arbitrary initial condition $p_0(x_0, 0)$ converges to $p_s(x)$ for $t \to \infty$ [20] and thus,

$$p_s(x) = \lim_{t\to\infty} p(x,t). \tag{3.19}$$

3.4. Additive and Multiplicative Noise

In this section, the difference between additive and multiplicative noise to the behavior of a system will be explained. The explanation follows again [20] in that we look at a system that is described in the 'non-noisy' case by the deterministic differential equation of the form

$$\dot{x} = h(x) + \lambda g(x) \tag{3.20}$$

λ is a dimensionless system parameter coupled to the system. For a better illustration, one may think of a biochemical reaction far from equilibrium between two substances, X and Y with the aid of two catalysts, A and B. Obviously, the total number $N = X + Y$ of particles in the system is conserved (the system is closed). The behavior of the fraction $\overline{X} = X/N$ can be described by eq. (3.20) and furthermore, λ can be expressed as a function of A and B so that it basically reflects a weighted ratio of the catalysts. The stable states of the system are thus the zeros of the right-hand side of (3.20) or, equivalently, one may write

$$\dot{x} = -\partial_x V(x), \quad V(x) = -\int (h(x) + \lambda g(x)) \mathrm{d}x. \tag{3.21}$$

The maxima (minima) of $V(x)$ are the unstable (stable) steady states of the system. What can be said about $p_s(x)$ in the presence of additive noise? It can be stated that the stationary probability density will consist of sharp delta peaks located at the positions of the minima of the potential well $V(x)$. The presence of additive white noise can then be translated in a graphic picture according to [20] as follows: Consider a ball in the potential $V(x)$ subjected to additive noise. The ball will jiggle around its likeliest position, i.e. the minimum of $V(x)$. As a consequence, the sharp peaks of $p_s(x)$ will widen reflecting the less certain whereabouts of the ball. The resulting probablility density is thus a consequence of the interplay of the organizing influence of $V(x)$ and the disorganizing influence of the noise $\xi(t)$. Thus, considering the case $V(x) = c, \quad c \in \mathbb{R}$, the ball would simply undergo a Brownian motion.
Indeed, it is possible to show for additive noise that the highest maximum of $p_s(x)$ coincides with the deepest potential well for all σ^2 by the following considerations [20]: Defining the auxiliary function

$$U(x) = \int \frac{f(x')}{g^2(x')} \mathrm{d}x'$$

to rewrite the stationary probability density as

$$p_s(x) = N \exp\left(\frac{2}{\sigma^2} U(x_m)\right) \exp\left[\frac{2}{\sigma^2}\left(U(x) - U(x_m) - \sigma^2 \ln g(x)\right)\right] \tag{3.22}$$

where x_m is the location of the highest maximum of $U(x)$, it then follows for that

$$U(x) = -\frac{V(x)}{c^2}. \tag{3.23}$$

The assumption of small white noise, $\sigma^2 \ll 1$, has been used to neglect the last term in the second exp function in eq. (3.22).

If however the influence of the external noise depends on the system itself, that is, if we deal with multiplicative noise, the deterministic state that gives rise to a maximum in $p_s(x)$ is not necessarily the one with the deepest potential well in the deterministic framework, i.e. multiplicative noise *can* change the most likely (most stable) configurations of the system while additive noise cannot. Keeping our vivid picture of the ball moving around in a potential landscape, these considerations can be summarized as follows:
Additive noise is shaking the ball around while multiplicative noise makes the landscape change randomly in that it makes the ground move up and down randomly *in addition* to the shaking of the ball. Hence, the most interesting type of noise clearly is multiplicative noise since it is able to qualitatively change the shape and therefore the steady states of a system. In [20], it is proposed that the best indicator for this qualitative change of behaviour is indeed $p_s(x)$. We remember equation (3.18) and write $g^{-2}(x) = \exp(-2\ln g(x))$ to obtain

$$p_s(x) = N \exp\left[\frac{2}{\sigma^2}\left(\int^x \frac{f(u)}{g^2(u)}\mathrm{d}u - \sigma^2 \ln g(x)\right)\right] \tag{3.24}$$

and define the *stochastic potential* as

$$\mathcal{V}(x) = \int^x \frac{f(u)}{g^2(u)}\mathrm{d}u - \sigma^2 \ln g(x) \tag{3.25}$$

since the extrema of $p_s(x)$ are the extrema of $\mathcal{V}$ because of the strict monotony of the exp function. It follows then that the extrema of $p_s(x)$ are given by the equation

$$f(x) - \sigma^2 g'(x)g(x) \stackrel{!}{=} 0 \tag{3.26}$$

so that we obtain for our example from the beginning (3.20):

$$h(x) + \lambda g(x) - \sigma^2 g(x)g'(x) = 0 \tag{3.27}$$

From this equation, it is clear that the change of location of the deterministic steady states can be neglected for $\sigma^2 \ll 1$, i.e. for 'small' white noise which in fact means a small variance. Thus

'valleys stay valleys and mountain tops stay mountain tops' [20]. On the other hand, it can be seen that a qualitative change will occur if the second term in (3.27) cannot be neglected that is, if σ^2 is sufficiently large and $g(x)$ is suitably nonlinear. The following example should clarify the matter.

Example: Occurence of a Noise-Induced Critical Point

The aim of this section is to apply the results of the previous sections to a model and to verify that multiplicative noise can indeed change the behaviour of a system drastically. The most instructive example to demonstrate noise-induced transitions is of course the occurence of such a transition in a system that deterministically is incapable of featuring any transition. We will thus stick to the model [22]

$$\dot{x} = \alpha - x + \lambda x(1-x), \quad x \in [0,1], \alpha \in \mathbb{R} \tag{3.28}$$

that has some relevance in theoretical biology and chemistry which we will for our purposes not care about. λ is a parameter that is coupled to the state of the environment of the system. In the following, we will investigate the consequences of a rapidly fluctuating value of λ, that is, we will set $\lambda_t = \lambda + \sigma\xi(t)$ in the deterministic equation (3.28). The Stratonovich SDE corresponding to eq. (3.28) can be transformed into an identical SDE in the Itô sense (see eq. (3.10)) to finally obtain

$$\mathrm{d}X_t = \left[\alpha - X_t + \lambda X_t(1-X_t) + \frac{\sigma^2}{2}X_t(1-X_t)(1-2X_t)\right]\mathrm{d}t + \sigma X_t(1-X_t)\mathrm{d}W_t \tag{3.29}$$

which, because of relation (3.27), yields an expression for the extrema of $p_s(x)$ which reads

$$\alpha - x + \lambda x(1-x) - \frac{\sigma^2}{2}x(1-x)(1-2x) = 0 \tag{3.30}$$

Without loss of generality, one can consider the deterministic case $\lambda = 0$, $\sigma = 0$ and $\alpha = \frac{1}{2}$ where the solution $x = \frac{1}{2}$ follows quickly as the only extremum. Introducing delta-correlated Gaussian white noise so that $\sigma \neq 0$, one obtains three extrema, namely

$$x_1 = \frac{1}{2}, \quad x_{2,3} = \frac{1}{2}(1 \pm \sqrt{1 - \frac{4}{\sigma^2}}) \tag{3.31}$$

as the solutions of the corresponding cubic equation. We can thus constate that, if $\sigma^2 < 4$, x_1 will be the only real - and therefore physically relevant - extremum. If however $\sigma^2 > 4$, one will observe three extrema with the former maximum x_1 being the minimum and x_2 and x_3 as two maxima symmetric to x_1. This noise-induced transition is illustrated qualitatively in fig. (3.3). It is remarked that most qualitative changes in a system's behavior occur upon a

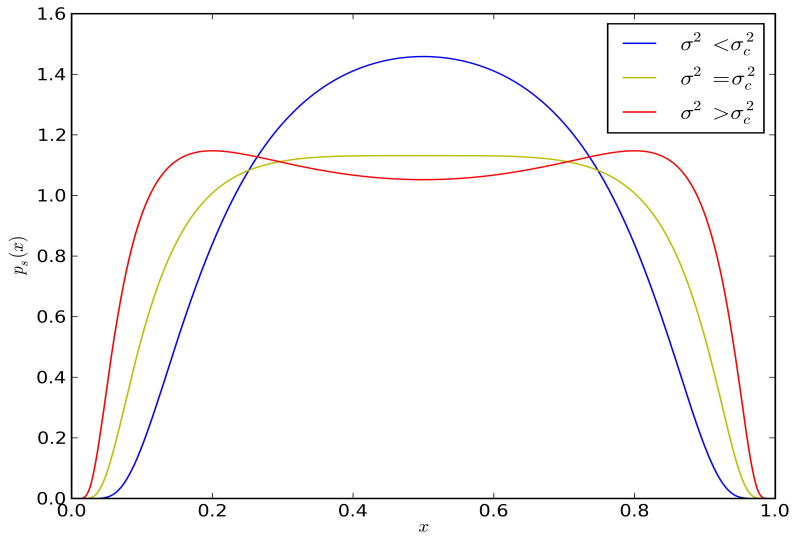

Figure 3.3.: The stationary probability density of (3.29), non-normalized. Note the qualitative change as σ^2 is increased.

change of a control parameter rather than a change of the noise amplitude. In spite of that, the general difference between additive and multiplicative noise is well-illustrated by this textbook example. To conclude, we shall name a few practical applications of this phenomenon that was introduced from a so far rather theoretical viewpoint. Kabashima and Kawagubo have extensively studied the occurence of noise-induced transitions in electrical circuits [24] while transitions of the kind introduced in this chapter have also been reported and studied in open chemical systems [25]. Very interesting from a physics perspective is the phenomenon of optical bistability reported by Graham and Haken [26] where laser light transmitted through a Fabry-Perot cavity filled with sodium vapour was investigated and shown to exhibit a hysteresis cycle when plotted versus the incident light [20]. And, last but not least, noise-induced transitions have been found to play an important role in theoretical biology and medicine, i.e. in predator-prey models of ecosystems and in models for the growth of tumors ([20] and references therein) to name only two.

4. The Stochastic Ide-Sornette Model

> With many calculations, one can win;
> with few one cannot.
>
> Sun Tzu,
> The Art of War

In this chapter, the Ide-Sornette model for financial markets will be extended towards multiplicative white noise. We will investigate the effects of this noise to the model and its components. This requires some technical preliminaries about numerics and stability in general and an introduction in the numerical simulation of nonlinear stochastic differential equations with a strong focus on the present problem will also be given along the way.

4.1. Introduction

Turning back to our model, we want to add a stochastic component in order to make it more realistic. Remembering that the model coefficients α and $\gamma \propto L^{-1}$, it is clear that they should fluctuate randomly depicting the behavior of the liquidity being transferred into or withdrawn from the market as investors decide whether they should enter or leave the market. It is therefore sensible to make the variables α and γ randomly fluctuating so that we can rewrite them as $\alpha_t = \alpha + \varepsilon_1 \xi_1(t)$ and $\gamma_t = \gamma + \varepsilon_2 \xi_2(t)$ where $\xi_i(t)$ is Gaussian delta-correlated white noise as defined in the previous chapter and ε_i are real numbers. We thus want to investigate a modified form of the Ide-Sornette model which reads

$$\frac{\mathrm{d}^2 x}{\mathrm{d}t^2} = \alpha_t \left| \frac{\mathrm{d}x(t)}{\mathrm{d}t} \right|^m - \gamma_t \left| x(t) \right|^n, \quad n, m > 1 \tag{4.1}$$

where it is stressed again that we refer to equation (4.1) and all its siblings considered in this thesis as SDE in the Itô sense. It is mathematical conventionalism[1] to rewrite such a stochastic equation in the form

$$\mathrm{d}\vec{X}(t) = a(t,\vec{X}_t)\mathrm{d}t + b(t,\vec{X}_t)\mathrm{d}\vec{W} \tag{4.2}$$

where $a \in \mathbb{R}^d$ and $b \in \mathbb{R}^{d\times m}$ with d being the space dimension and m being the dimension of the driving Wiener process. In our case $d = m = 2$ but this is not generally true since one can always think of any m dimensional Wiener process that acts on the equation of interest, no matter what dimension $\vec{X}$ lives in. For a very good illustration of such processes, the reader is requested to refer to [29]. Some rather easy calculation leads to

$$\mathrm{d}\begin{pmatrix} x(t) \\ r(t) \end{pmatrix} = \begin{pmatrix} r(t) \\ \alpha\,|r(t)|^m - \gamma\,|x(t)|^n \end{pmatrix}\mathrm{d}t + \begin{pmatrix} 0 & 0 \\ \varepsilon_1\,|r(t)|^m & -\varepsilon_2\,|x(t)|^n \end{pmatrix}\mathrm{d}\vec{W}(t) \tag{4.3}$$

where $\mathrm{d}\vec{W}(t) = (\mathrm{d}W_1(t), \mathrm{d}W_2(t))$. Unfortunately, there is no transform such that the diffusion matrix $b(t,X_t)$ has only constant entries, i.e. the Lamperti transform in several dimensions does not work.

4.2. Simulation of SDEs: Facts, Problems and Possibilities

The simulation of SDEs, both linear and nonlinear is a very active research area ([29], [32], [37], [36]) and a lot of work is still left to be done [31], especially in the nonlinear case and there particularly in cases of nonlinear diffusion coefficients that are irreducible to constants - as in the present model. To illustrate the issues when dealing with such simulations, we explicitly quote Gardiner [35]: 'Uninformed intuition can lead to completely meaningless results, excessive waste of time and even complete failure to solve the problem in question.' Obviously, 'uninformed intuition' refers to the misbelief that numerical schemes that are known to work well in a deterministic setting like the Runge-Kutta scheme, to name only one, are transferred to the stochastic setting without thorough reconsideration of the mathematical justification in terms of stochastic convergence and numerical stability. Note that all of what

[1] since the notation with differentials is the only one mathematically justified. Notations like the one given in eq. (4.1) can be found throughout the literature belonging to the intuitive but sloppy physicist's notation: Strictly speaking, the stochastic process X_t is nowhere differentiable and thus, notations like (4.1) are formally incorrect.

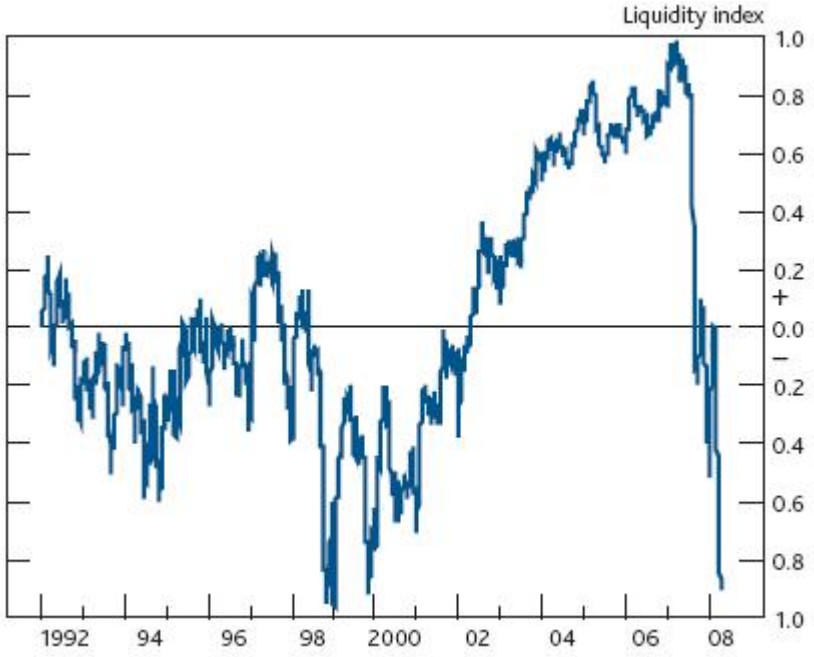

Figure 4.1.: Index of financial market liquidity as calculated by the Bank of England [49]. This index shows the number of standard deviations from the mean and is a simple unweighted average of nine liquidity measures (normalised on the period 19992004) [50]. Note the sharp nose-dive starting in mid-2007 indicating the severe upcoming crisis.

is said in this thesis refers to methods of *time discrete approximation* which means that the stochastic process $X(t)$ is evaluated only at discrete points of the time domain such that the time discretization $(t)_\delta$ of the time interval $[0,T]$ reads

$$0 = \tau_0 < \tau_1 < \cdots < \tau_N = T$$

so that in the simplest possible case, we have

$$\delta = \frac{T}{N}$$

and moreover

$$\tau_{n+1} - \tau_n = \delta.$$

To clarify these points, we have to define in a first step what stochastic convergence means:

Definition 1. *A numerical scheme is said to have* strong order of convergence *equal to β if there exists a constant $C \in \mathbb{R}$ such that*

$$\mathbb{E}(|X_T - X(\tau)|) \leq C\delta^\beta \tag{4.4}$$

where $\mathbb{E}$ *denotes the expectation value.*

In other words, the expectation value of the difference of the true value of the stochastic process X_T and its approximated value for any fixed τ can be characterized by the number β. Thus, the higher the strong order of convergence, the better our numerical result given a fixed discretization time stepsize δ. It should also be clear that the smaller δ is chosen, the better the numerical approximation, albeit at the cost of computing time. On the other hand, we have

Definition 2. *The notion* weak order of convergence *of order* β *means that there exists a constant* $C \in \mathbb{R}$ *for some class of functions* f *such that*

$$\mathbb{E}(f(X_T)) - \mathbb{E}(f(X(\tau))) \leq C\delta^{\beta} \tag{4.5}$$

at any fixed $\tau = k\delta \in [0,T]$ *and* δ *sufficiently small.*

In a nutshell, if one is looking for a good pathwise approximation of a given process, one needs a good strong order of convergence, whereas a good simulation of the statistical properties of a process requires a good weak order of convergence. This is clear if we remember that the most important quantities characterizing a distribution are its *moments* which are nothing different than special functions of the value of the random variable X_T. For example, the rth moment of a distribution (in a time discrete setting) is defined as

$$M_r = \frac{1}{N}\sum_{j=1}^{N}(x_j - \overline{x})^r.$$

We see that the first moment amounts to the average value of the variable. Similarly, we obtain the variance ($r = 2$), the skewness ($r = 3$) and the kurtosis ($r = 4$) of the distribution. Coming back to simulational issues, in [39] it is shown that the confusion among the scientific community concerning appropriate approaches to simulate SDEs is still prevailing, eventually leading to the publication of articles ([44], [45]) in renowned journals such as Physical Review Letters that feature numerical schemes that cannot be justified from a numerical point of view. Known issues when heuristically converting deterministic schemes to stochastic ones include:

- The solution is converging to the Stratonovich solution where it is supposed to converge to the Itô solution. This naturally gives rise to consistency problems.

- These heuristic adaptions can be shown to have a very low order of convergence regardless of the order of convergence of the underlying deterministic scheme [33]. The explanation for this behavior is that the only information about the driving white noise process is contained in the Brownian increment $\Delta W = W_{\tau_{i+1}} - W_{\tau_i}$ which is insufficient for any higher order convergence. On the other hand, a slow order of convergence, be it convergence in the strong or weak sense, can only be countered by choosing a very small discretization step size δ which leads to considerably higher computation times.

Thus, to adequately simulate any SDE, special numerical schemes have to be employed, often customized for the equation in question [30]. The most widely used scheme is the Euler[2]-Maruyama[3] scheme which is a simple generalization of the Euler discretization scheme known for ordinary differential equations. The standard Euler-Maruyama (EM) scheme reads

$$X_{i+1} = X_i + f(X_i)\Delta t + g(X_i)\Delta W \tag{4.6}$$

work in numerous cases. The first two terms on the right-hand-side exactly correspond to the the Euler scheme, the third expression is termed Maruyama term to honour the idea of Japanese mathematician Gisiro Maruyama who introduced it in the 1950s. The EM scheme is very widely used in finance because of its ease of use and implementation. However, many financial models exhibit rather 'tame' coefficients f and g and - as mentioned earlier - to the authors knowledge at the time of writing, *virtually any* model in finance is a SDE of *first* order in time. In case of the stochastic Ide-Sornette model for financial markets, f and g are neither 'tame' nor do they live in only one dimension. Numerical tests in the deterministic setting showed that the EM scheme was too inaccurate at reasonable discretization time steps ($\delta = 10^{-4}$) as compared to the Runge-Kutta implementation we had used for the deterministic Ide-Sornette model. In effect, it was unavoidable to look for an appropriate replacement. The easiest higher order algorithm is the Milstein scheme

$$X_{i+1} = X_i + f(X_i)\Delta t + g(X_i)\Delta W + \frac{1}{2}g(X_i)g'(X_i)\left((\Delta W)^2 - \Delta t\right) \tag{4.7}$$

which in this case does not lead to any improvement since this scheme requires the drift and diffusions coefficients of the equation in question to be twice continuously differentiable, an assumption that is obviously not valid in the present case[4]. Higher order Milstein schemes exist but require the implementation of multiple stochastic integrals which is not easy to accomplish, prone to errors and currently constituting a separate field of research [31, 43].

[2]Leonard Euler (1707-1783), Swiss mathematician
[3]Gisiro Maruyama (1916-1986), Japanese mathematician
[4]consider for example the case $|r|^{3/2}$ at $r = 0$

Milstein and Tretyakov [32] have suggested a method for nonlinear SDEs with nonglobal Lipschitz coefficients that has been proved to work under certain assumptions for additive noise in a sense that 'bad trajectories' can be disregarded. However, the authors do not investigate the case of multiplicative noise which is of interest in the present case and the Lamperti transform does not work in this particular case. A thorough literature search and consultation of several renowned experts in the field brought to our attention that our equation might be *stiff*.

Definition 3. *A d dimensional SDE is said to be stiff if it holds that*

$$\lambda_d \ll \lambda_1$$

where

$$\lambda = \lim_{t\to\infty} \sup \frac{1}{t} \log |Z_t|$$

are the d Lyapunov exponents and Z_t is the linearized *version of the original process X_t.*

The problem thus reduces to determining the Lyapunov[5] exponents of the problem which is in most cases not explicitly possible [58, 31]. Concretely, stiffness of an SDE means that there are at least two vastly differing time scales that operate in the system[6]. When dealing with stiff equations, one can however resort to implicit numerical schemes which are known to work well even for comparably large step sizes. An implicit numerical scheme is any scheme of the form

$$X_{i+1} = h(X_i, X_{i+1}) \tag{4.8}$$

where h is any real-valued function. Consequently, implicit schemes are computationally much more expensive since in every time step (usually far more than 1000), equation (4.8) has to be solved which is numerically done with the Newton[7]-Raphson[8] iteration. Higham and coworkers [41] have remarked that the stochastic Θ method is the best possible implicit scheme known in both the strong and weak sense of convergence without using multiple stochastic integrals. For this reason, the class of stochastic diagonally drift-implicit Runge-Kutta (DDISRK) schemes due to Rößler and Debrabant [29] was selected for implementation which contains the stochastic Θ method as a special case. A brief introduction to this class of methods can be found in Appendix B. In our case, the scheme reads

$$X_{i+1} = X_i + \frac{\delta}{2}\left(a(X_i + a(X_{i+1}))\right) + I_{(1),i} b^1(X_i) + I_{(2),i} b^2(X_i) \tag{4.9}$$

[5] Alexander Michailowitsch Ljapunow (1857-1918), Russian mathematician and physicist
[6] a situation usually often found in equations describing noisy chemical reactions
[7] Sir Isaac Newton (1643-1727), British mathematician and physicist
[8] Joseph Raphson (1648-1715), British mathematician

with $I_{(j),i}$ being a Gaussian distributed random number and using the notations from eqn. (4.2) where b^k denotes the kth column of the diffusion matrix b. This translates as

$$x_{i+1} = x_i + \frac{\delta}{2}(r_i + r_{i+1}) \tag{4.10}$$

$$r_{i+1} = r_i + \frac{\delta}{2}(\alpha |r_i|^m - \gamma |x_i|^n + \alpha |r_{i+1}|^m - \gamma |x_{i+1}|^n) \tag{4.11}$$

For the sake of completeness, it should be noted that the field of researching and developing high-order integration schemes for SDE is widely still considered in its 'infancy' [31], especially in the case of high-order strong integration schemes for SDEs with nonlinear coefficients [40, 41, 31]. This section is concluded with a graphical illustration of our findings which may serve as a guide for the perplexed modeler.

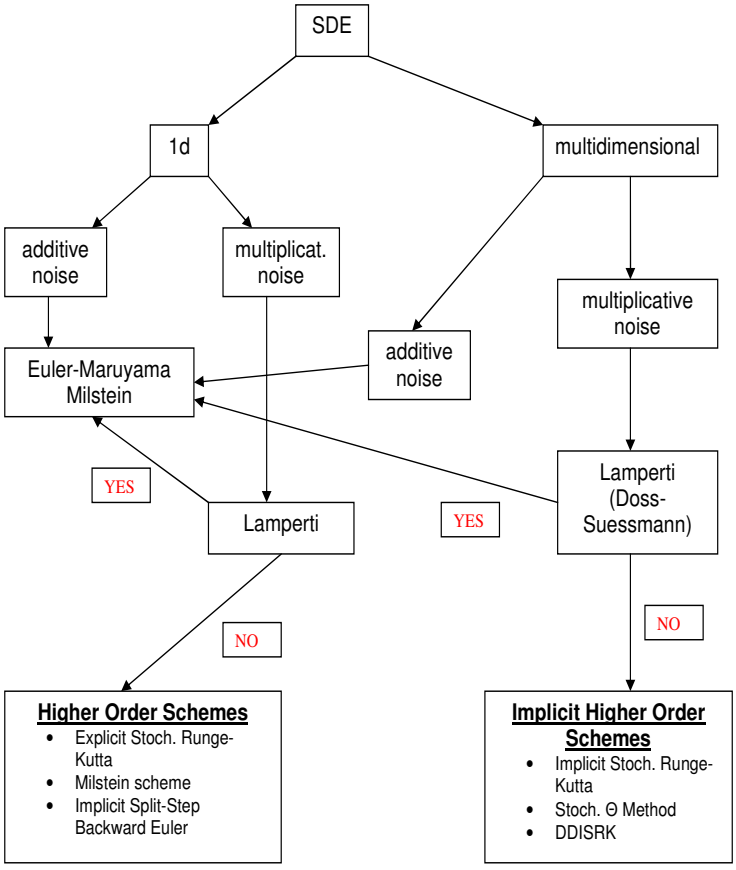

Figure 4.2.: A guide for modelling SDEs (compilation of the author). The red boxes indicate whether the Lamperti (Doss-Suessmann) transform has been successful or not.

4.3. A Brief Introduction to Survival Analysis

In this section which follows the compendium by Rinne [68], we will give a short introduction to the field of survival analysis which is sometimes also referred to as reliability analysis. Survival analysis has applications in many different fields such as biostatistics, medicine, mechanical engineering and social sciences and is used whenever some object of interest has a finite lifespan so that one is typically interested in prediction and measurement of failure probability and quantification of optimization potentials. Such objects of interest may involve

- Electrical parts such as transistors, capacitors and modules comprised of them
- Objects of daily use such as bicycles, cars or televisors
- Objects that are relevant for general security such as nuclear power plants, airplanes and satellites
- In empirical social sciences, social states such as being married or (un-)employed

In the present work, we deal with singularities (i.e. a mortality) deterministically occurring at fixed time instants $t_{C,i}$ depending of the parameter choices in the Ide-Sornette model. Extending this model towards Gaussian white noise, it is expected that the times at which the singularities occur will turn into a random variable with a certain distribution. In the following, we will thus quickly introduce the most important measures to characterize such distributions of critical times.

4.3.1. Kernel Density Estimation

All relevant functions and measures in survival analysis basically derive from the probability density function (PDF) $p(t)$ of the critical times. It is therefore important to have a good estimate of $p(t)$ based on a given array of critical times. The kernel density estimation[9] does just that, i.e. it gives an estimate of the underlying PDF based on a given sample time series or array of values. In other words, the kernel density estimator returns the PDF from which the given sample is most probably[10] drawn. Although most computer languages have pre-defined routines for kernel density estimation, we quickly give its definition: Be $x_1, \ldots, x_n \in \mathbb{R}$ a sample and k a kernel, then the corresponding kernel density estimator is defined as mapping

$$\tilde{f}_n : \mathbb{R} \to \mathbb{R}_+ : \quad \tilde{f}_n(t) = \frac{1}{nh} \sum_{j=1}^{n} k\left(\frac{t - x_j}{h}\right) \tag{4.12}$$

where h is the so-called bandwidth on which the quality of approximation heavily depends[11]. The theorem of Nadaraja which we will - for the sake of brevity - not give here ensures that the sequence $\tilde{f}_n$ converges to the true PDF with probability one. When lacking information

[9] also termed kernel density regression

[10] A statement like 'this distribution is obviously a power law distribution' is *never* a priori justified. Telling what kind of distribution one sees in any given data sample is actually a science of its own and a subfield of statistics: Test and estimation theory

[11] Again, in most programming languages, the best possible choice of the bandwidth h is automatically chosen by default

about the PDF of some process, the kernel k is usually set equal to the Epanechnikov[12] kernel which is defined by [52]

$$k_E(t) = \frac{3}{4\alpha}(1 - (\frac{t}{\alpha})^2) \quad \text{for} \quad |t| < \alpha \quad \text{and} \quad k_E = 0 \quad \text{else.} \tag{4.13}$$

The Epanechnikov kernel is the 'best choice' for k in a sense that it minimizes the mean squared deviation of the corresponding kernel density estimator under all possible kernels [67]. However, it should always be made sure that the kernel density regression maps the raw data

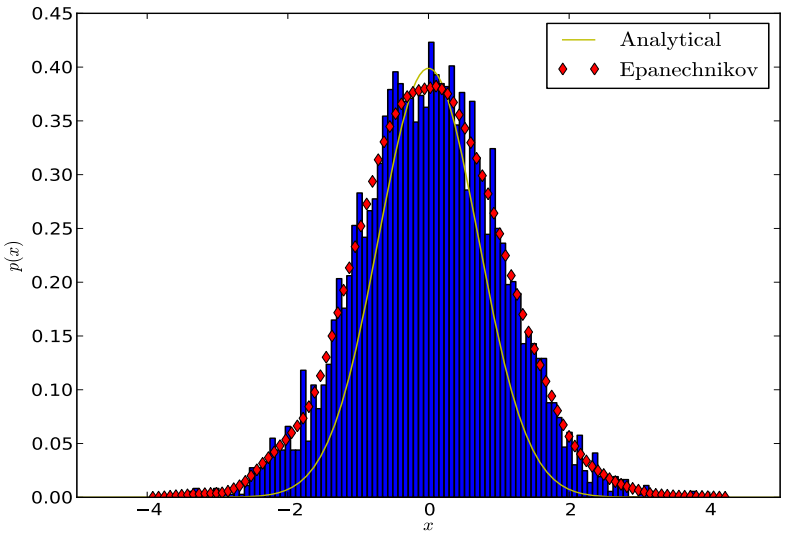

Figure 4.3.: Kernel density estimation using an Epanechnikov kernel (red diamonds) versus raw data from which the PDF is estimated (blue histogram) and analytical Gaussian PDF (yellow).

correctly.

4.3.2. Functions Derived From $p(t)$

Several important functions for the survival analysis can be derived directly from $p(t)$:

1. Distribution function:
   The distribution function $F(t) = P(t_C \leq t), \quad t > 0$ at time t is defined as the monotonically increasing function
   $$F(t) = \int_0^t p(t')\mathrm{d}t' \tag{4.14}$$

[12] V. A. Epanechnikov, Russian statistician

and is consequently also referred to as cumulative probability function (CPF). It quantifies the probability for the object of interest to die until time t where it holds that $0 \leq F(t) \leq 1$, $F(0) = 0$ and $F(\infty) = 1$.

2. Survival function:
   Closely related is the survival function $S(t) = P(t_C \geq t) = 1 - F(t)$ which measures the probability for some object of interest to survive until time t. It is thus monotonically decreasing with boundary values $S(0) = 1$ and $S(\infty) = 0$ where $S(t) \in [0,1] \, \forall t \geq 0$.

4.3.3. Typical Distributions of Survival Analysis

As we have mentioned above, testing whether a distribution is of kind X rather than Y is a challenging task in statistics. Nonetheless, the most common distributions that occur in survival analysis are briefly introduced to help the reader digest later results.

4.3.3.1. Weibull Distribution

Originally published in the context of material sciences, the Weibull[13] distribution Wei(a,b) is the most important distribution in survival analysis, together with the exponential distribution. Its PDF reads

$$f(x) = abx^{b-1}e^{-ax^b} \tag{4.15}$$

and is displayed in the following graph. This distribution is most commonly used in mechanical engineering and related fields but was also found to describe the yearly distribution of wind speeds.

4.3.3.2. Γ Distribution

For $x \geq 0$, the Γ distribution has the PDF

$$f(x) = \frac{b^p}{\Gamma(p)} x^{p-1} e^{-bx} \tag{4.16}$$

The distribution is most prominently used in queueing theory and in insurance mathematics for modelling small and intermediate damages.

[13] Ernst Hjalmar Waloddi Weibull (1887-1979), Swedish engineer and mathematician

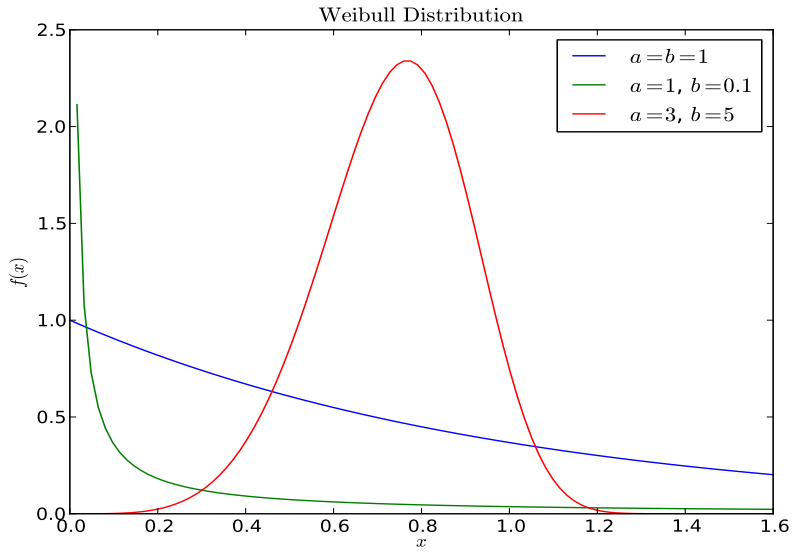

Figure 4.4.: The Weibull distribution.

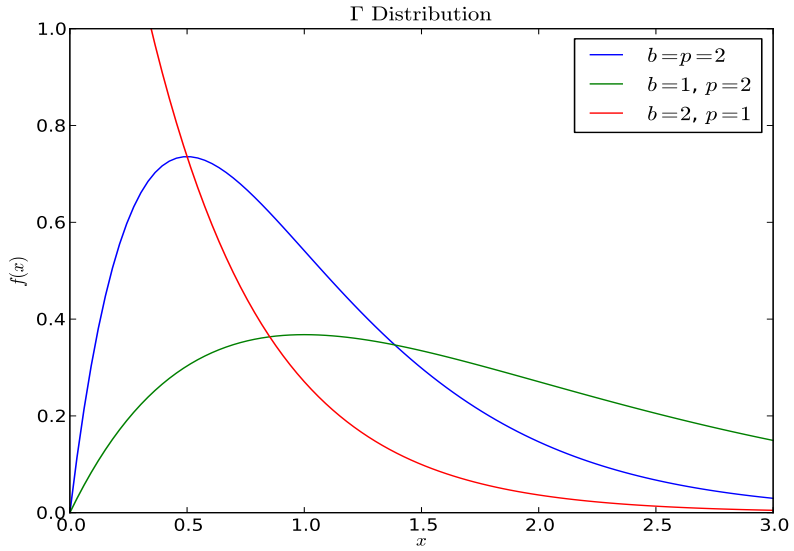

Figure 4.5.: The Γ distribution.

4.3.3.3. Erlang Distribution

The Erlang[14] distribution was originally developed to statistically model interval lengths between phone calls and thus also belongs to the field of queueing theory. Its PDF is given

[14] Agner Krarup Erlang (1878-1929), Danish mathematician and engineer, one of the founders of traffic engineering and queueing theory. The Erlang formulas remain highly relevant for the efficient design of phone networks to this date.

by

$$f(x) = \frac{(\lambda x)^{n-1}}{(n-1)!}\lambda e^{-\lambda x}; \quad x > 0. \tag{4.17}$$

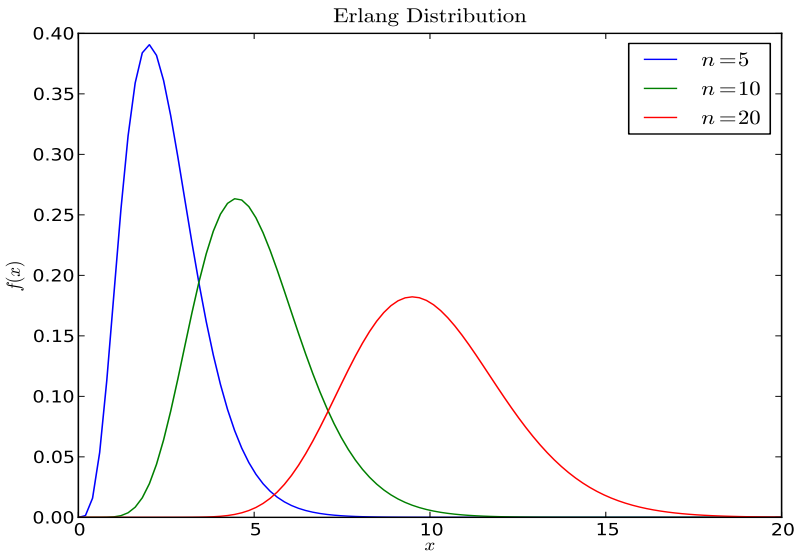

Figure 4.6.: Erlang distribution for $\lambda = 1$ and various values of n.

4.4. Investigation of the Stochastic Ide-Sornette Model

As we have gathered all necessary ingredients now, we will look for both, qualitative and quantitative changes in the system's behavior. This means that we will remember the analysis scheme of the deterministic Ide-Sornette model from chapter 2 and look at the noisy model components and, in a last step, assemble the results to obtain a bigger picture.

4.4.1. $\alpha = \varepsilon_1 = 0$

As was demonstrated in Chapter 2, the assumption that a market consists only of fundamental value investors who assess their investment decisions solely on the behavior of the price of an asset relative to its fundamental price leads to a second order nonlinear oscillatory ODE

$$\ddot{x} + \gamma \left| x(t) \right|^n = 0, \quad n > 1. \tag{4.18}$$

where γ is inversely proportional to the market liquidity L. Letting the parameter γ fluctuate randomly over time, i.e we pose $\gamma_t = \gamma + \varepsilon\xi(t)$ we obtain a stochastic dynamical system[15]

$$\mathrm{d}\vec{X}_t = \begin{pmatrix} r \\ -x^n \end{pmatrix} \mathrm{d}t + \begin{pmatrix} 0 & 0 \\ 0 & \varepsilon x^n \end{pmatrix} \mathrm{d}\vec{W}_t \tag{4.19}$$

where $\mathrm{d}W_t$ is a twodimensional Brownian increment. As we have pointed out in chapter 3, we a priori understand this equation in the Itô sense of stochastic integration. In this particular case however, we stress that both interpretations *coincide*. To see this, we use the Itô - Stratonovich drift conversion theorem in multiple dimensions:

Theorem 1. *The Stratonovich SDE*

$$\mathrm{d}Z_t^i = \underline{a}^i(Z_t,t) + \sum_{j=1}^{M} b^{ij}(Z_t,t) \circ \mathrm{d}W_t \tag{4.20}$$

for $i = 1, ..., N$; $j = 1, ..., M$ with the same solutions as the N-dimensional Itô SDE with an M-dimensional Wiener process

$$\mathrm{d}Z_t^i = a^i(Z_t,t) + \sum_{j=1}^{M} b^{ij}(Z_t,t)\mathrm{d}W_t \tag{4.21}$$

[15]for ease of reading, we skip the indices '2' in the following

has a drift coefficient that is defined given a component-wise by

$$\underline{a}^i(Z_t,t) = a^i(Z_t,t) - \frac{1}{2}\sum_{k=1}^{N}\sum_{j=1}^{M} b^{kj}(Z_t,t)\frac{\partial b^{ij}(Z_t,t)}{\partial z^k} \tag{4.22}$$

The diffusion coefficients are the same in both the Itô and Stratonovich SDEs.

It follows from the shape of the diffusion matrix $\mathbf{b}$ that the only possible contribution to the drift correction amounts to $i = j = k = 2$. However, the second component (z^2) of the stochastic process (4.19) is r and $b^{22} = \varepsilon x^n$. Hence, we obtain

$$\frac{\partial}{\partial r}\varepsilon x^n = 0$$

and therefore, this correction also vanishes and we have $\vec{\underline{a}} = \vec{a}$, i.e. Itô and Stratonovich coincide. It is thus possible to use Stratonovich calculus[16] to analyze the behavior of the system although we are not initially dealing with the Stratonovich interpretation of equation (4.19) since we have shown that both interpretations lead to the *same* FPE and consequently to the same PDF, i.e. time evolution.

4.4.1.1. Case $n = 1$

As reported by Mallick and Marcq [74], the ensemble mean energy $\langle E\rangle$ for the linear case $n = 1$ is found to obey

$$\langle E\rangle = \frac{1}{2}\langle r^2\rangle + \frac{\gamma}{2}\langle x^2\rangle \propto e^{\mu t} \tag{4.23}$$

where the growth rate μ is the positive real root of the equation

$$\mu^3 + 4\gamma\mu = 2\varepsilon. \tag{4.24}$$

These results are obtained by considering the equivalent FPE and a scaling analysis. In our market model picture, this is already surprising: According to equation (4.23), in spite of the presence of only fundamentalists, this predicts large ranges for the price and return time series to act in rather than small fluctuations around some fundamental value.

[16] this means that the rules from deterministic calculus apply

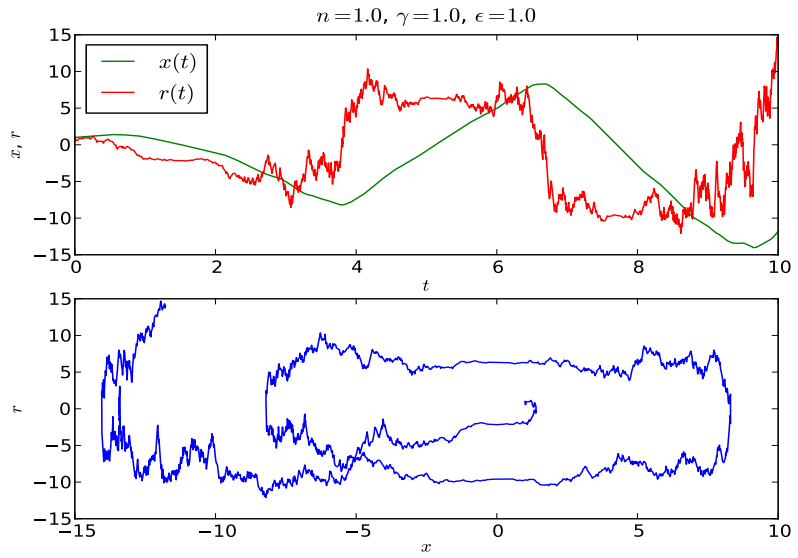

Figure 4.7.: Sample path of the linear noisy oscillator without friction (upper panel) along with the corresponding phase portrait.

4.4.1.2. Case $n > 1$

In this section, we use the aforementioned idea of Mallick and Marcq [74] for our case to learn about the behavior of our fundamentalist market for $n > 1$, i.e. a greater mean-reversion parameter. Considering the equation $\ddot{x} + \gamma_t x^n = \varepsilon\xi(t)x^n$ (in Stratonovich interpretation), we find that the energy is defined as

$$E = \frac{\dot{x}^2}{2} + \gamma\frac{x^{n+1}}{n+1} \tag{4.25}$$

from which it follows that

$$\frac{\mathrm{d}E}{\mathrm{d}t} = \dot{x}\left(\ddot{x} + \gamma x^n\right) = \dot{x}\varepsilon\xi(t)x^n \tag{4.26}$$

As was shown in [74], one can either do an exact calculation via energy-angle variables, hyperelliptic integrals and the corresponding Fokker-Planck equation to yield exact relations with all prefactors (see Appendix A) or do a scaling analysis which gives the same qualitative insights for such oscillatory systems, but with minimal efforts. We will stick to the scaling analysis here and refer the reader to Appendix A to get an overall idea of the course of these calculations or the original publication [74] for a far more detailed and complete overview. From eq. (4.25), we know that

$$E \sim \dot{x}^2 \quad \wedge \quad E \sim x^{2r} \quad \Leftrightarrow \quad x \sim E^{\frac{1}{2r}} \quad \wedge \quad \dot{x} \sim E^{\frac{1}{2}} \tag{4.27}$$

This means that

$$\frac{\mathrm{d}E}{\mathrm{d}t} = \dot{x}\varepsilon\xi(t)x^n \sim \varepsilon\xi(t)E^{\frac{3n+1}{2(n+1)}} \tag{4.28}$$

which leads to an energy growth rate growing itself with time and thus a finite-time singularity (see Chapter 2) if and only if

$$\frac{3n+1}{2(n+1)} > 1 \tag{4.29}$$

which is easily shown to be true for any $n > 1$. Given this result, we conclude that our nonlinear oscillator market model will blow-up in finite time if $\varepsilon \neq 0$ since $n > 1$ by definition. A direct integration of eq. (4.28) again similar to the one performed in Chapter 2 then yields

$$E(t) = \left[\frac{1}{D - \varepsilon(\zeta - 1)W(t)}\right]^{\frac{1}{\zeta - 1}} \tag{4.30}$$

where we have abbreviated $\zeta = \frac{3n+1}{2(n+1)}$ and where D is an integration constant determined by the initial energy E_0. The occurrence of the finite-time singularity (at the critical time t_C) thus reduces to the problem of first passage of the random walk $W(t)$ at some point D. The critical time is thus turned into a random variable and depends on the particular realization of the Brownian motion $W(t)$. Transferring the idea of Mallick and Marcq, we have provided strong evidence that the noisy nonlinear oscillator of degree n without friction (and therefore our market model only consisting of fundamental value investors) is separated into two mutually different dynamical regimes at $n_C = 1$. The regime $n > n_C$, which corresponds exactly to the domain of definition of our market model, will be characterized in the following paragraph while we show two sample realizations in the following figures.

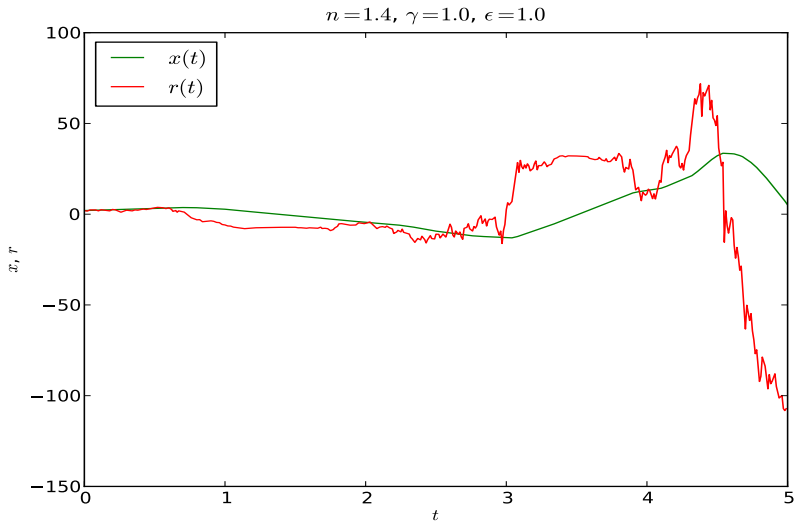

Figure 4.8.: Sample path of the nonlinear oscillator before occurrence of a FTS. Note the increase in the energy reflected by increasing amplitudes of r and x

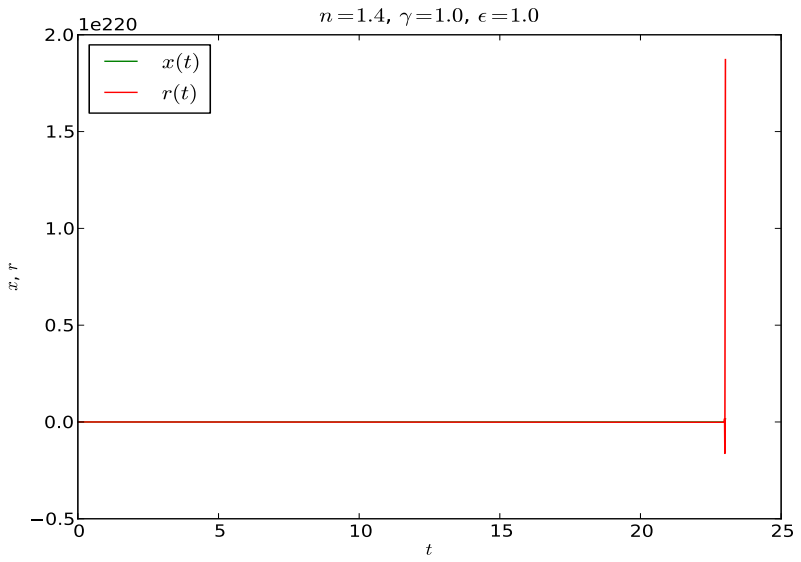

Figure 4.9.: Sample path of the nonlinear oscillator with $n > n_C$ exhibiting singular behavior in $r(t)$ at $t_C \approx 23.03$

4.4.1.2.1. Numerical Investigations After the theoretical finding that for $n > 1$ any trajectory will exhibit a finite-time blow-up, we investigate and characterize this behavior numerically. We remark that, in order to be relevant for finance, it has to be made sure that $\gamma_t > 0 \ \forall t$ since there is no such thing as a negative market liquidity. However, from the nonlinear oscillator perspective, it is a priori clear that such a constraint will have no impact on the results. Indeed, simulations with this constraint implemented only needed more time to run as many paths were killed before the FTS occurred with the same outcome (in terms of distributions of critical times) as without the constraint. It was thus skipped for computational efficiency. All simulations were carried out using the same set of initial conditions and parameters: $\gamma = \varepsilon = X_0 = R_0 = 1.0$, the discretization step width was fixed at $\delta = 10^{-2}$ and a relatively large number of integration steps was chosen, $N = 50000$, to cover an as big as possible time domain. The prediction of $n_C = 1$ as bifurcation value was also tested as simulation trials for $n = 0.8, 0.9, 0.99, 1.0$ were also run. Concerning these values, not a single FTS was detected in spite of using $N = 10^5$ which is in perfect agreement with the behavior expected from our scaling analysis. We chose $\varepsilon = 1.0$ to keep the computing time as short as possible although for $n \to 1$, a simulation runtime > 3 hours per trial of $M = 1000$ paths was observed. However, we did do some control samples for $\varepsilon = 0.5$ and various $n > 1$ which consistently gave the expected zero survival rate.

4.4.1.2.1.1. Survival Analysis The analysis is performed in several steps: First, we simulate $M = 1000$ paths for different values of n in the neighborhood of the critical value $n_C = 1$. From this, the histogram of critical times at which the FTS occurs is constructed together with the corresponding PDF using a kernel density regression algorithm where it is checked for every n that the regression gives an estimation of the PDF that is consistent with the raw data (see also [78]). In a second step, we construct the CPF and the survival function from the PDF. The results can be seen in figs. 4.10-4.12.

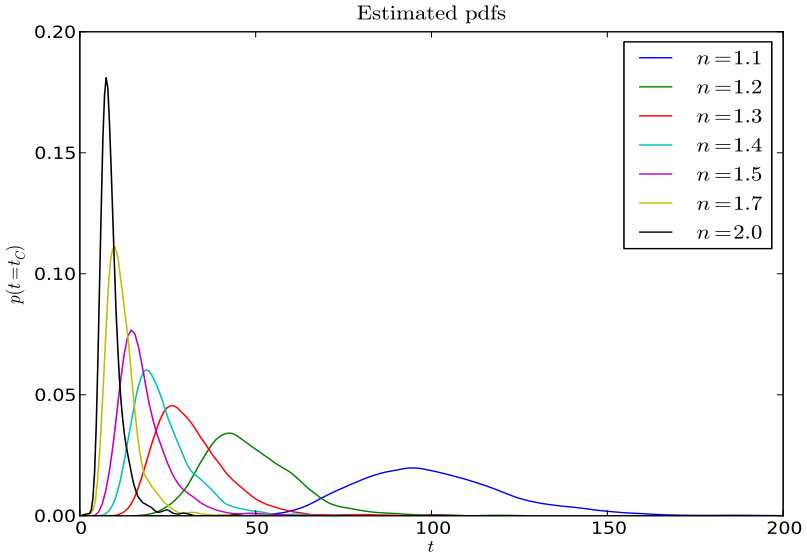

Figure 4.10.: Estimated probability densities for various values of n near the critical value $n_C = 1$. Note the smearing out of the PDF as $n \to 1$. The exponent n plays the role of an 'inverse time' compared to the smearing out of Gaussian wave packets as solutions of the Schrödinger equation in quantum mechanics as the PDFs become more definite as n is increased (compared to Gaussian wave packets that become more indefinite as t grows). Notice also the formal resemblance of the curves to the ones typically found in survival analysis as introduced in the previous section.

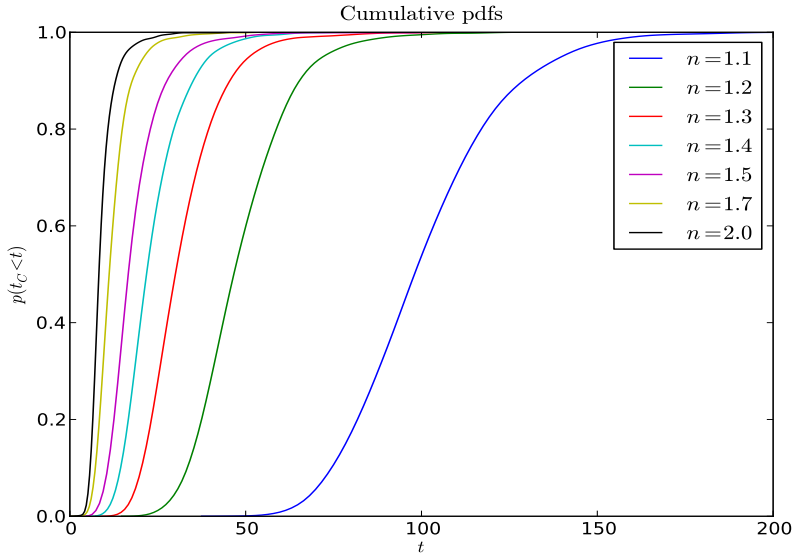

Figure 4.11.: Cumulative probability density as constructed from figure 4.10. For every time instant t, the value of the CPF gives the probability for an ensemble path to have died until t.

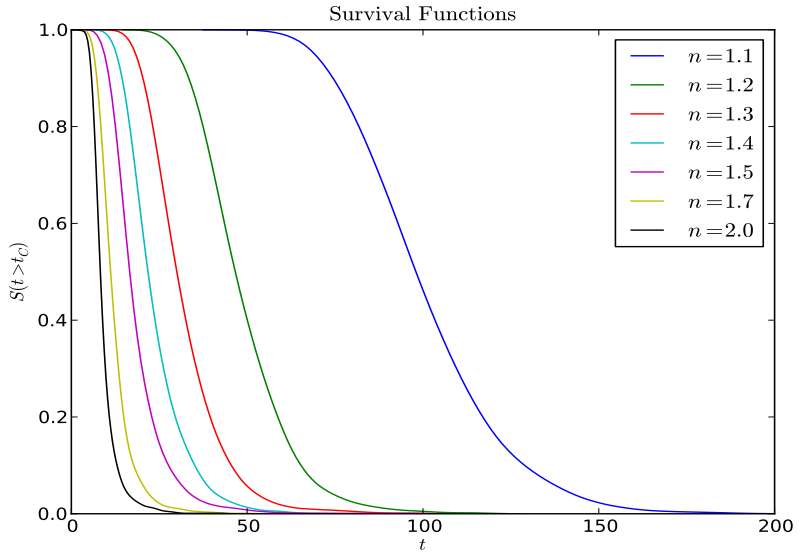

Figure 4.12.: Survival functions corresponding to figure 4.11. For every t, $S(t)$ quantifies the probability for an ensemble path to survive until t.

4.4.1.2.1.2. Dependence of Ensemble Critical Times on n In a next step, we present the behavior of the median[17] of the critical times, $\widetilde{t_C}$, as a function of n for the same data sets as above. A Levenberg-Marquard fit of these data points to the function

$$\widetilde{t_C}(n) = C(n-1)^a \tag{4.31}$$

shows a very accurate match (see figure (4.13)).

[17] the median is less impacted by outliers and insofar better when dealing with skew or heavy-tailed distributions

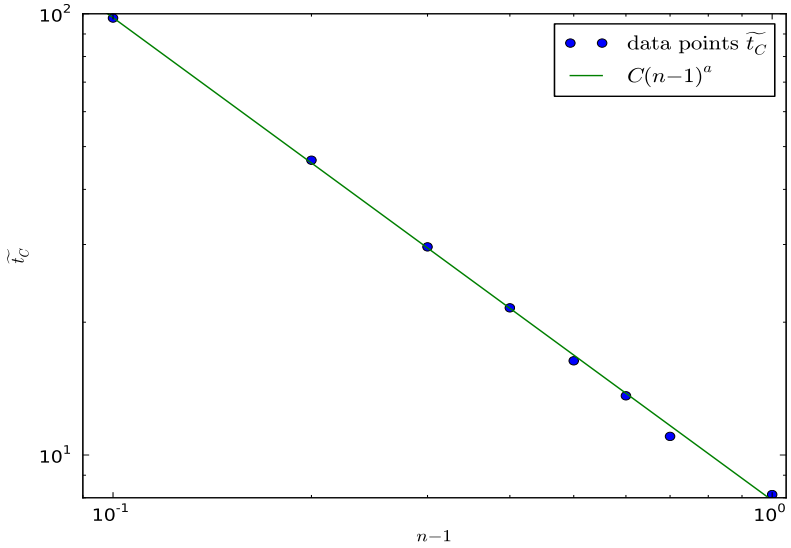

Figure 4.13.: The behavior of $\widetilde{t_C}(n)$: Fitting parameters were $C = 7.79$ and $a = -1.10$ while $R^2 = 0.998$.

4.4.1.2.1.3. Dependence of the Entropy on n To quantify the smearing out of the PDFs, we also constructed Shannon's entropy from our data. Shannon's entropy is defined as

$$S = -\sum_{t_C \in \{t_C\}} p_{t_C} \log_2 p_{t_C} \tag{4.32}$$

and is thus a measure for the definiteness of the corresponding PDF as a higher value of $S(n)$ reflects a wider PDF. To account for the influence of binning, we looked at three different choices for the number of bins at a pre-defined interval on the time axis $\mathcal{I} = [0,200]$ in order to make our results comparable. The so obtained entropy was found to obey a stretched exponential function of the form

$$S(n) = A \exp(-\alpha n^\beta) \tag{4.33}$$

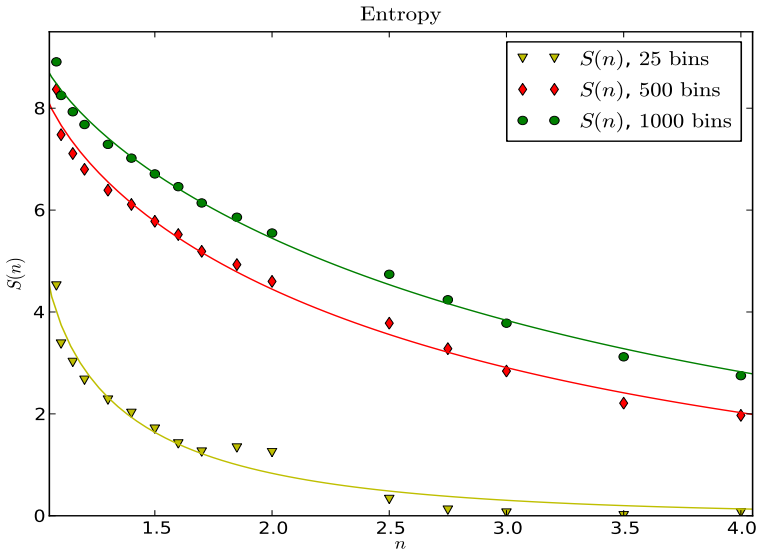

Figure 4.14.: Entropy over nonlinearity n for three different numbers of bins. The fitting parameters were found to be $A = 9.19$, $\alpha = 0.523$ and $\beta = 0.74$ (green curve, $R^2 = 0.999$), $A = 8.78$, $\alpha = 0.68$ and $\beta = 0.70$ (red curve, $R^2 = 0.999$) and $A = 6.41$, $\alpha = 2.04$ and $\beta = 0.58$ (yellow curve, $R^2 = 0.985$).

4.4.1.3. Discussion

Stochastic oscillatory equations have been omnipresent in the physics literature ever since stochastic calculus was invented [74, 75, 76] as the (non-) linear oscillator is somewhat the workhorse of physicists. However, in this section, we have investigated an oscillatory equation that has not been analyzed previously: The frictionless nonlinear oscillator coupled to multiplicative noise which is contained as the special case $\alpha = \varepsilon_1 = 0$ in the Ide-Sornette model for financial markets. It was demonstrated theoretically as well as numerically that the energy of this nonlinear stochastic oscillator exhibits a singularity in finite time if the degree of nonlinearity exceeds a critical boundary, i.e. if $n > n_C$ where it was found that $n_C = 1$. In the context of the Ide-Sornette model, this is particularly surprising since the equation in question can be derived in an economical framework under the assumption that no trend following investors at all are present in the market, as seen in Chapter 2. This means that, by construction, the occurrence of a finite-time blow-up of the 'energy' (the sum of squared prices and returns) is highly unintuitive and unexpected since, in essence, this means that - given a fluctuating liquidity, i.e. cash is randomly injected in or withdrawn from the market - not even a 'fundamentalists only' market keeps prices and returns at an accurate level that reflects the true value of the asset being traded. Moreover, the FTS will occur no matter how small the noise amplitude ε is chosen since a smaller ε will - on average - only postpone

the occurrence of it. In the end, judgement day turns out to be literally unavoidable. These findings therefore perfectly fortify our reasonings from Chapter 3 where the impact of additive and multiplicative noise on the behavior of a system was explained at length.

4.4.2. $\gamma = \varepsilon_2 = 0$

In this section, we look at the second component of the Ide-Sornette model and investigate the influence of multiplicative noise on the distribution of critical times. This means that we investigate the SDE given by

$$\mathrm{d}\begin{pmatrix} x(t) \\ r(t) \end{pmatrix} = \begin{pmatrix} r(t) \\ \alpha\,|r(t)|^m \end{pmatrix}\mathrm{d}t + \begin{pmatrix} 0 & 0 \\ \varepsilon\,|r(t)|^m & 0 \end{pmatrix}\mathrm{d}\vec{W}(t) \tag{4.34}$$

where we have again skipped the index of the noise amplitude ε for ease of reading. As we have seen in Chapter 2, the deterministic critical times are given by

$$t_C = \frac{r_0^{1-m}}{\alpha(m-1)} \tag{4.35}$$

This means that we can compare the observed critical times at which the FTS occurs in the noisy case with the expected critical times based on this analytical expression.
At this point, it is noteworthy that this case is different from the Sornette-Andersen model introduced in [5]. This is due to the fact that in their aformentioned paper, the authors introduce their model

$$\mathrm{d}B_t = aB_t^m + bB_t^m\mathrm{d}W \tag{4.36}$$

in the *Stratonovich* framework while we understand (4.34) as *Itô* SDE from the start. Consequently, what is known in the literature as Sornette-Andersen model is the equation

$$\mathrm{d}B_t = \left(aB_t^m + \frac{am^2}{2}B_t^{2m-1}\right) + bB_t^m\mathrm{d}W \tag{4.37}$$

Furthermore, we work with a second order SDE here while Sornette and Andersen use the one dimensional case.

4.4.2.1. Survival Analysis

At first, we look at a fixed but small noise amplitude ($\varepsilon_1 = 0.1$) for different values of m. The procedure is almost exactly the same as in the preceding section on the stochastic nonlinear oscillator: For every value of m, we simulate $M = 1000$ paths, letting $\alpha = 1$, $x_0 = r_0 = 5$ (to make sure that $t_{C,th}$ remains relatively close to $t = 0$ which minimizes the simulation runtimes), detect the singularity as given in Appendix C and store the so-obtained critical times in an array from which we can construct the histogram and perform a kernel density estimation. As in the preceding numerical investigation of the stochastic nonlinear oscillator, it has again been checked whether an additional constraint that the liquidity be strictly positive for all times, i.e. $\alpha_t > 0 \quad \forall t$ had an impact on our results. Again, we did not find any effect except that the necessary simulation runtime was longer (as paths were possibly also terminated due to the positivity constraint imposed on α_t rather than reaching the FTS). The following pictures display our results.

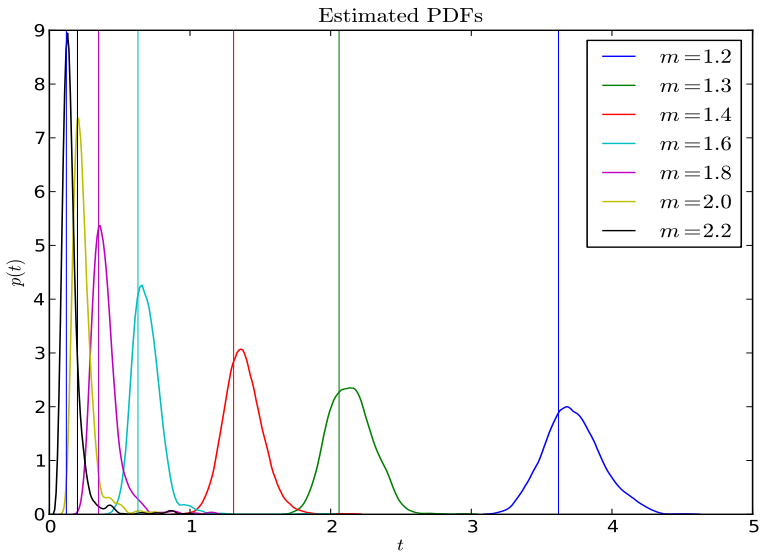

Figure 4.15.: PDFs estimated from our data: The peaks of the distributions are roughly where we would expect them from the deterministic setting (thin vertical lines) each and move from right to the left as the cooperation parameter m is increased.

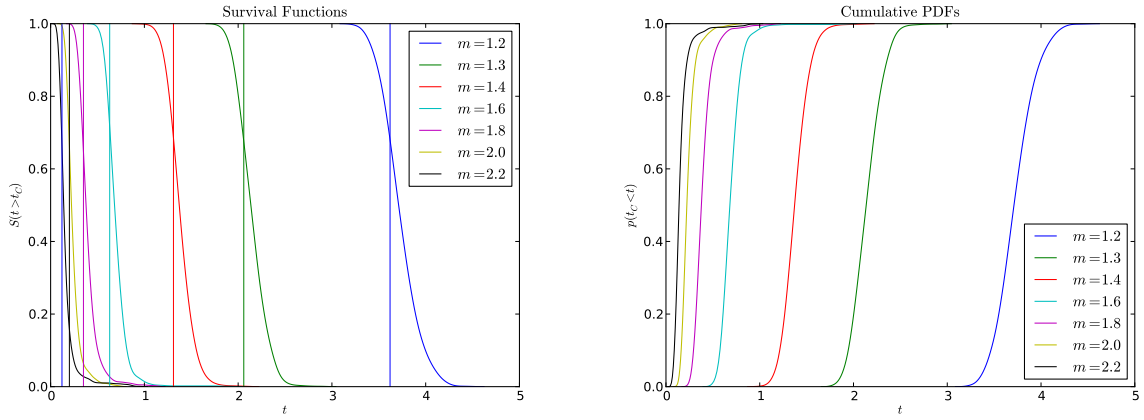

Figure 4.16.: Survival functions and cumulative PDFs as obtained from figure 4.15. The behavior remains qualitatively the same for larger noise amplitudes but the PDFs are found to move to the right, i.e. stronger noise extends the expected lifetimes of paths. Furthermore, higher noise amplitudes are found to broaden the PDF reflecting that it is less clear when to expect the FTS to occur. This is illustrated by the entropy graphs in Section 4.4.2.3.

4.4.2.2. Dependence of Ensemble Critical Times on m and ε

In the following graph, figure 4.17, we compare the numerically determined values of $\widetilde{t_C}(m)$ to the deterministically expected values, as given by equation (4.35). It can be observed that the overall behavior remains the same while the small noise produces an offset to slightly higher values of $\widetilde{t_C}(m)$. For stronger amplitudes of noise, we observe that the shape of the

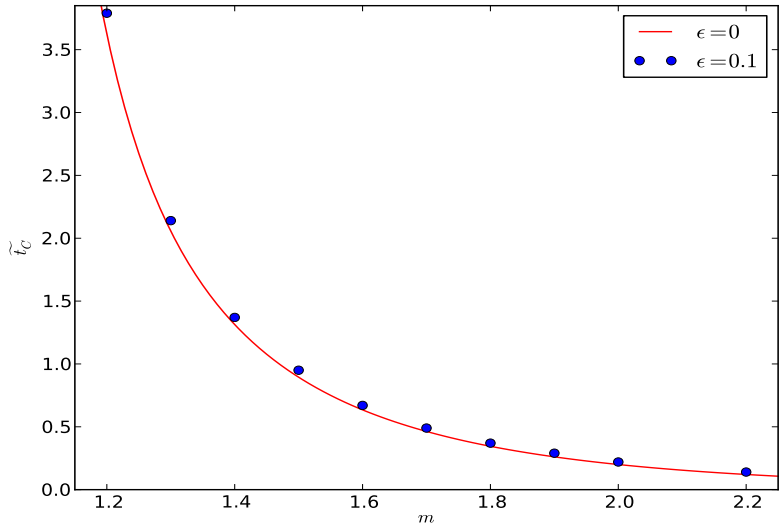

Figure 4.17.: The median of the critical times is slightly moved upwards for very weak noise ($\varepsilon = 0.1$) as compared to the deterministic case, but has the same overall shape.

$\widetilde{t_C}(m)$ curve cannot be explained by a power law similar to equation (4.35) as measured by the goodness of fit value R^2. To test this, we considered a modified version of equation (4.35) where we let $m' = m + \kappa$ with fitting parameter κ where the underlying assumption is that noise alters the 'true' value of m while the remaining parameters r_0 and α are treated as given and remain unaffected. A good fit however was only accomplished for the case $\varepsilon = 0.1$ where we found $\kappa = -0.007$ while $R^2 = 0.999$. In the other cases using the same setting, we obtained $R^2 = 0.838$ for $\varepsilon = 0.5$ and $R^2 = 0.802$ for $\varepsilon = 1.0$ Instead, it is again found that the observed median critical time values can be described much better by a stretched exponential function that accounts for the smoother change of slope in the data (see figure 4.18) that we obtained as compared to the modified power law similar to (4.35).

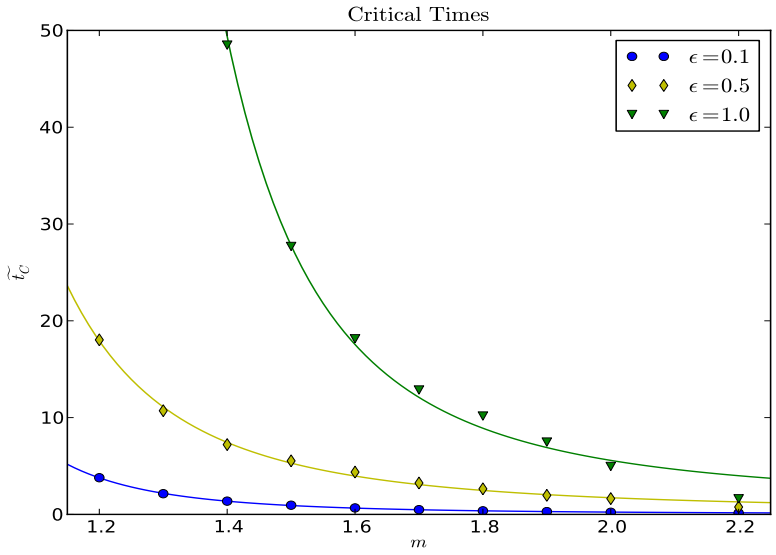

Figure 4.18.: Least square fits of stretched exponential functions (4.33) to the medians of critical times $\widetilde{t_C}(m)$. The following fitting parameters were obtained: $A = 0.077$, $\alpha = -5.304$ and $\beta = -2.909$ (blue curve, $R^2 = 0.893$), $A = 1.92$, $\alpha = -1.39$ and $\beta = -1.59$ (yellow curve, $R^2 = 0.999$) and $A = 4.7 \cdot 10^{-4}$, $\alpha = -10.08$ and $\beta = -0.134$ (green curve, $R^2 = 0.999$).

4.4.2.3. Dependence of the Entropy on m and ε

The entropy was calculated as in Section 4.4.1.2.1.3 with one important difference: In this case, we also accounted for three different noise amplitudes ($\varepsilon \in \{0.1, 0.5, 1.0\}$). For all three curves, the same interval of critical times $\mathcal{I} = [0{,}500]$ and number of bins (500) was used so that the curves can also be compared absolutely to each other. Having said this, the message of the graph is two-fold: Firstly, one can see that the greater the noise amplitude, the greater the absolute value of the entropy. This means that a higher noise level leads to a less definite and broader PDF and vice versa. Secondly, the $S(m)$ curves were again found to decay like stretched exponential functions (see equation (4.33)) as in the case of the nonlinear stochastic oscillator.

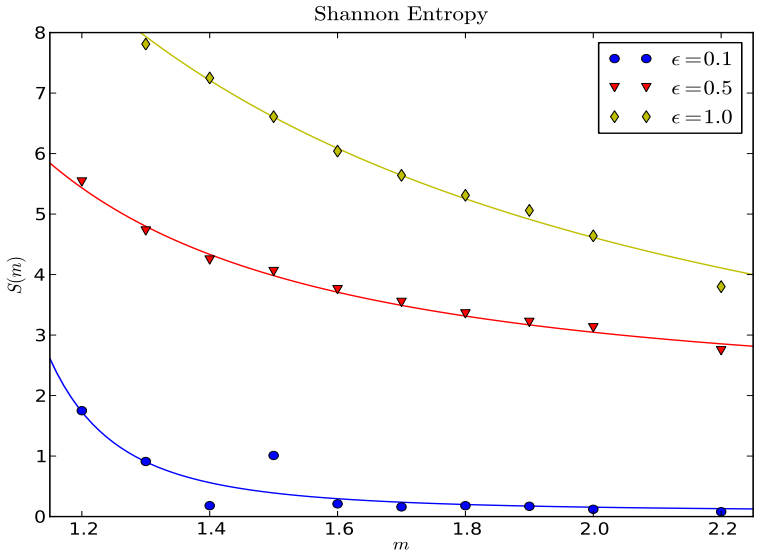

Figure 4.19.: Entropy over nonlinearity m for three different noise amplitudes ($\varepsilon \in \{0.1, 0.5, 1.0\}$). The fitting parameters were found to be $A = 4.7 \cdot 10^{-4}$, $\alpha = -10.08$ and $\beta = -0.134$ (yellow curve, $R^2 = 0.999$), $A = 1.92$, $\alpha = -1.39$ and $\beta = -1.59$ (red curve, $R^2 = 0.999$) and $A = 0.077$, $\alpha = -5.304$ and $\beta = -2.909$ (yellow curve, $R^2 = 0.893$.

4.4.2.4. Discussion

In this section, we have investigated the impact of different levels of parametric noise on the behavior of the PDF, the median of critical times $\widetilde{t_C}(m)$ and the Shannon entropy $S(m)$ as a measure for the definiteness of the t_C distribution in the Ide-Sornette model with $\gamma = \varepsilon_2 = 0$. We have seen that there is a positive correlation between noise amplitude and entropy reflecting the fact that the t_C distribution broadens and exhibits less sharp peaks as the noise amplitude is augmented. Moreover, the medians of critical times $\widetilde{t_C}$ (as well as its ensemble averages $\langle t_C \rangle$) for a given value of m are consistently larger than its deterministic counterpart as given by the analytical expression (4.35). In the framework of the financial market interpretation of our model, this means that the cooperation of the trend followers amomgst each other is perturbed by a randomly varying market liquidity leading to longer average and median waiting times for the finite-time singularity to occur. This resembles the noisy buzz of activity on the trading floor which is practically observed rather than a silent entourage of traders that watch their computer screens. On the other hand, based on our analysis, there is no evidence for a qualitative change in the behavior of the system as in the case of the stochastic nonlinear oscillator: Singularities remain singularities, albeit not with a well-defined critical time instant as in the deterministic case. The behavior observed here is thus somewhat more in line with intuitive expectations than the ones reported for the nonlinear oscillator.

4.4.3. $\varepsilon_1 \neq 0$, $\varepsilon_2 \neq 0$

In a final step, we demonstrate the effect of noise on the full Ide-Sornette model with multiplicative white noise which we have found to read

$$\mathrm{d}\begin{pmatrix} x(t) \\ r(t) \end{pmatrix} = \begin{pmatrix} r(t) \\ \alpha\,|r(t)|^m - \gamma\,|x(t)|^n \end{pmatrix} \mathrm{d}t + \begin{pmatrix} 0 & 0 \\ \varepsilon_1\,|r(t)|^m & -\varepsilon_2\,|x(t)|^n \end{pmatrix} \mathrm{d}\vec{W}(t) \qquad (4.38)$$

In what follows, we will restrict ourselves to the scenario most relevant for practical applications to finance. This implies that we think of the liquidity as a variable varying *slowly* over time, i.e. we let $\varepsilon_1 = \varepsilon_2 = 0.1$ since both parameters $\alpha, \gamma \sim \frac{1}{L}$ by definition (see Chapter 2, eqs. (2.6)). Based on our findings in Chapter 2, we will look at the two regimes that we have found in the deterministic case, $m > 2$ and $m < 2$ for some fixed value of m each, and check for qualitative similarities and differences compared to the deterministic case as n is varied according to $n < m$, $n > m$ and $n = m$ in each regime. The survival analysis will be displayed for each case separately while the analysis of the critical times and entropy will be plotted in

the same graph, respectively, to allow for a convenient comparison of both cases.

4.4.3.1. $m > 2$

In the following paragraphs, we investigate the Ide-Sornette model for the supposed regime $m > 2$.

4.4.3.1.1. Survival Analysis The procedure we employ basically remains the one explained in Section 4.4.1.2.1, the only difference being that we obviously have both parameters α_t and γ_t in the game.

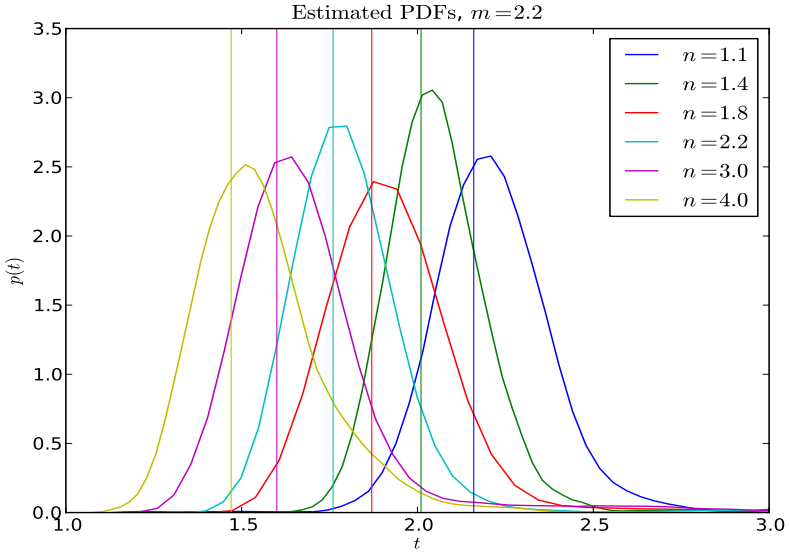

Figure 4.20.: Estimated PDFs for different values of n and fixed $m = 2.2 > 2$. Interestingly, a greater exponent n which corresponds to a stronger mean- reversion for large prices $x(t)$ does not only not help to postpone the FTS but leads to its earlier occurrence instead. Note also that the PDFs show a substantial overlap as the median critical times lie very close to each other.

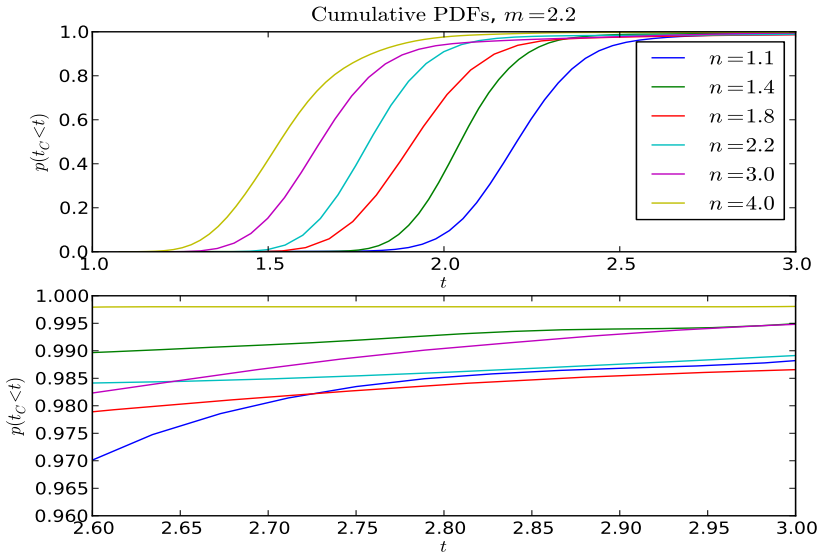

Figure 4.21.: The CPFs intercept close to $p(t_C < t) = 1$ reflecting that the hazard rate for long lasting sample paths to die is not the same for every n investigated. In fact, especially the value $n = 1.8$ seems to have a particularly good chance for a comparably long life, see also figure 4.22.

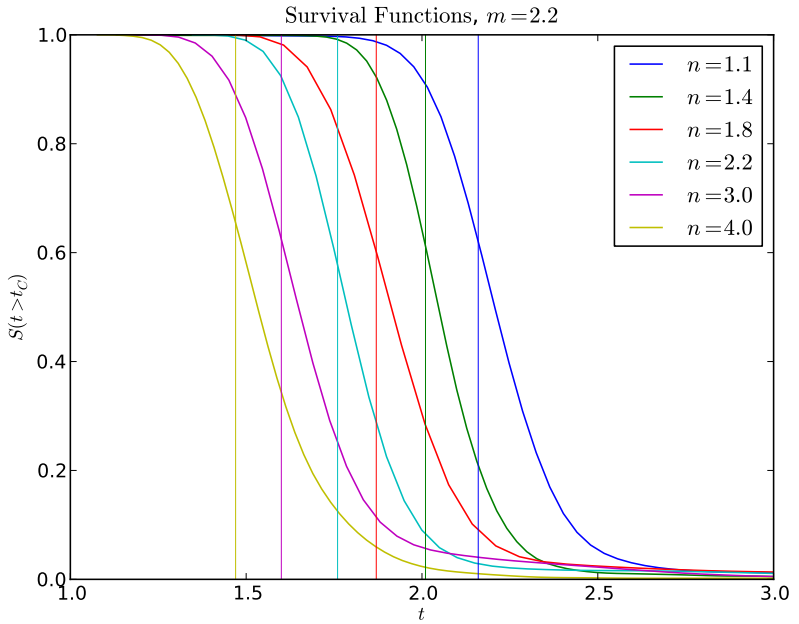

Figure 4.22.: The survival functions for $m = 2.2$ and several values of n

4.4.3.1.2. Dependence of Critical Times on n As in the corresponding preceding chapters, we plot the behavior of $\widetilde{t_C}(n)$ for fixed $m > 2$ and compare this to the deterministic findings which are obtained by two mutually different implementations of the Ide-Sornette

model: The DDIRDI2 scheme (see Chapter 3 and Appendix B) which serves again as our main program for the stochastic case and a classical four-stage Runge-Kutta scheme which we employ to test the results obtained from DDIRDI2 which is in the case $\varepsilon_1 = \varepsilon_2 = 0$ nothing different than an alternative implementation of the deterministic model. The deterministic critical times as well as the medians of the stochastic ensemble critical times are found to follow a power law function

$$t_m(n) = Bn^{\nu} \tag{4.39}$$

The calculation and discussion of Shannon's entropy will follow in the upcoming section of

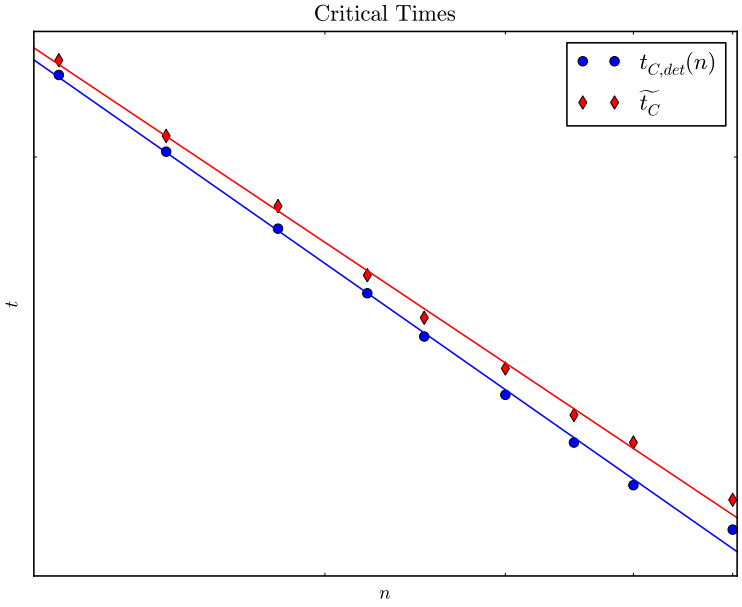

Figure 4.23.: Deterministic critical times and ensemble median critical times as a function of n. The double-logarithmic plot suggests a power law decay which is found to be in excellent agreement with the data: For the blue curve, we obtained $B = 2.216$ and $\nu = -0.292$ while for the red curve, $B = 2.24$ and $\nu = -0.279$. In both cases, $R^2 = 0.999$.

the analysis, for the sake of a better direct comparison.

4.4.3.2. $m < 2$

In the following paragraphs, we investigate the Ide-Sornette model for the supposed regime $m < 2$.

4.4.3.2.1. Survival Analysis In this regime, we chose $m = 1.4$ and varied n in the range from 1.1 to 1.75. The results can be seen in the following graphs. We stress again that it has been checked for every simulation run if the kernel density regression does give a good estimate for the 'true' PDF by comparing the regression to the raw data (histogram).

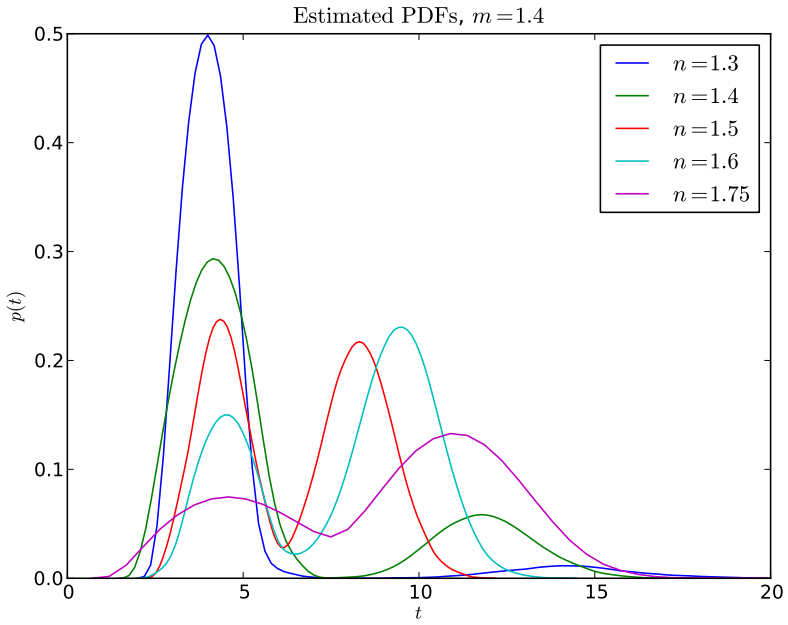

Figure 4.24.: Estimated PDFs for various values of n in the range from 1.3 to 1.75. For the sake of lucidity, the PDFs for $n = 1.2$ and $n = 1.1$ are omitted as they have an unimodal appearance and would clearly disturb the message of the graph: As n approaches m, the PDF starts to switch from an unimodal to a bimodal appearance indicating that there are two time domains in which the hazard rate for a sample path is significantly higher than normal.

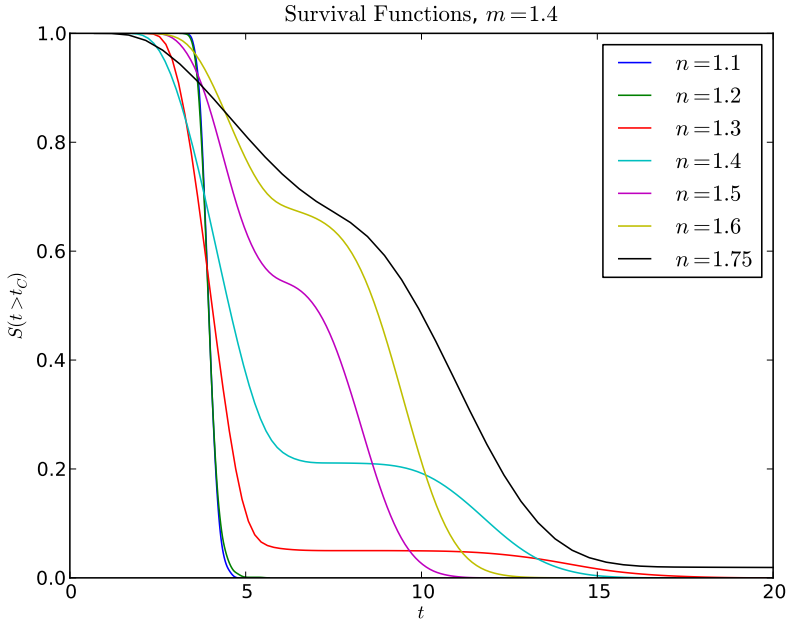

Figure 4.25.: Survival functions for $m = 1.4$ and various values of n.

4.4.3.2.2. Dependence of Entropy on n As remarked earlier on, we calculate Shannon's entropy for both, $m > 2$ and $m < 2$ in this last paragraph of the analysis. Figure 4.26 illustrates our findings where the blue curve is a fit of our data to the curve

$$S_m(n) = \frac{a}{1 + b\exp(-cn)} + d \tag{4.40}$$

which is a logistic function with offset d to the n axis.

4.4.3.3. Discussion

The impact of small multiplicative white noise ($\varepsilon_1 = \varepsilon_2 = 0$) on the full Ide-Sornette model was investigated in this section for a limited set of parameter combinations. For the cases investigated, we find that the PDF of critical times is unimodal and quasi-constant in its width as measured by the Shannon entropy for $m = 2.2$ (supposed regime $m > 2$) while for $m = 1.4$ (supposed regime $m < 2$), the PDF of critical times is bimodal for $n \geq 1.3$ and unimodal for $n \leq 1.2$. Moreover, the critical times are found to follow a power law behavior for $m = 2.2$ similar to the situation found in the stochastic nonlinear frictionless oscillator while for the small noise amplitude that has been considered, we find that the median ensemble critical times are larger than the deterministic ones, as estimated from numerical simulations. Interestingly, the stretched exponential decay of the entropy S that we have have found in

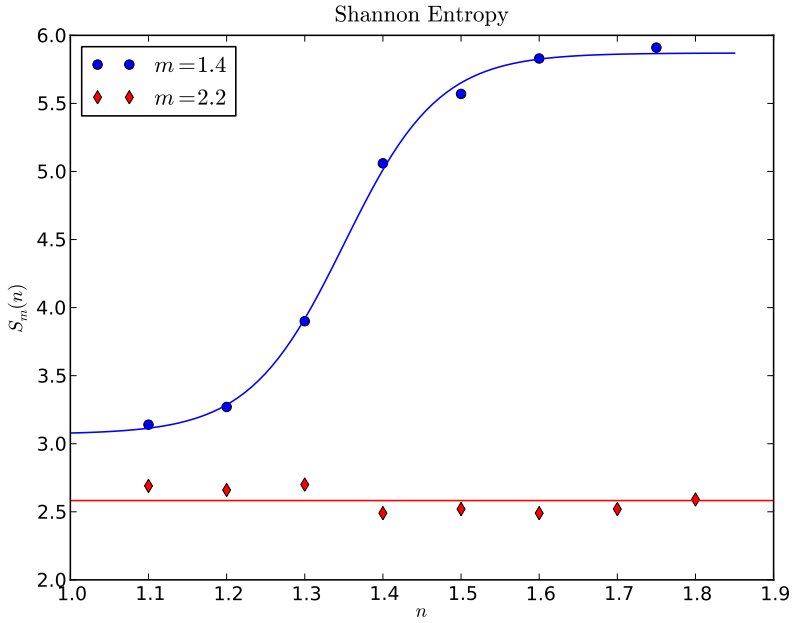

Figure 4.26.: The Shannon entropy $S_m(n)$ for both regimes considered, $m > 2$ and $m < 2$. For $m = 2.2$, $S_{2.2}(n)$ is found to be scattered around a constant value of $S_{2.2}(n) = 2.58$ ($R^2 = 0.999$) whereas we find a good agreement of our numerical data to a modified sigmoidal curve. For the parameters of (4.40), we obtain $a = 2.80$, $b = 4.757 \cdot 10^9$, $c = 16.50$ and $d = 3.07$ while we again recover $R^2 = 0.999$.

the components comprising the model, is not recovered in the full model. Instead, we find a logistic growth behavior of $S_m(n)$ for $m = 2.2$, i.e. the entropy *grows* with n as opposed to the stochastic oscillator case where $\partial_n S(n) < 0$.

4.5. Summary and Outlook

This first part of the thesis was concerned with the impact of multiplicative (i.e. parametric) white noise on the Ide-Sornette model for financial markets. Apart from the software developmental implications, the main goal was to study the noisy version of the model, to compare its behavior to the deterministic case and to find differences if there are any.
We have documented the necessary theoretical background and our results in the following way: In Chapter 1, we have given a short introduction to the relatively new field of science called complex system theory and we have explained how the wording 'complex adaptive systems' is to be understood. In Chapter 2, we introduced the main ideas and assumptions that led to the deterministic Ide-Sornette model and provided a detailed analysis of the model in the spirit of the original work [6]. We have moreover expanded the analysis from the original paper by also providing an analytical closed-form solution of the frequency-amplitude relation of the nonlinear frictionless oscillator exploiting the work of Mohazzabi [12]. In Chapter 3, we have introduced the basics of stochastic calculus, stochastic differential equations and the most important stochastic processes, namely the Wiener process and the Ornstein-Uhlenbeck process (mean-reverting random walk) which we will need in the second part of this work. In addition, the important difference between additive and multiplicative noise to the behavior of the system was explained and demonstrated using a textbook example from [20]. In Chapter 4, we have tackled the challenge to extend the Ide-Sornette model towards parametric white noise in order to bring the model closer to the reality observed in financial markets. The rather technical but nonetheless necessary background concering the numerical aspects of this work have also been laid out in this chapter followed by a short introduction to survival analysis. Analyzing the subparts of the model, we find several effects of noise: Firstly, looking at the median of critical times, we find that the occurrence of FTS is, on average, postponed as compared to the deterministic version in case of the Sornette-Andersen model while the noisy nonlinear oscillator is driven to a FTS, an entirely unexpected noise-induced phenomenon which we have successfully supported by a scaling argument that was previously used in the literature [74]. As to the interpretation of these effects, we have argued that both types of traders, fundamentalists and trend-followers, are somewhat perturbed in following their strategies in the presence of noise, even leading to a FTS in the case of only fundamentalists in the market.

Having said that, the conclusion concerning the full version of the model is split: Indeed, we recovered two mutually different regimes as in the deterministic case, however in a different sense: Deterministically, we referred to the behaviour of the frequency at the approach of t_C while in the stochastic case, we referred to the distribution of the critical times and the

behavior of the Shannon entropy which was derived from this distribution.

In the present work, we have restricted ourselves to only a very limited fraction of the parameter space and remark that the best possible certainty about the general behavior of the system would require a search of the whole parameter space along with an automatized data handling and analysis. However, the foundation is now laid and ready for further investigations. These might include:

- What features of *real* financial market time series does the model show? These features are usually referred to as 'stylized facts' and the interested reader can find a brief introduction to the field in Appendix D. For example, it is supposed that the PDF of the return time series will be at least bimodal (but in general multimodal) resulting from the oscillatory component. At the time of writing, this is only a conjecture. However, it seems to be supported by a few tests using 'bare eyes' that the author has conducted. A more quantitative and systematic approach would require the implementation of a robust statistical test for multimodality as the one proposed recently by Henderson [79]. Due to the sixdimensionality of the parameter space $(\alpha, \gamma, n, m, \varepsilon_1, \varepsilon_2)$, the minimum required number of price and return time series per parameter combination (at least 1000, but the more, the better...) and the possible extra-efforts of statistical tests such as bootstrapping one data sample 5000 times (as in [79])), answering the stylized facts question will require a very efficient and stable code for data analysis. The basis for obtaining such data has been created in this work.

- Calibration of the model: If it reflects the behavior of any real price or return time series, at which time scale does it do so ((milli-)seconds, hours, days, weeks, years)?

- Given that we have answered the preceding questions, can we estimate the parameters n and m from financial market data to draw conclusions about levels of trend-following and mean-reversion in the market? Can such an estimate give evidence of the idea of an inertia being present in the market?

- What are the pros and cons of this model compared to other financial market models that exhibit (or fail to exhibit) stylized facts? Can these models somehow be merged for the better good?

Part II.

Singularities All Around?

5. Modelling the Short-Term Riskless Interest Rate

Often you have to rely on intuition

Bill Gates

In this chapter, we will investigate the possibility of a singularity in finite time in a widely-used class of models in mathematical finance. The occurrence of a FTS in these models would be relevant for example in certain econometric tests that rely on an infinite lifetime of the process.

5.1. Introduction

For many applications in finance, economics and business administration, it is important to model the short-term riskless interest rate. For example, two Nobel prize winning models that use the short-term riskless rate r as one of their key parameters are the Capital Asset Pricing Model (CAPM) by Markowitz[1] which provides the basis for modern portfolio theory and the Black[2]-Scholes[3] formula for option pricing[4]. In a general framework, all of the known models to describe the behavior of r (and in some cases also of the price) are a subclass of the SDE of first order in time

$$\mathrm{d}Z_t = (\alpha + \mu Z_t)\mathrm{d}t + \sigma Z_t^m \mathrm{d}W \tag{5.1}$$

[1] Harry Markowitz, born 1927, American economist, Nobel price for Economics 1990

[2] Fisher Sheffey Black, 1938-1995, American economist

[3] Myron Scholes, born 1941, American economist

[4] American economist Robert C. Merton, born 1944, was the first to publish a model concerned with option pricing that coined the term 'Black-Scholes model' in 1973. Merton was awarded the Nobel price for economics together with Scholes in 1997 with Black being mentioned by the Swedish Academy as 'an important contributor' (being ineligible for the Nobel price having died in 1995).

with nonnegative constants α, μ, σ and m. Understanding the different models that arise from this class of processes is thus the key to finding optimal investment strategies for different types of investors (risk-averse or willing to take risks). As it was shown in the literature [63, 64], models with $m \geq 1$ perform better in terms of goodness of fit to empirical financial market data than models which require the parameter m to be smaller than one. In this part of the thesis, we demonstrate a few new findings about models which require $m \geq 1$, namely we will be looking at the CIR-VR (Cox[5]-Ingersoll[6]-Ross[7] with variable rate, 1980) and the CEV (constant elasticity of variance, Cox, 1975) and provide a closed form analytical solution of the corresponding model class CIR-CEV.

5.2. The CIR-CEV Class of Models

The CIR-CEV class of models arises from equation (5.1) and reads

$$\text{CIR} - \text{VR}: \qquad \mathrm{d}Z_t = \sigma Z^{\frac{3}{2}} \mathrm{d}W_t \tag{5.2a}$$

$$\text{CEV}: \qquad \mathrm{d}Z_t = \mu Z_t \mathrm{d}t + \sigma Z_t^m \mathrm{d}W_t \tag{5.2b}$$

Equation (5.2a) has been put forward in the context of variable rate loan contracts [71] which uses $m = \frac{3}{2}$ while most other models have been introduced and analyzed predominantly for $0 < m \leq 1$ which is surprising in a sense that there is no reasonable economic *a priori* reason for this restriction [65]. Actually, for $m > 1$, eqs. (5.2) exhibit a positive feedback mechanism, i.e. the stochastic growth rate Z_t feeds back upon itself. We will therefore investigate the long-term behavior and the possibility of FTS in this model class for $m > 1$ in the following.

5.2.1. Outline of Investigations

To study the CIR-CEV model class, we will let us guide by the following scheme and look at the problem from four different angles:

- Simulation of the SDE
- Simulation of the corresponding FPE

[5] John Carrington Cox, born 1943, American economist
[6] Jonathan Edwards Ingersoll, born 1949, American economist
[7] Steven Allen Ross, born 1943, American economist

- Theoretical analysis using Schrödinger's potential formalism
- Derivation of an analytically exact solution of the process class given by eqs. (5.2)

5.2.2. Construction of the Probablility Density by Simulation of the SDE

For computational ease, we investigate the Lamperti transformed version of the original process (5.2) via

$$Y_t = \frac{1}{\sigma(1-m)} Z_t^{1-m}, \quad Z_t > 0 \tag{5.3}$$

to obtain the equivalent substitute process Y_t using Itô's formula

$$\mathrm{d}Y_t = \left(\mu(1-m)Y_t - \frac{m}{2(1-m)}\frac{1}{Y_t}\right) + \mathrm{d}W_t. \tag{5.4}$$

Looking at equation (5.4), we thus want to investigate whether or not $p(y \to 0, t) = 0$. A non-vanishing PDF at the origin would then correspond to a blow-up in finite time. This problem is non-trivial since, intuitively we would expect a FTS from eqs. 5.2 while we would not from equation (5.4). The dynamic properties therefore remain an interesting question.
The probability density function (PDF) $p(x,t)$ can be numerically constructed from the SDE in the following way: At first, the parameter μ and Y_0 of the model has to be chosen where we consider - without loss of generality - the case $\mu = 1$ and $Y_0 = -7$. In a second step, one has to define the numerical parameters such as step width and number of steps from which the instant T follows at which the PDF is to be constructed. Then, the process described by the SDE has to be simulated $M \geq 1000$ times in order to obtain a meaningful result (of course, the greater M, the better - but at the cost of additional computation time). In this case, $M = 5000$ which took about 80 minutes on a conventional laptop PC[8] to run. For every M, the last value of the process at instant T, i.e. $Z(T)$ is saved in an array. The histogram of this array is subsequently constructed which is, for large M, a good approximation of the actual PDF at instant T. The following figures illustrate our results while it is worth noting that the number of bins is affecting the shape of the approximated PDF, a fact already encountered when dealing with the Shannon entropy in the first part of this work.

[8]Pentium IV, 1.67 GHz, 1 GB RAM

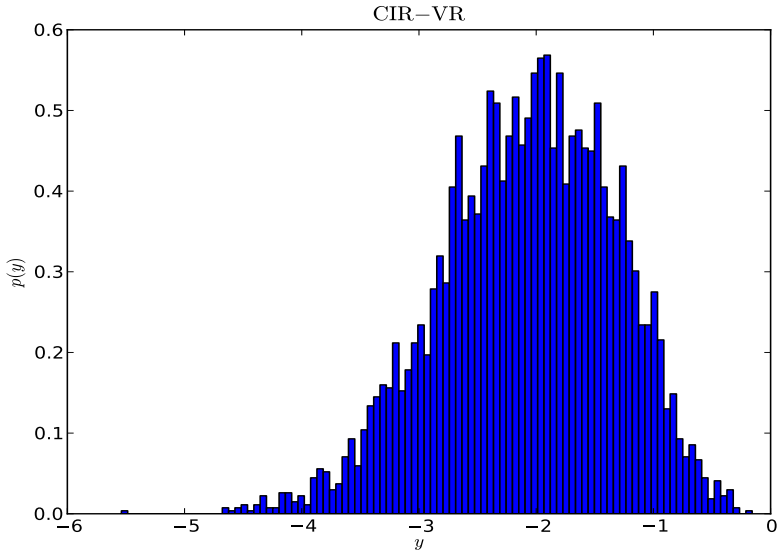

Figure 5.1.: Histogram (100 bins) of the endpoints of 5000 sample paths of the original CIR-VR process ($m = 1.5$) at instant $T = 4$ ($\Delta t = 0.002, N = 2000$). The median of the end points was found to be ≈ -2.03.

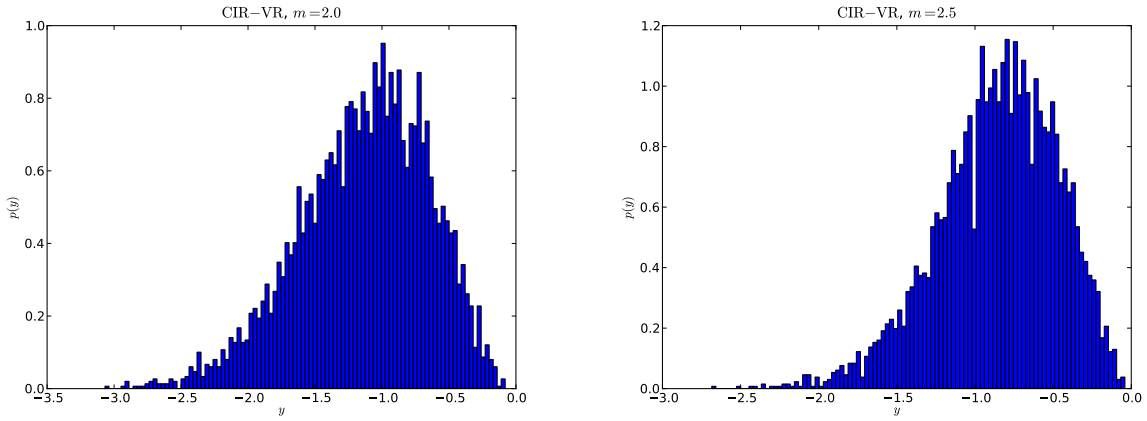

Figure 5.2.: Approximate PDFs (histograms with 100 bins, as above) constructed as explained above for greater values of m: In the left picture, $m = 2.0$ while in the right figure, $m = 2.5$. The medians (as a measure for the maximum of the PDF) move towards $y = 0$ without reaching it, giving -1.09 (left panel) and -0.82, respectively.

5.2.3. Direct Simulation of the Probability Density via the Corresponding FPE

In this section, we quickly give the results of the simulation of the FPE corresponding to the process (5.4) for various values of m. The equation under study reads

$$\frac{\partial}{\partial t}p(y,t) = -\frac{\partial}{\partial y}\left(\mu(m-1)y + \frac{m}{2(m-1)y}\right)\cdot p(y,t) + \frac{1}{2}\frac{\partial^2}{\partial y^2}\cdot p(y,t)) \tag{5.5}$$

The results are found to be in very good agreement to the previous section. The following pictures illustrate these results where it is remarked that the simulation computed the values of the PDF at $t = 6$ where the time domain was discretized in steps of 10^{-2} and the solution domain was treated as a onedimensional grid $\mathcal{G} = [-5{,}0]$ with a step width of $\Delta x = 10^{-2}$. For further numerical details, the interested reader is referred to Appendix C.

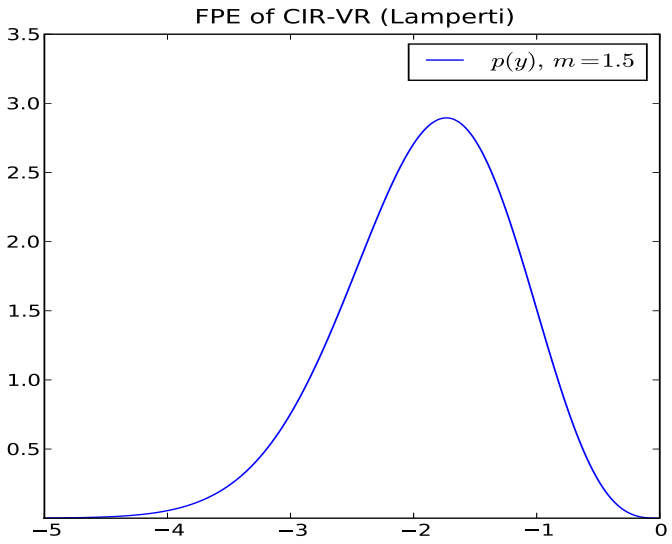

Figure 5.3.: PDF for $m = 1.5$ as obtained from a Finite-Elements simulation of the corresponding FPE.

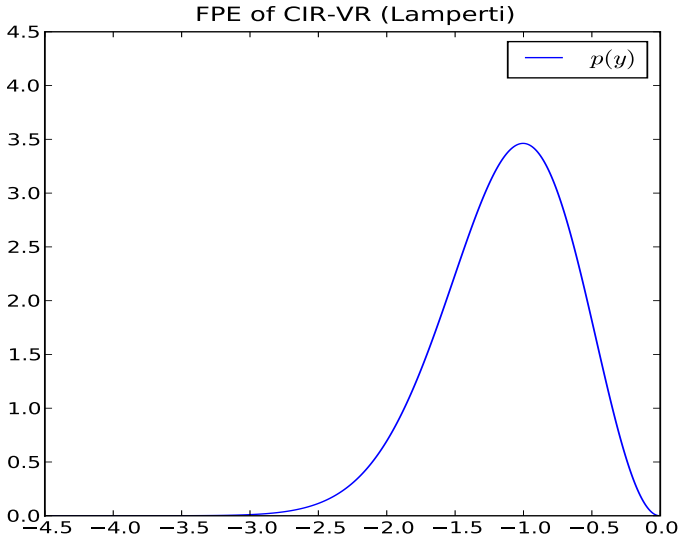

Figure 5.4.: Same graph as figure 5.3 for $m = 2$.

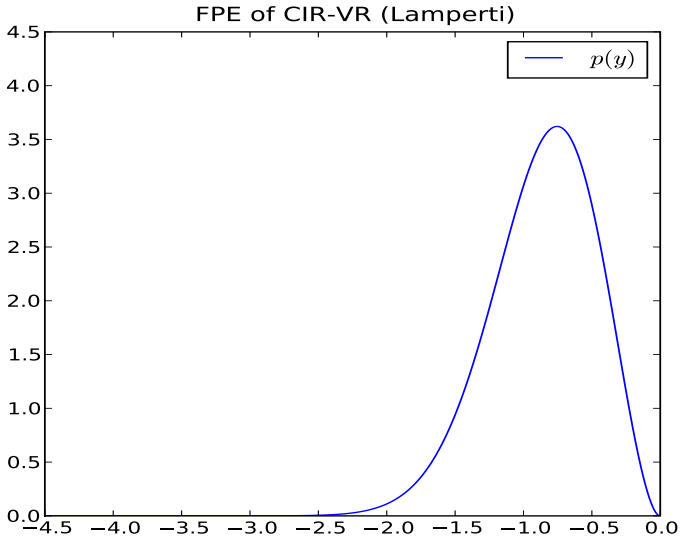

Figure 5.5.: PDF for $m = 2.5$

5.2.4. Schrödinger's Formalism

In this section, we will employ a method from the book by Risken [46] introduced as as 'Schrödinger[9]'s formalism' due to its formal similarity to quantum mechanics. For the ease of

[9]Erwin Schrödinger (1887-1961), Austrian physicist, Nobel price for physics in 1933

the reader, we start from equation (3.6) which reads

$$\mathrm{d}X_t = f(t, X_t)\mathrm{d}t + g(t, X_t)\mathrm{d}W_t$$

We remember the definition of the FPE

$$\frac{\partial}{\partial t}p(x,t) = -\frac{\partial}{\partial x}(f(x,t)\cdot p(x,t)) + \frac{1}{2}\frac{\partial^2}{\partial x^2}(g(x,t)\cdot p(x,t))$$

and realize that the case $g(x,t) = \text{const}$ amounts to solving a Schrödinger-like equation

$$\partial_t\psi(y,t) = \left[D\partial_y^2 - V(y)\right]\psi(y,t) \tag{5.6}$$

with some potential $V(y)$ appropriate to the problem. We thus employ the Lamperti transform on our original SDE to obtain an equation of the form

$$\mathrm{d}Y_t = \tilde{f}(t, Y_t)\mathrm{d}t + \mathrm{d}W_t \tag{5.7}$$

with the equivalent FPE

$$\partial_t p(y,t) = \left[\frac{1}{2}\partial_y^2 - \partial_y\tilde{f}(y,t)\right]p(y,t) \tag{5.8}$$

In the aformentioned book, Risken introduces Schrödinger's potential V_S corresponding to the problem as

$$V_S = \frac{1}{4D}(\tilde{f}(y))^2 - \frac{1}{2}\partial_y\tilde{f}(y) \tag{5.9}$$

and study the behavior of this potential as an equivalent analysis. In our case, this calculational scheme for equation (5.4) yields

$$V_S(y) = \frac{1}{2}\left[\mu(m-1)y + \frac{m}{2(m-1)y}\right]^2 + \frac{1}{2}\mu(m-1) + \frac{m}{4(m-1)}\frac{1}{y^2} \tag{5.10}$$

where we have again used equation (5.4). The shape of this potential for different values of m is illustrated in figure 5.6 and is in excellent agreement with our previous findings.

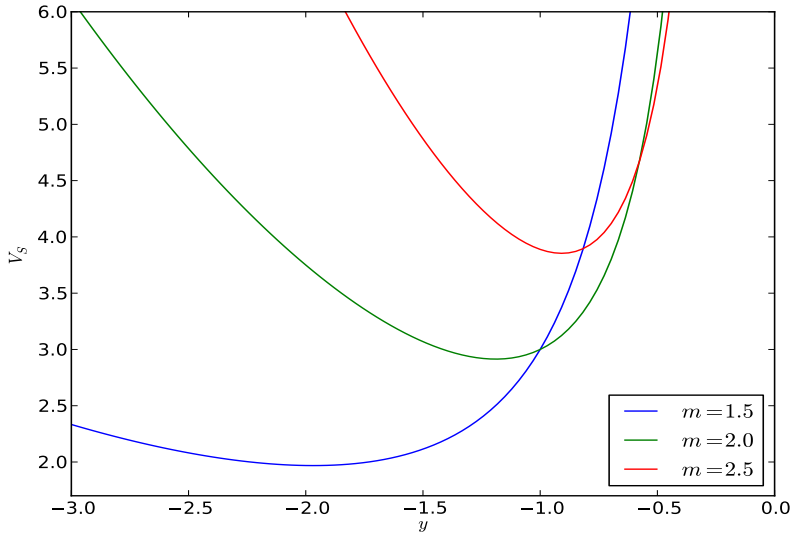

Figure 5.6.: V_S for three different values of the parameter m. The potential's minimum moves exactly as expected and is in excellent agreement with our findings so far.

5.2.5. Exact Solution of the SDEs

The analytical solution of stochastic differential equations is often very hard (and more often impossible) as there is no such thing as a solution theory for SDEs. There is not even a standard procedure as in the case of certain ODEs. However, during our computational analysis, it came to our attention that equation (5.4) together with the choice $\mu = 0$ is also known as Bessel[10] process which is defined by the SDE

$$\mathrm{d}R_t = \frac{d-1}{2R_t}\mathrm{d}t + \mathrm{d}W_t \tag{5.11}$$

which is, as we have just shown, obviously nothing different than the Lamperti transformed version of the CIR-VR process. The Bessel process however (5.11) is known to have the analytical solution

$$R_t = \left(\sum_{i=1}^{d} W_i^2(t)\right)^{\frac{1}{2}} = \sqrt{W_1^2(t) + \cdots + W_d^2(t)} \tag{5.12}$$

where the parameter d corresponds to the dimension of the underlying random walk. To see that the process (5.12) indeed solves the SDE (5.11), we start from the definition of R_t as $R_t = \left\|\vec{W}(t)\right\|_{L^2}$ such that $R_t^2 = \sum_i W_i^2(t)$ where $\vec{W}(t) = (W_1, \ldots, W_d)^T$. Then, we compute

[10] Friedrich Wilhelm Bessel, 1784-1846, German astronomer and mathematician

the stochastic differential exploiting Itô's formula again

$$\mathrm{d}f(\vec{W}(t)) = \sum_{i=1}^{d} \frac{\partial f}{\partial W_i}\mathrm{d}W_i + \frac{1}{2}\sum_{i=1}^{d} \frac{\partial^2 f}{\partial W_i^2}\mathrm{d}t \tag{5.13}$$

Applying this to our analytical expression (5.12) yields

$$\begin{aligned} \mathrm{d}R_t &= \sum_{i=1}^{d} \frac{W_i}{R_t}\mathrm{d}W_i + \frac{1}{2}\sum_{i=1}^{d}\left(\frac{1}{R_t} - \frac{W_i^2}{R_t^3}\right)\mathrm{d}t \\ &= \frac{1}{R_t}\sum_{i=1}^{d}\left[W_i\mathrm{d}W_i + \frac{1}{2}\left(1 - \frac{W_i^2}{R_t^2}\right)\mathrm{d}t\right] \end{aligned} \tag{5.14}$$

Now, the first factor on the right-hand side of the last expression, $\frac{1}{R_t}\sum_{i=1}^{d} W_i\mathrm{d}W_i$, is a real-valued Brownian motion since $\mathbb{E}\left[\frac{1}{R_t}\sum_{i=1}^{d} W_i\mathrm{d}W_i\right] = 0$ and $\mathbb{E}\left[\left(\frac{1}{R_t}\sum_{i=1}^{d} W_i\mathrm{d}W_i\right)^2\right] = \mathrm{d}t$ so that

$$\mathrm{d}R_t = \mathrm{d}W + \sum_{i=1}^{d}\frac{1}{2R_t}\left(1 - \frac{W_i^2}{R_t^2}\right)\mathrm{d}t \tag{5.15}$$

Furthermore, it holds that

$$\sum_{i=1}^{d}\left(1 - \frac{W_i^2}{R_t^2}\right) = d - 1$$

so that SDE (5.11) follows right away. We have thus found the analytical solution of the CEV process with $\mu = 0$ as the back transform of eq. (5.3) in cases where d is integer:

$$\begin{aligned} Z(t) &= (\sigma(1-m)R(t))^{\frac{1}{1-m}} \\ &= (\sigma(1-m))^{\frac{1}{1-m}}\left[W_1^2(t) + \cdots + W_d^2(t)\right]^{\frac{1}{2-2m}} \end{aligned} \tag{5.16}$$

Furthermore, the parameter m is related to the dimension of the Brownian motion via

$$d - 1 = \frac{m}{m-1} \quad \Leftrightarrow \quad d_m = \frac{2m-1}{m-1} \tag{5.17}$$

from which it follows that $\lim_{m\to\infty}\delta_m = \searrow 2$ which means that for any economically reasonable m, $\delta_m > 2$. For example, the standard CIR-VR process with $m = \frac{3}{2}$ yields $d = 4$ so that the process $Z(t)$ is shaped by a fourdimensional standard Wiener process (Brownian motion). Because of the general form of the solution (5.16), it is clear that the process $R(t)$ will never reach the value zero and in consequence, $Z(t)$ remains finite for any t. Our conjecture about the occurrence of FTS in the CIR-VR process is moreover no longer justified. However, it is known that in a space-time-continuous setting, there is always a non-zero probability for

a d-dimensional random walk to visit in finite time some small area of radius ε around the origin before escaping to infinity [66] so that it can be concluded that there will be large excursions of the process $Z(t)$ before it eventually settles down to zero. Figure (5.7) provides some illustration.

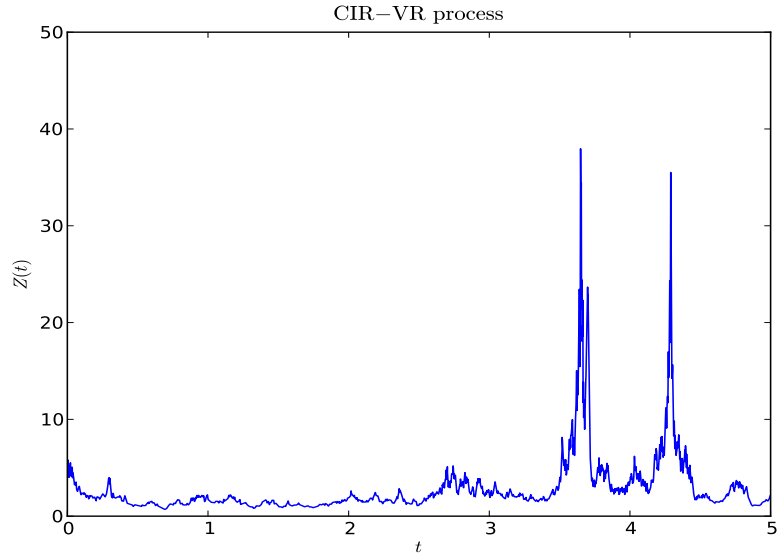

Figure 5.7.: Sample realization of $Z(t)$ obtained by simulation of the corresponding SDE, $Z_0 = 5$.

The remaining question is if we can specify an analytical solution in the case $\mu > 0$. To test this, we test the process $Y_t = \left(\sum_{i=1}^{d} M_i^2\right)^{\frac{1}{2}}$ where the M_i are d independent mean-reverting random walks, i.e. Ornstein-Uhlebeck processes where

$$\mathrm{d}M_i = -\beta M_i \mathrm{d}t + \sigma \mathrm{d}W_i. \tag{5.18}$$

In complete analogy to the proof of the case $\mu = 0$, we obtain

$$\begin{aligned}
\mathrm{d}Y_t &= \frac{1}{Y_t}\sum_{i=1}^{d}\left(M_i \mathrm{d}M_i + \frac{1}{2}\left(1 - \frac{M_i^2}{Y_t^2}\right)\right) \\
&= \frac{1}{Y_t}\sum_{i=1}^{d}\left[M_i(-\beta M_i \mathrm{d}t + \sigma \mathrm{d}W_i) + \frac{d-1}{2}\mathrm{d}t\right] \\
&= \left[\frac{d-1}{2Y_t} - \frac{1}{Y_t}\sum_{i=1}^{d}\beta M_i^2\right]\mathrm{d}t + \sigma \mathrm{d}W \\
&= \left[-\beta Y_t + \frac{1}{2}\frac{m}{m-1}\frac{1}{Y_t}\right]\mathrm{d}t + \sigma \mathrm{d}W
\end{aligned} \tag{5.19}$$

These results were obtained in collaboration with Stefan Reimann and Didier Sornette [65]. One can thus identify $\beta = \mu(m-1)$ with a mean-reversion level $\mu' = 0$ in the standard OU process. $\mu(m-1)$ is thus the mean-reversion rate. Y_t is thus bounded by definition (as it is mean-reverting) which means that Z_t will *not* go to zero at long times but will remain stationary while also exhibiting very large excursions as Y_t visits neighbourhoods of zero.

5.3. Summary and Outlook

In summary, we have again seen how hard it is to draw conclusions about the behavior of a stochastic process by pure intuition, i.e. by looking at the equations using 'common sense'. The undisputed advantage of this venture is that we have demonstrated that there are analytical closed-form solutions for Z_t, namely

$$Z_t = \left[\sigma(1-m)\left(\sum_{i=1}^{d} W_i^2\right)^{\frac{1}{2}}\right]^{\frac{1}{1-m}} ; \quad \mu = 0 \tag{5.20}$$

$$Z_t = \left[\sigma(1-m)\left(\sum_{i=1}^{d} M_i^2\right)^{\frac{1}{2}}\right]^{\frac{1}{1-m}} ; \quad \mu > 0 \tag{5.21}$$

which tells us that there are no true FTS in neither of the processes but on the other hand, there will be large excursions that may resemble singular behavior. It can also be remarked that the results of this analysis offer a new perspective on the well-known phenomenon of herding in financial markets: If we think of the process (5.2a) as a general model for financial markets with variable $m > 1$, then, according to our reasoning concerning eqs. (5.17), herding reduces the dimension of the underlying d dimensional Wiener process $\vec{W}(t)$ as herding would correspond to greater values of m implying smaller values of d_m. This is like new light through old windows since this compactly grasps the actual nature of herding. A possible future application resulting from this is the estimation of the parameter m from real financial market price or return trajectories exploiting the fact that a d_m dimensional radial Ornstein-Uhlenbeck process produces random variables that are χ^2 distributed [65].

A. Scaling Analysis

In this appendix, the power of the very simple scaling analysis due to Mallick and Marcq [74] is demonstrated. For this, the exact derivation is outlined in a non-exhaustive way to provide the reader with the involved technicalities and to motivate our decision to stick to the scaling analysis in the main text of this work along with numerical evidence. The aforementioned exact calculation considers the system without noise first ($\ddot{x} + \gamma x^{2r-1} = 0$) whose energy is known to be

$$E = \frac{\dot{x}^2}{2} + \gamma \frac{x^{2r}}{2r} \tag{A.1}$$

The exact solution of this mechanical system is also known (see also calculations in Chapter 2, Section 2.2.2):

$$x = E^{\frac{1}{2r}} S_r \left[(2rE)^{\frac{r-1}{2r}} t \right] \tag{A.2}$$

$$\dot{x} = (2n)^{\frac{r-1}{2r}} S_r' \left[(2rE)^{\frac{r-1}{2r}} t \right] \tag{A.3}$$

where S_r is the inverse function of an hyperelliptic integral of the form $\int \frac{\mathrm{d}u}{\sqrt{1-\frac{u^{2r}}{2r}}}$. The main idea is that one can switch to energy-angle variables, i.e. (E, ϕ) coordinates, using these notations. The noise is introduced as in the main text of this thesis, i.e. $\dot{E} = \sigma x \dot{x} \xi(t)$, so that

$$\dot{E} = \sigma (2r)^{\frac{r-1}{2r}} E^{\frac{r+n}{2r}} S_r'(\phi) S_r^n(\phi) \xi(t) \tag{A.4}$$

Using eqs. (A.4) and (A.3) and introducing the shortcut $\Omega = (2r)^{\frac{r+1}{2r}} E^{\frac{r-1}{2r}}$, one finally arrives at the system

$$\dot{\Omega} = (r-1) S_r(\phi) S_r'(\phi) \xi(t) \tag{A.5}$$

$$\dot{\phi} = \frac{\Omega}{(2r)^{\frac{1}{r}}} - \frac{S_r^2(\phi)}{\Omega} \xi(t) \tag{A.6}$$

which fully describes the evolution of the noisy frictionless oscillator (4.18) without any approximation. Considering the FPE associated with this system and a few averaging manip-

ulations, the phase-averaged FPE is obtained which reads

$$\partial_t p = \frac{\sigma M_r}{2}\left(\partial_\Omega^2 p - \frac{2}{r-1}\partial_\Omega \frac{p}{\Omega}\right) \tag{A.7}$$

where M_r is a prefactor depending on r. This FPE is known to be exactly solvable and its solution $p(\Omega, t)$ can be used to calculate the ensemble mean energy. Assembling the findings gives

$$\langle E \rangle = \frac{1}{(2r)^{\frac{r+1}{r-1}}} \cdot \frac{\Gamma(\frac{3r+1}{2r-2})}{\Gamma(\frac{r+1}{2r-2})}(2\sigma M_r t)^{\frac{r}{r-1}} \tag{A.8}$$

where the factor M_n is defined over

$$M_r = \frac{(r-1)^2}{r+1}(2r)^{\frac{2}{r}} \cdot \frac{\Gamma(\frac{3}{2r})\Gamma(\frac{3r+1}{2r})}{\Gamma(\frac{1}{2r})\Gamma(\frac{3r+3}{2r})} \tag{A.9}$$

In the original article, this calculation takes several pages and is, at first sight, rather technically involved. A much easier and faster way is the scaling analysis, which would start from equation (A.1) and the noisy equation $\ddot{x} + \gamma x^{2r-1} = \sigma\xi(t)x$ to obtain

$$\dot{E} = E^{\frac{r+1}{2r}}\xi(t)$$

Approximating $\dot{E} \sim \frac{E}{t}$ and remembering $\xi(t) \sim t^{-\frac{1}{2}}$, one obtains

$$E \sim t^{\frac{1}{2}\cdot\frac{2r}{r-1}} = t^{\frac{r}{r-1}}$$

which is, in essence, the same result as (A.8).

B. The DDIRDI2 Integration Scheme

This numerical integration scheme belongs to the class of derivative free stochastic Runge-Kutta methods due to Rößler which have been introduced only very recently (2006-now). The notation is as easy as possible and follows the standard literature. We start from equation (4.2)

$$\mathrm{d}\vec{X}(t) = a(t,\vec{X}_t)\mathrm{d}t + b(t,\vec{X}_t)\mathrm{d}\vec{W}, \qquad X_{t_0} = x_0 \tag{B.1}$$

with drift term $a(t,\vec{X}_t) \in \mathbb{R}^d$ and diffusion matrix $b(t,\vec{X}_t) \in \mathbb{R}^{d\times m}$. In general, m denotes the dimension of the driving Wiener process and d the dimension of the stochastic process. In our case, $m = d$. The jth column of the diffusion matrix will in the following be denoted by b^j and time discrete approximations are considered, $Y_h = (Y_t)_{t\in(0,T_N)}$ The d-dimensional approximation process Y^h with $Y_n = Y_{t_n}$ is given by the following SRK method of s stages with $Y_0 = x_0$ and

$$\begin{aligned} Y_{n+1} = Y_n \;&+\; \sum_{i=1}^{s} \alpha_i a(t_n + c_i^{(0)}h_n, H_i^0)h_n \\ &+\; \sum_{i=1}^{s}\sum_{k=1}^{m} \left(\beta_i^{(1)} I_{(k),n} + \beta_i^{(2)} \frac{I_{(k,k),n}}{\sqrt{h_n}}\right) b^k(t_n + c_i^{(1)}h_n, H_i^{(k)}) \\ &+\; \sum_{i=1}^{s}\sum_{k=1}^{m} \left(\beta_i^{(3)} I_{(k),n} + \beta_i^{(4)}\sqrt{h_n}\right) b^k(t_n + c_i^{(2)}h_n, \widehat{H}_i^{(k)}) \end{aligned} \tag{B.2}$$

for $n = 0,1,\ldots,N-1$ with stage values

$$\begin{aligned} H_i^{(0)} &= Y_n + \sum_{j=1}^{s} A_{ij}^{(0)} a(t_n + c_j^{(0)}h_n, H_j^{(0)})h_n + \sum_{j=1}^{s}\sum_{l=1}^{m} B_{ij}^{(0)} b^l(t_n + c_j^{(1)}h_n, H_j^{(l)})\hat{I}_{(l),n} \\ H_i^{(k)} &= Y_n + \sum_{j=1}^{s} A_{ij}^{(1)} a(t_n + c_j^{(0)}h_n, H_j^{(0)})h_n + \sum_{j=1}^{s} B_{ij}^{(1)} b^k(t_n + c_j^{(1)}h_n, H_j^{(k)})\sqrt{h_n} \\ \hat{H}_i^{(k)} &= Y_n + \sum_{j=1}^{s} A_{ij}^{(0)} a(t_n + c_j^{(0)}h_n, H_j^{(0)})h_n + \sum_{j=1}^{s}\sum_{\substack{l=1\\ l\neq k}}^{m} B_{ij}^{(2)} b^l(t_n + c_j^{(1)}h_n, H_j^{(l)})\frac{\hat{I}_{(k,l),n}}{\sqrt{h_n}} \end{aligned} \tag{B.3}$$

The random variables of the method are defined by

$$\hat{I}_{(k,l),n} = \begin{cases} \frac{1}{2}(\hat{I}_{(k),n} - \sqrt{h_n}\tilde{I}_{(k),n}) & \text{if } k < l \\ \frac{1}{2}(\hat{I}_{(k),n} + \sqrt{h_n}\tilde{I}_{(l),n}) & \text{if } l < k \\ \frac{1}{2}(\hat{I}^2_{(k),n} - h_n & \text{if } k = l \end{cases} \tag{B.4}$$

for $1 \leq k,l \leq m$ with independent random variables $\hat{I}_{(k),n}$ for $1 \leq k \leq m$ and $\tilde{I}_{(k),n}$ for $1 \leq k \leq m-1$ and $0 \leq n < N$. In effect, only $m-1$ independent random variables have to be generated in each step. The coefficient family of the SRK method (B.2) can be displayed in an extended Butcher[1] array.

$$\begin{bmatrix} c^{(0)} & |A^{(0)} & |B^{(0)} & \\ c^{(1)} & |A^{(1)} & |B^{(1)} & \\ c^{(2)} & |A^{(2)} & |B^{(2)} & \\ & |\alpha^T & |\beta^{(1)^T} & |\beta^{(2)^T} \\ & | & |\beta^{(3)^T} & |\beta^{(4)^T} \end{bmatrix} \tag{B.5}$$

where $\alpha = (\alpha_i)$ and $\beta^{(k)} = \beta_i^{(k)}$ for $1 \leq k \leq 4$ are the vectors of weights and $A^{(k)} = (A^k_{ij})$ and $B^{(k)} = (B^k_{ij})$ for $k = 0,1,2$ the corresponding coefficient matrices. The class of weak order one diagonally drift implicit stochastic Runge-Kutta (DDISRK) methods is then given by

$$c^{(0)} = \begin{pmatrix} c_1 \\ c_2 + c_3 \end{pmatrix}, \quad A^{(0)} = \begin{pmatrix} c_1 & 0 \\ c_2 & c_3 \end{pmatrix}, \quad B^{(0)} = \begin{pmatrix} 0 & 0 \\ c_4 & 0 \end{pmatrix}$$
$$\alpha^T = (1 - c_5 \quad c_5), \qquad \beta^{(1)^T} = (1 \quad 0)$$

where every other coefficent is zero. The general DDIRDI2 scheme follows by putting $c_1 = 0$, $c_2 = 1 - \Theta$, $c_3 = \Theta$, $c_4 = 1$ and $c_5 = \Theta$ and some $\Theta \in [0,1]$. In this work, we have chosen $\Theta = \frac{1}{2}$ due to the the kind suggestion of Andreas Rößler [58].

[1] John C. Butcher, born 1933, New Zealand mathematician. Any numerical scheme can be described conveniently using a Butcher array, hence its widespread use in numerical mathematics

C. The Python Source Code

In line with this thesis, all required programs were written in the Python programming language, versions 2.5 and 2.6. This appendix contains the main program where the stochastic version of the Ide-Sornette model is implemented along with some analysis procedures which were developed for investigation of the time series created by the main loop. All routines were written from scratch by the author.

C.1. SDE

The implementation of the second order SDE that has been subject of the better part of this work was far more challenging to achieve than expected. Beside the usual period of vocational adjustment concering the programming itself, a great deal of time had to be spent in order to search for appropriate literature and code resources. Because of the very special form of the Ide-Sornette SDE, it was necessary to review the most recent developments in stochastic numerics. Surprisingly, the issue of stiffness of a SDE turned out to be so special that only *one* of the leading experts in the field I have contacted during my work (D. Higham (U. of Strathclyde, Scotland), P. Kloeden (U. of Frankfurt, Germany) and others) came up with the idea that stiffness might me the key to the solution of the serious numerical stability problems I encountered.

```
"""
    Simulation of the Stochastic Ide-Sornette model using Roessler's DDIRDI 2
    method
            -- Version 2 --
    Oliver Engler

    Date of last modification: February 3, 2010.
    Mod log: Estimation for t_C in the main loop (10-15-09)
    Implementation of t_C estimation by break condition (10-23-09)
```

```
    Tried out very small alpha and gamma (11-16-09)
    Implementation of leverage, vclustering according to Cont (11-17-09)
    Implementation of ensemble average of NLO energies according to Mallick
    (01-27/28-10)
    If-statement to kill trajectories that are uneconomic in a sense that
    g - W < 0 (02-03-10)

    a = 0: Nonlinear Oscillator of Degree n
    g = 0: Sornette-Andersen model
    else: Ide-Sornette
    If s1, s2 neq 0: Noisy models
"""

from scipy.optimize import fsolve
from pylab import *
import matplotlib
from numpy import *
from mpmath import gamma
import random
import statistics

#import psyco
#psyco.full()

""" The main set of parameters """

#random.seed(8)
dt = 0.01               # Time increments used
n  = 2.5             # The exponent n in the oscillatory deq
m = 1.4
X  = [ 5.0]            # Setting up arrays for x and v providing initial conditions
R  = [ 0.05]
t  = [ 0.0]             # Creating a time array
N  = 60000       # No. of evaluation points
dWx = [0]
dWy = [0]
Wx = []
Wy = []
a = 0.0             #alpha
g = 50.0            #gamma
s1 = 0.0           #epsilon1 (alpha)
s2 = 1.0         #epsilon2 (gamma)
Z = [0]
W = [0]
Wt= [0]
dR= [0]                 #R increments (volatility)
A = []
tC = []
M = 50
```

```
Rs= []
Rmax= []

""" Theoretical prediction for t_C in case gamma = 0 (Sornette-Andersen) """
def critical(r_0, M, alpha):
        return ((r_0)**(1.0-M))/(alpha*(m-1.0))

""" Theoretical prediction for w(n,A) according to Mohazzabi """
##def omega(A,n):
##        return (sqrt(pi*g/(2.0*(n+1))))*(A**(0.5*(n-1.0))) \
##        *(gamma((n+3)/(2*(n+1)))/(gamma((n+2)/(n+1))))

""" Our theoretical prediction for w(t) """
##def omega(g,n,m,x_0,r_0,alpha,T,t_C):
##        return (((r_0)**(2-m))/alpha*(2-m))*sqrt((g*pi)/(2*(n+1)))* \
##               gamma((n+3)/(2*(n+1)))/gamma((n+2)/(n+1))*(x_0 + \
##                (1-T/t_C)**((m-2)/(m-1))-1.0)**(0.5*(n-1))

""" Stylized Facts """
""" Defining the autocorrelation function of the time series x """
def autocorr(x):
    result = correlate(x, x, mode='full')
    return result[result.size/2:]/max(result)

def leverage(x):
        l = correlate(x, (abs(x))**2, mode = 'full')
        return l[l.size/2:]/max(l)

def vclustering(x):
        k = correlate((abs(x))**0.5, (abs(x))**0.5, mode = 'full')
        return k[k.size/2:]/max(k)

""" Defining F(x) """

def func(x, xold, rold, wx, wy):
    lhs = [x[0] - xold - (dt/2.0)*(rold + x[1]), x[1] - rold -
            (dt/2.0)*(a*rold*(abs(rold))**(m-1)
            - g*xold*(abs(xold))**(n-1) + a*x[1]*(abs(x[1]))**(m-1)
            - g*x[0]*(abs(x[0]))**(n-1)) - s1*wx*(abs(rold))**m +
           s2*wy*(abs(xold))**n]
    return lhs


""" The main loop """
for k in xrange(0,M):
        print k

        for i in xrange(0,N):
            dWx.append((sqrt(dt))*(random.gauss(0,1.0)))  # creating random numbers
```

```
            dWy.append((sqrt(dt))*(random.gauss(0,1.0)))
            #Wx = cumsum(dWx)
##            Wy = cumsum(dWy)
##            if g - Wy[i] < 0:
##                    print 'Process killed'
##                    break
            """
                In every call, take the last values of x and v as initial guess for
                fsolve and treat args as given parameters
            """
            result = fsolve(func, [X[i], R[i]], args = (X[i], R[i], dWx[i], dWy[i]))
            X.append(result[0])
            R.append(result[1])
            Rs.append(R[i]*R[i])
            t.append(t[i] + dt)
##            if X[i]*X[i+1]<=0:
##                Z.append((t[i] + t[i+1])/2.0)   #store zeros in t
##                Rmax.append((R[i]+R[i+1])/2.0)
##                Rs.append(Rmax[len(Rmax)-1]*Rmax[len(Rmax)-1])
               ##W.append(pi/(Z[len(Z)-1] - Z[len(Z)-2]))
##                Wt.append(omega(g,n,m,X[0],R[0],a,t[i],4.2))
            if R[i+1] - R[i] == 0:
                  tC.append((i+1)*dt)
                  print 'Critical time:'
                  print (i+1)*dt
                  print '--------------'
                  break
        ####        print 'Theoretical prediction (Sornette-Andersen):'
        ##        print critical(R[0], m, a)
        del dWx[1:len(dWx)]
        del dWy[1:len(dWy)]
        del X[1:len(X)]
        del R[1:len(R)]
        del t[1:len(t)]
##print 'median:'
##print '------------'
##print statistics.median(R)

print statistics.median(tC)
print statistics.mean(tC)
print len(tC)

""" Distribution of Critical Times """
subplot(211)
hist(tC, 50, normed = True, label = '$\mathrm{pdf}$')
legend(loc=0)

subplot(212)
y,x = statistics.pdf(tC)
```

```
plot(x,y, label = '$\mathrm{KDE}(p)$')
legend(loc=0)

""" Calculating energy ensemble average """
##energy = []
##summe = []
##c = arange(M)
##
##for j in xrange(0,N):
##        for k in c:
##                summe.append(sum(Rs[j+c[k]*N])) # len(Z) ~ N
##        energy.append(statistics.mean(summe[j]))
##
""" Theoretical prediction according to Mallick """
def f(x):
        return x**3 + 4*x - 2.0

""" Curve fitting procedures """
##from scipy.optimize import leastsq
##
##def residuals(p, rs, h):
##        err = rs - peval(h, p)
##        return err
##
##def peval(x,p):
##        return s2**(p[0])*h**(p[1]*((n+1)/(n-1)))
##
#h = linspace(0,N*dt,N)
##p0 = 0.0
##p1 = 1.0
##p = array([p0, p1])
##plsq = leastsq(residuals, p, args = (h, Rs))
##print plsq
##
""" Plotting the stuff """
#mu = fsolve(f, 0)

##plot(h, energy, label = '$<E(t)>$')
##plot(h, h**((n+1)/(n-1)))
###plot(h, exp(0.1*mu*h), label = '$e^{\mu t}$')
###plot(h, exp(0.0473466*h))
###plot(h,peval(h, plsq[0]), label = 'fit')
##xscale('log')
###xlim(1,N*dt)
##yscale('log')
##xlabel('$t$')
##ylabel('$<E(t)>$')
###legend(loc=0)
##show()
```

```
##""" Calculating trading days """
#t2 = array(t)
#t3 = t2/0.003

""" Calculate autocorrelation of absolute returns """
##R2=array(R)
##D = autocorr(abs(R2))

""" Calculate autocorrelation of returns """
#E = autocorr(R2)

#print R[len(R)-1]
#print(omega(X[0], n))

""" Plotting """

""" Trajectories """
##subplot(211)
##plot(t,X, '-g', label='$x(t)$')
##plot(t,R, '-r', label='$r(t)$')
##legend(loc=0)
##title('$n=%.1f$, $\gamma=%.1f$, $\sigma=%.1f$' %(n,g,s2))#$m=%.1f$, $a=%.3f$, $\epsilon_1=%
##xlabel('$t$')
##ylabel('$x$, $r$')
##xlim(2.5,)

""" Autocorrelation """
##subplot(311)
###plot(t,D, 'y-', label = 'autocorr($|r|$)')
##plot(E, label = 'autocorr ($r$)')
##xlabel('$\mathrm{time}$ $\mathrm{lag}$')
##ylabel('$C_{1}$')
###xlim(0,200)
###xscale('log')
###yscale('log')
##legend(loc=0)

""" Kernel Density Estimation """
##subplot(212)
##y,x = statistics.pdf(R)
###b,a = statistics.pdf(A, kernel = 'Gaussian')
##plot(x,y, 'y-', label='$\mathrm{KDE}$')
##hist(R, 50, normed = True, label = '$\mathrm{hist}$')
###plot(a,b, 'b-', label = '$\mathrm{Gauss}$')
##xlabel('$r$')
##ylabel('$p(r)$')
###xlim(-100,100)
###xscale('log')
```

```
###yscale('log')
##legend(loc=0)

""" Histogram of returns """
##subplot(312)
##hist(R, 200, normed = True, label = 'PDF')
###xlim(-100,100)
##legend(loc = 0)

""" ACF of absolute returns """
##plot(t, D, label = 'autocorr($|r|$)')
##legend(loc = 0)

##subplot(312)
###plot(t, cumsum(R), label='cumsum($r(t)$)')
##plot(t,X, label='$x(t)$')
###plot(t, X)
##legend(loc=0)

""" Numerical Test for w(t) """
##plot(Z[2:len(Z)-1],W[2:len(W)-1], 'y+', label='$\mathrm{num. estimated}$ $\omega (t)$')
##plot(Z[2:len(Z)-1],Wt[2:len(Wt)-1], 'r-', label='$\mathrm{predicted}$ $\omega (t)$')
#yscale('log')
#xlim(2.5, 4.0)
#ylim(4,8)
##plot(X, R, '-y')
##xlabel('$x$')
##ylabel('$r$')
#legend(loc = 0)

""" Plotting the volatility (std(returns)) """
##subplot(212)
##plot(t, dR, label='$\sigma (r)$')
##ylabel('$\mathrm{volatility}$')
###xlim(1.6,2.0)
###ylim(-3,3)
##legend(loc=0)

""" volatility clustering """
##subplot(312)
##vc = vclustering(R2)
##plot(vc, label = '$C_{1}(t)$')
##t1 = array(t)
##plot(t1**(-0.5))
###xscale('log')
###yscale('log')
###title('V-clustering and Leverage Effect')
##legend(loc=0)
```

```
""" Leverage Effect """
##subplot(313)
##l = leverage(R2)
##plot( l, label = '$L(t)$')
##xlabel('time lag')
##ylabel('$L$')
##legend(loc=0)

""" Plotting a sample Brownian Path """
##subplot(313)
###plot(t, Wx, 'b-', label='$W_x$')
##plot(t, dWy, 'y-', label='$W_y$')
###ylabel('$W(t)$')
##legend(loc=0)

""" Phase portrait """
##subplot(212)
##plot(X,R)
##xlabel('$x$')
##ylabel('$v$')

#savefig('Freq_Comparison', dpi=600)

show()
```

C.2. FPE

For simulation of the corresponding Fokker-Planck-Equations, the FiPy package [77] was employed which uses an object-oriented implementation of the class of Finite-Volume methods to discretize any given partial differential equation of the form

$$\partial_t(\rho\phi) - [\nabla \cdot (\Gamma_i \nabla)]^n \phi - \nabla(u\phi) - S_\phi = 0 \tag{C.1}$$

```
"""
    This script simulates the Fokker-Planck equation of the Lamperti transformed
    CIR-VR process

    d_t p(y,t) = -d_y[-m/(2*(1-m))*y^(-1)]p(y,t) + 0.5*d^2_y p(y,t)

    These terms are named transient, convection and diffusion term,
    respectively.
```

```
    Author: Oliver Engler
    December 9, 2009
"""

""" Initializations """
from fipy import *
from numpy import *
from pylab import *

""" Building a 1d linear grid with nx evaluation points that are equally spaced
    with interval dx """

nx = 900
dx = -0.01
mesh = Grid1D(nx=nx, dx=dx)

"""
    Suggested by D. Wheeler, seems not to work however. Intention was to
    build a solution domain (grid like (-5,...,0,...,1.0))
"""
##x0 = -5.0
##xn = 1.0
##nx = 100
##mesh = Grid1D(nx=nx, dx=(xn - x0) / nx) + ((x0,)))

m = 1.5
D = 0.5

y = mesh.getFaceCenters()

""" Initial Conditions """


p = CellVariable(name = '$p(y),$ $m=1.5$', mesh = mesh, value = 1.0, hasOld=False)


""" Boundary Conditions """

bc=(FixedValue(faces=mesh.getFacesRight(), value=0.0))

""" Defining the integration time """

timeStepDuration = 0.01
steps = 50
t = timeStepDuration*steps

""" The main loop """

eq1 = TransientTerm() == -ExponentialConvectionTerm(coeff = \
```

```
    m/(2*(y)*(m-1.))) + ImplicitDiffusionTerm(coeff=D)
eq2 = TransientTerm() == -ExponentialConvectionTerm(coeff = \
    m/(2*(y)*(m-1.))) + ExplicitDiffusionTerm(coeff=D)
eqCN= eq1 + eq2
#eq1.solve(var=p, boundaryConditions=bc)

for step in range(steps):
    eqCN.solve(var = p, dt = timeStepDuration)

if __name__ == '__main__':
    viewer=Viewer(title='PDF of Lamperti transformed CIR-VR (FPE)',
                  vars=(p))
    viewer.plot()   # save image requires filename = 'xy.pdf' in brackets
```

D. Empirical Findings in Financial Markets: Stylized Facts

D.1. Overview

In this section, we give a short overview of the empirical facts that are known about markets and asset returns in general. Our guideline for this is the review article by Rama Cont published in 2001 [28]. The wording 'stylized facts' can be dated back to 1961 when economist Nicholas Kaldor[1] first used it in a debate about the expansion of a model he had introduced four years earlier [59, 60]. In [61], a stylized fact is defined as 'a simplified presentation of an empirical finding' in the social sciences and particularly economics. Although there may be inaccuracies in detail due to the broad and generalized character of summarizing statistical computations into short stylized facts, they are essentially true statements about the considered systems. For example, 'Education significantly raises lifetime income.' is a stylized fact about the labour market although holding a PhD - the highest possible educational degree - may actually *lower* lifetime income since many PhD holders stay in the academics rather than entering much better paid fields and most PhD candidates do not get wages that reflect their actual market value [62]. These stylized facts are known to be found in *any* market which might be surprising: After all, it is unclear why properties of various assets such as commodity futures, blue chip stocks or the Euro/Dollar exchange rate should be similar. And, as financial market history has shown, not only similar but essentially equal. It is therefore a very important feature of any economic model to reflect at least some of these stylized facts. Thus, a thorough examination if a model, i.e. a stochastic model process, exhibits certain stylized facts and if so, which ones, is of great interest since 'most currently existing models fail to reproduce all of these statistical features at once' [28]. The most important stylized facts for which we will investigate our model in the following are:

[1] British economist, 1908 - 1986, most renowned for his contributions to welfare economics and economic growth theory.

1. Short-range correlation of returns
   The linear autocorrelation of asset returns

$$C(\tau) = \mathrm{corr}(r(t), r(t+\tau)) \tag{D.1}$$

   in *liquid markets* decays to zero very fast reflecting no significant serial dependence in the data, very much like a white noise process (see D.1). This absence of autocorrelation [69, 70] has been put forward as empirical evidence of the 'efficient market hypothesis' and is comparably easy to understand in that it excludes the possibility of statistical arbitrage which is a trading strategy with positive expected earnings based on the correlation of returns. Therefore, statistical arbitrage 'tends to whiten the spectrum of price changes' [28] and time series analysis methods cannot distinguish between price changes and a white noise process. It should be noted that autocorrelation has been found no longer absent when the time scale of the underlying data is increased [28]. In consequence, monthly returns often do show significant autocorrelation.

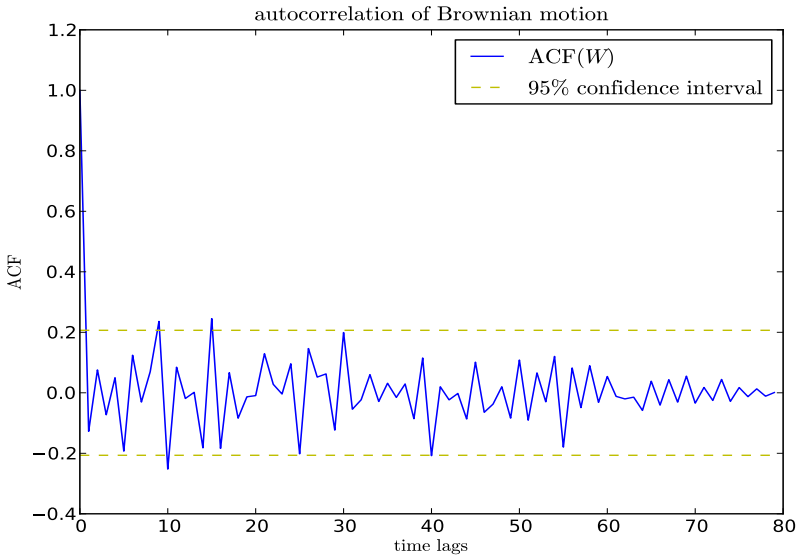

Figure D.1.: Autocorrelation (ACF) as a function of time lag τ of a standard Wiener process. The 95% confidence interval indicates that only values out of it are *significantly* differing from zero.

2. Long-range correlation of volatility
   The phenomenon of significant serial dependence in financial data is also referred to as *volatility clustering* and reflects the experience of probably anyone who has ever tried to invest in the stock market: 'High volatility events tend to cluster in time'. A 'normal' volatility time series thus features sudden bursts of volatility where returns exhibit a

high degree of variability (see figure D.3). A measure commonly used to quantify this stylized fact is

$$C_\alpha(\tau) = \mathrm{corr}(|r(t+\tau)|^\alpha, |r(t)|^\alpha) \tag{D.2}$$

where the usual choice is $\alpha = 2$.[2] Several studies that have used this measure remark that this ACF is in general positive and remains positive decaying slowly to zero [72, 28]. The VDAX of the Deutsche Boerse AG maps the behavior of the volatility of the German DAX over time and is often referred to as a measure for fear in the market. Figure D.2 shows the VDAX for the time period from 01/2000 through 11/2009.

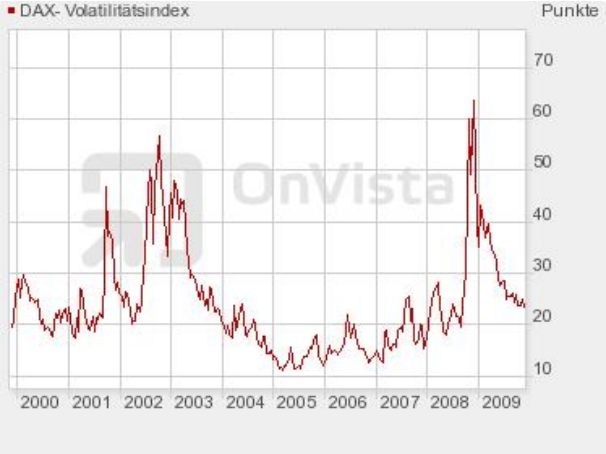

Figure D.2.: The VDAX as a measure of volatility in the market [51]. One can see that times of a low level are intermittently interrupted by times of comparably high levels that can last up to several months especially after external shocks such as 9/11, the beginning of the US invasion of Iraq (February 2003) or the full impact of the bursting of the US real estate bubble on Europe's economy (end of 2008).

3. Leverage effect

As has been pointed out by Black [53] and Bouchaud [47], financial markets exhibit a negative correlation between past returns and future volatility, a fact sometimes also termed 'volatility asymmetry' This means that the higher an assets' past returns have been the smaller its future volatility will be and vice versa. While indentified as a stylized fact and thus more or less present in any financial market, economic interpretation and even the causality of the effect ('volatility increase induced by price drop or do prices simply drop after a volatility increase?' [28]) are subject to a lively scientific debate. The psycological fact this seems to mirror is that investors tend to be more nervous if preceding price moves have been downwards whereas they rather tend to believe that the

[2] contrary to the finding that absolute values of returns ($\alpha = 1$) seem to be 'more predictable' [28] in that the correlation is highest in that case - in the majority of publications, this constitutes another stylized fact on its own and hence its state in this work.

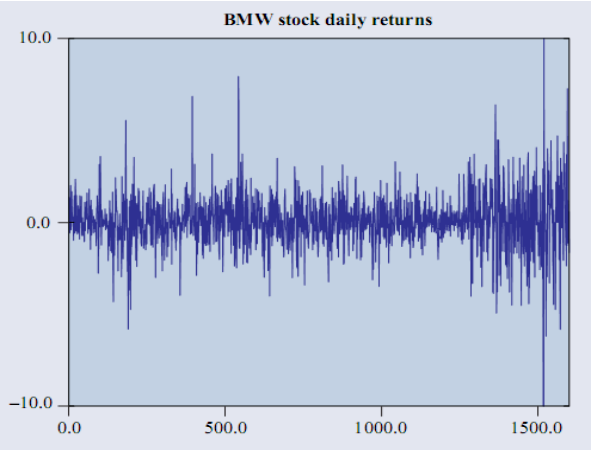

Figure D.3.: Daily returns of BMW shares from 1992-98, taken from [28]

'boom will last forever' if preceding moves were up, a conjecture that might be closely related to the formation of financial bubbles. In the literature [28, 47], the leverage is defined as

$$L(\tau) = \mathrm{corr}(|r(t+\tau)|^2, r(t)) \tag{D.3}$$

and has been reported to 'start from a negative value' and to 'decay to zero' [28]. The leverage effect is commonly interpreted as an evidence of the conjecture that volatilities are correlated while returns are not.

4. Bubbles and crashes

   Bubbles and the following crashes have been documented ever since markets in our modern sense of the word exist. The following table D.1 lists a few very prominent speculative excesses.

t	**Name**	*Time Period*	*Affected Countries*	*Object of speculation*
	Tulip Mania	1636-37	Netherlands	tulip bulbs, stocks (Dutch East India Company)
	South Sea Bubble	1720	GB	stocks (British South Sea Company)
	Railway Bubble	1847-57, 1873	GB, Europe, USA	stocks (railway companies), real estate, wheat
	Noble Metal Mania	1893	USA, Australia	silver, gold, gold mines and land
	Great Crash and Depression	1929-38	USA, world	credit backed stock investments, investment trusts
	Black Monday	1987	USA, world	stocks, Dollar, luxury real estate
	Japan Inc.	1990-?	Japan	stocks (NIKKEI), real estate
	Asian Crisis	1997	Hongkong, Singapore, Korea ...	real estate, bank credits, local currencies and stocks
	Dotcom Bubble	1996-2001	USA, world	stocks ('New Market')
	Real Estate Bubble	2002-2007	USA, world	real estate investments, mortgage backed securities

Table D.1.: A few of the most prominent bubbles of economic history, after [15, 16]

5. Heavy tails

   Return distributions usually exhibit power law tails which reflects the finding that comparably large gains and losses or too frequent to be explained by an underlying Gaussian normal distribution. More concretely, the distribution of a random variable X is said to be heavy-tailed if

$$\mathbb{P}(X > x) \overset{x\to\infty}{\propto} x^{-\alpha}, \quad \alpha > 0. \tag{D.4}$$

   where $\mathbb{P}(X > x)$ denotes the probability for the stochastic process X to take a value greater than x. Empirically, one has found that for the *tail index* α of financial market return distribution data, it holds that $2 < \alpha < 5$ [28]. Precise tail index estimation is not always easy and it has been subject to discussion whether a simple log-log regression

is always appropriate [55, 56].

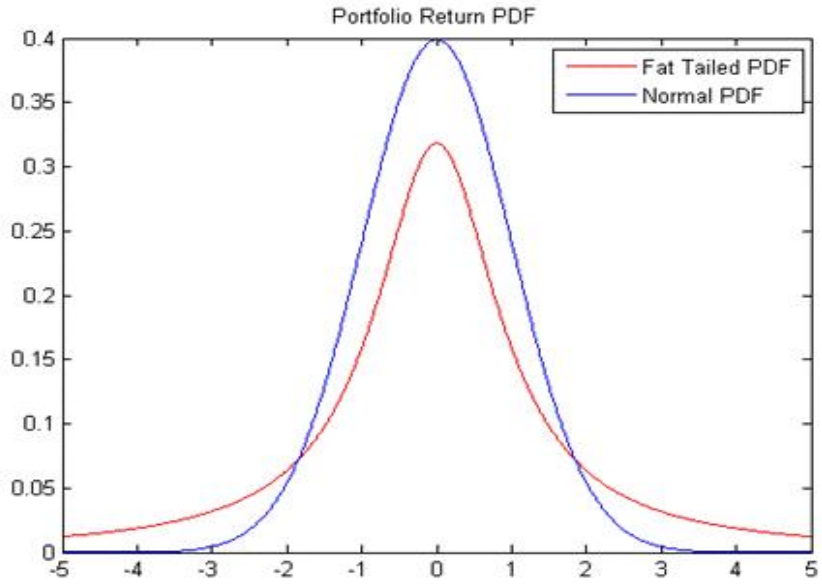

Figure D.4.: A 'fat tailed' distribution in comparison to the Gaussian normal distribution, picture taken from web site [54].

6. Slow decay of autocorrelation in absolute returns

   It has been found that, unlike the autocorrelation of returns, the autocorrelation of *absolute* returns decays very slowly (as a function of time lag) and roughly as power law with an exponent β within [0.2, 0.4], i.e.

$$C_\alpha \propto \frac{A}{\tau^\beta} \tag{D.5}$$

Other points often closely related to these stylized facts include the observed *gain/loss asymmetry* in return time series which alludes to the observation that large drawdowns are over-represented compared to upward movements of similar amplitude. However, this is not true for currency exchange rates where a higher symmetry has been documented. Moreover, Cont [28] lists *intermittency* as a stylized fact for return time series emphasizing that 'a high degree of variability' should be present 'at any time scale' and the *volume/volatility correlation* which means that the 'trading volume is correlated with all measures of volatility'. However, the author considers these as rather obvious facts about such time series and concludes with the example of the Volkswagen stock which skyrocketed from a 200 EUR level to over 1000 EUR within only two days in October 2008! When looking at the actual number of transactions involving the VW stock compared to the respective transaction volumes, this can be seen as a good example for the volume/volatility correlation.

Figure D.5.: October 2008 - Volkswagen skyrockets to over 1000 EUR after Porsche announced to take over 75 % of the VW company, picture taken from [57].

D.2. Known Issues About Asset Return Time Series

Allthough this work is not focussing on empirical analysis of asset returns or prices, it is still worth mentioning a few issues about statistical methods and estimations which we will do very briefly in the following paragraph.

D.2.1. Stationarity

It is a common misbelief among investors - and at this point, we are coming back to the assumptions of the Ide-Sornette model from the very beginning - that past returns can be simply extrapolated to the future. Such an attitude might be characteristic for the trend followers in the present model since they will enter the market if the preceding moves were up and vice versa. Obviously, such an investment behavior is enforced and promoted by investment consultants who often begin to massively advertise their products with their respective past performances suggesting the trend would go on forever. However, it is not clear whether return time series verify this property, i. e. that for *any* set of time instants and *any arbitrary* time lag τ, the joint distribution of the returns $r(t_1), \ldots, r(t_k)$ is the same as the joint distribution of returns $r(t_1 + \tau), \ldots, r(t_k + \tau)$.

D.2.2. Ergodicity

Ergodicity in a system implies that 'time average equals ensemble average'. As an example, consider rolling one dice a thousand times and taking the average of pips which should give a value of 3.5 as expected value for the number of pips (otherwise the dice we used would not be fair). The ergodic theorem now tells us that, instead of rolling one dice a thousand times, we might as well throw one thousand dices at once without affecting the result of our experiment. In a more physical language: consider the hypersurface $H(\vec{q},\vec{p}) = E$ associated with some process. Ergodicity of the system hence implies that the neighbourhood of any point $x \in H$ is actually visited by the system infinitely often[3].
Despite the undisputed power of the ergodic theorem which is the basic axiom of statistical physics as we know it today, it is worth noting that the theorem breaks down in case of spontaneous symmetry breaking, especially in case of phase transitions. Note also that the ergodic theorem is still not rigorously proven [27]. Moreover, Bouchaud [48] has pointed out that ergodicity can fail if a physical system exhibits long-range dependencies.

D.2.3. Reliability of Autocorrelation Functions

We have seen that the empirical stylized facts for financial markets are mostly defined over ACFs of the returns or some functions of them. However, it can be problematic to interpret these ACFs if the features of the underlying model or process are either not known at all or not the ones that ACFs were originally developed for. According to Cont [28] ACFs were developed to analyze dependence in *linear* and *Gaussian* time series data whereas Mikosch and Davis [73] have demonstrated that the presence of heavy-tailed distributions can give rise to non-standard statistical properties of the ACF and even invalidate some econometric testing procedures. In particular, the sample ACF remains a reliable estimator for the theoretical ACF but with a much slower rate of convergence ultimately widening the confidence bands for the sample ACFs. Another problem is that some sample ACFs use squares of returns such as introduced in the measures for volatility clustering and the leverage effect which causes 'a great deal of variability in sample autocorrelations of returns' [28]. It is therefore not always meaningful to draw quantitative conclusions from sample ACFs of heavy-tailed nonlinear return time series, especially where functions of returns or their absolute values are used. To conclude, it remains to be said that estimation of the confidence bands for nonlinear and non-Gaussian time series is a science of its own.

[3] this is sometimes also referred to as 'molecular chaos' meaning that any point on the hypersurface is equally probable

Bibliography

[1] M. Michael Waldrop: Complexity - the emerging science at the edge of order and chaos. Harmondsworth, Penguin.

[2] K. Richter, J.-M. Rost: Komplexe Systeme, Fischer Taschenbuch Verlag, Frankfurt am Main, October 2002.

[3] T. Lux, M. Marchesi: Scaling and criticality in a stochastic multi-agent model of a financial market, Nature 297 (1999), 498-500.

[4] J. D. Farmer: Market force, ecology and evolution, Industrial and Corporate Change, Volume 11, Number 5 (2001), 895-953.

[5] D. Sornette, J. V. Andersen: A Nonlinear Super-Exponential Rational Model of Speculative Financial Bubbles„ Int. J. Mod. Phys. C 13 (2002), 171-188.

[6] K. Ide, D. Sornette: Oscillatory finite time singularities in finance, population and rupture, Physica A 307 (2002), 63-106.

[7] A. H. Nayfeh., D.T. Mook: Nonlinear Oscillations, Wiley-IEEE, first edition 1979.

[8] J.-H. He: Some asymptotic methods for nonlinear equations, International Journal of Modern Physics B, Vol. 20, No. 10 (2006) 1141-1199.

[9] R. A. Mahaffey: A harmonic oscillator description of plasma oscillations, Phys. Fluids, Vol. 19, 1976, 1387-1391.

[10] I. Maeda, M. Yokomori: Systems of Multiply Connected Nonlinear Oscillators and Their Application to Seismic Phenomena, J. Fac. Sci. Hokkaido Univ. Ser. 7, Vol. 11, No. 3 (1999), 633-655.

[11] A. Drozdov, S. Hayashi: Quantum Statistics of Multidimensional Nonlinear Oscillators, Prog. Theor. Phys., Vol. 101, No. 1, 25-37, 1999.

[12] P. Mohazzabi: Theory and examples of intrinsically nonlinear oscillators, Am. J. Phys., Vol. 72, No. 4, April 2004, 493-498.

[13] J. V. Andersen and D. Sornette: Fearless versus Fearful Speculative Financial Bubbles, Physica A 337 (2004), 565-585.

[14] T. J. Sargent: "Rational expectations," The New Palgrave: A Dictionary of Economics, v. 4 (1987), 76-79.

[15] M. Otte: Der Crash kommt, Econ-Verlag, August 2006.

[16] D. Sornette: Critical Market Crashes, Physics Reports, Volume 378, Number 1, April 2003 , 1-98.

[17] W.-X. Zhou, D. Sornette:Antibubble and Prediction of China's stock market and Real-Estate, Physica A 337 (2004), 243-268.

[18] E. Nelson: Dynamical Theories of Brownian Motion, Princeton, 1967.

[19] M. Gitterman: The Noisy Oscillator - The First 100 Years, From Einstein Until Now, World Scientific Publishing, 1st edition, 2005, p. 11.

[20] W. Horsthemke, R. Lefever: Noise-Induced Transitions, Springer Series in Synergetics, Volume 15, 1984.

[21] N. G. van Kampen: Itô vs. Stratonovich, Journal of Statistical Physics 24 (1), January 1981, 175-187.

[22] L. Arnold, W. Horsthemke, R. Lefever: White and coloured external noise and transition phenomena in nonlinear systems, Z. Phys. B29, 1978, p. 867.

[35] C. W. Gardiner: Handbook of Stochastic Methods for Physics, Chemistry and the Natural Sciences, Springer Series in Synergetics, 3rd edition, 2003.

[24] S. Kabashima, T. Kawagubo: Observation of a noise induced phase transition in a parametric oscillator, Phys. Lett. A 70, 1979 p. 375.

[25] J. J. Tyson, P. C. Fife: Target patterns in a realistic model of the Belousov-Zhabotinskii reaction, J. Chem. Phys. 73, 1980, p. 2224.

[26] R. Graham, H. Haken: Laser light - a first example of a second order phase transition far away from thermal equilibrium, Z. Phys. 237, 1970, p. 30.

[27] P. Nielaba: Statistical Mechanics and Thermodynamics, Lecture in physics curriculum at University of Constance, winter semester 2006/07.

[28] R. Cont: Empirical properties of asset returns: stylized facts and statistical issues, Quant. Finance (1) 2001, 223-236.

[29] K. Debrabant, A. Rössler: Diagonally drift-implicit Runge-Kutta methods of weak order one and two for Itô SDEs and stability analysis, Appl. Num. Math (59) 2009, 595-607.

[30] P. Kloeden, E. Platen, H. Schurz: The Numerical Solution of Nonlinear Stochastic Differential Equations, Int J Bifur Chaos, Vol. 1, No. 2, 1991, 277-286.

[31] P. Kloeden, E. Platen: Numerical Solution of Stochastic Differential Equations, Applications of Mathematics (23) - Stochastic Modelling and Applied Probability, Third printing 1999, Springer Berlin.

[32] G. Milstein, M. Tretyakov: Numerical Integration of Stochastic Differential Equations with Nonglobally Lipschitz Coefficients, SIAM J. Numer. Anal. 43(3),1139-1154, 2005.

[33] W. Ruemelin: Numerical treatment of stochastic differential equations, SIAM J. Numer. Anal. 19, 604-613, 1982.

[34] P. Glasserman: Monte Carlo Methods in Financial Engineering, 1st ed., Springer, 2003.

[35] C. W. Gardiner: Handbook of Stochastic Methods, 3rd ed., Springer, 2003.

[36] J. Timmer: Parameter estimation in nonlinear stochastic differential equations, Chaos, Solitons and Fractals 11(2000) 2571-2578.

[37] J. Nicolau: Method for simulating non-linear stochastic differential equations in $\mathbb{R}^1$, J. Stat. Comp. and Sim., Vol. 75 (8), 2005, 595-609.

[38] D. Higham: An Algorithmic Introduction to the Numerical Simulation of SDE, SIAM Review, Vol. 43 (3), 525-546.

[39] K. Burrage, P. Burrage, D. Higham, P. Kloeden, E. Platen: Comment on "'Numerical methods for stochastic differential equations"', Phys. Rev. E 74, 068701, 2006.

[40] K. Burrage, P. M. Burrage: High Strong Order Explicit Runge-Kutta Methods for Stochastic Ordinary Differential Equations, Appl. Num. Math. 22, 1996, pp. 81-101.

[41] D. J. Higham, X. Mao, A. M. Stuart: Strong Convergence of Euler-Type Methods for Nonlinear Stochastic Differential Equations, SIAM J. Appl. Math. Vol. 40 (3), 2003, pp. 1041-1063.

[42] Michael Kohlmann, Universität Konstanz, private communication, August 2009.

[43] Lukas Szpruch, University of Strathclyde, private communication, September 2009.

[44] J. Wilkie: Phys. Rev. E 70, 017701, 2004.

[45] J. Wilkie, M. Cetinbas: Phys. Rev. A 337, 166, 2005.

[46] H. Risken: The Fokker-Planck Equation, Springer Berlin/Heidelberg, 1989.

[47] J.-P. Bouchaud, A. Matacz, M. Potters: Leverage Effect in Financial Markets: The Retarded Volatility Model, Phys. Rev. Lett. 87 (No. 22), 2001.

[48] J.-P. Bouchaud: Power laws in economics and finance, J. Quant. Finance 1, 2001, 105-12.

[49] http://www.generationaldynamics.com/cgi-bin/D.PL?xct=gd.log0805, 11/11/2009.

[50] www.bankofengland.co.uk/publications/fsr/2007/FSR07Oct3.ppt, 11/11/2009.

[51] http://www.onvista.de, 11/11/2009.

[52] V. A. Epanechnikov: Nonparametric estimation of a multidimensional probability density, Teor. Veroyatnost. i Primenen., 14:1 (1969), 156161

[53] F. Black in Proceedings of the 1976 American Statistical Association, Business and Economical Statistics Section (American Statistical Association, Alexandria, VA, 1976), p. 177.

[54] http://complexity.orconhosting.net.nz/fattail.gif , 11/12/2009.

[55] N. Wagner, T. Marsh: On Adaptive Tail Index Estimation for Financial Return Models, UC Berkeley: Research Program in Finance, Institute of Business and Finance. Retrieved from http://escholarship.org/uc/item/2651k8f5, publ. in 2000.

[56] P. Gopikrishnan, P. Meyer, L. A. N. Amaral, H. E. Stanley: Inverse cubic law for the distribution of stock price variations, Eur. Phys. J. B 3, 1998 , 139-40.

[57] http://boerse.ard.de, 11/12/2009.

[58] Andreas Rößler, private communication, September 2009.

[59] N. Kaldor: 'Capital Accumulation and Economic Growth' in: Lutz/Hague (eds.): The Theory of Capital, London, pp. 177-222.

[60] N. Kaldor: A model of economic growth, The Economic Journal 67 (268), 1957, pp. 591-624.

[61] T. Cooley, ed.: Frontiers of Business Cycle Analysis, Princeton University Press, 1995, p3.

[62] http://en.wikipedia.org/wiki/Stylized_fact, 11/23/09.

[63] K. C. Chan, G. Karolyi, F. A. Longstaff, A. B. Sanders: An Empirical Comparison of Alternative Models of the Short-Term Interest Rate, Journal of Finance, Vol. XLVII (3), July 1992, 1209-1227.

[64] L. Broze, O. Scaillet, J.-M. Zakoian: Testing for continuous-time models of the short-term interest rate, Journal of Empirical Finance 2(1995), 199-223.

[65] D. Sornette, S. Reimann, J.-O. Engler: Super-Exponential Bubble in the CIR-CEV Model with Positive Feedback, ETH internal working paper, January 2010.

[66] M. A. Rajabpour: Bessel Process and Conformal Quantum Mechanics, arXiv:0906.1728v1 [cond-mat.stat-mech], 9 June 2009.

[67] R. Schlittgen, B. Streitberg: Zeitreihenanalyse, R. Oldenbourg Verlag München Wien, 9th edition 2001.

[68] H. Rinne: Taschenbuch der Statistik, 4th edition, Verlag Harri Deutsch, Frankfurt 2008, pp. 856-884.

[69] A. Pagan: The econometrics of financial markets, Journal of Empirical Finance 3, 1996, pp. 15-102.

[70] E. F. Fama: The behavior of stock market prices, Journal of Business 38, 1965, pp. 34-105.

[71] J. C. Cox, J. E. Ingersoll, S. A. Ross: An analysis of variable rate loan contracts. The Journal of Finance 35(2), pp. 389-403, 1980.

[72] R. Cont, J. Yong: Statistical properties of financial time series, Mathematical Finance: Theory and Practice. Lecture Series in Applied Mathematics, Vol. 1, 1999, (Beijing: Higher Eductaion Press).

[73] T. Mikosch, R. A. Davis: Limit theory for the sample ACF of stationary processes with heavy tails with applications to ARCH, Ann. of Statistics 26, 1998, pp. 2049-80.

[74] K. Mallick, P. Marcq: Anomalous diffusion in nonlinear oscillators with multiplicative noise, Phys. Rev. E 66 (4), 2002, pp. 041113(1-13).

[75] P. S. Landa, A. A. Zaikin: Noise-induced phase transitions in a pendulum with a randomly vibrating suspension axis, Phys. Rev. E 54 (4), 1996, pp. 3535-3543.

[76] M. M. Klosek-Dygas, B. J. Matkowsky, Z. Schuss: Stochastic Stability on Nonlinear Oscillators, SIAM Journal on Applied Mathematics, Vol. 48, No. 5 (Oct., 1988), pp. 1115-1127

[77] J. E. Guyer, D. Wheeler, J. A. Warren: FiPy: Partial Differential Equations with Python, Comput. Sci. Eng. 11 (6), 2009, pp. 6-15.

[78] E. Bura, A. Zhmurov, V. Barsegov: Nonparametric density estimation and optimal bandwidth selection for protein unfolding and unbinding data, J. Chem. Phys. 130, 015102 (2009)

[79] D. J. Henderson: A Test for Multimodality of Regression Derivatives with an Application to Nonparametric Growth Regressions, MPRA paper no. 15, available online at: http://mpra.ub.uni-muenchen.de/8768/, 01/15/2010.